UC Davis
UC Davis Electronic Theses and Dissertations

Title
Ocean and climate change in the Northeast Pacific through the Holocene

Permalink
https://escholarship.org/uc/item/1js6r1gv

Author
Palmer, Hannah

Publication Date
2021

Peer reviewed|Thesis/dissertation

eScholarship.org Powered by the California Digital Library
University of California

Ocean and climate change in the Northeast Pacific through the Holocene

By

HANNAH MARIE PALMER
DISSERTATION

Submitted in partial satisfaction of the requirements for the degree of

DOCTOR OF PHILOSOPHY

in

Earth and Planetary Sciences

in the

OFFICE OF GRADUATE STUDIES

of the

UNIVERSITY OF CALIFORNIA

DAVIS

Approved:

Tessa M. Hill, Chair

Peter Roopnarine

Dawn Sumner

Committee in Charge

2021

Table of Contents

Table of Contents ii
Abstract v
Acknowledgements vi

Chapter 1: Southern California margin benthic foraminiferal assemblages record recent centennial-scale changes in oxygen minimum zone

Abstract 1
1. Introduction 2
   1.1. Benthic foraminifera record changes in coastal margin biogeochemistry 2
   1.2. Regional setting 4
2. Methods 5
   2.1. Study site 5
   2.2. Oceanographic data collection 5
   2.3. Sediment cores 6
   2.4. Foraminiferal assemblages 6
   2.5. Radiocarbon based chronology 7
3. Results 8
   3.1. Vertical profiles, sediment characterization of San Diego margin 8
   3.2. Benthic foraminiferal assemblage across modern environmental gradient 8
   3.3. Comparison of benthic foraminifera in two size fractions 10
   3.4. Multivariate analyses of benthic foraminiferal assemblage 11
   3.5. Age model development 12
   3.6. Temporal change in benthic foraminiferal assemblages 12
4. Discussion 13
   4.1. Benthic foraminiferal assemblages across modern environmental gradient 13
   4.2. Temporal change in benthic foraminiferal assemblages record environmental change through time 18
5. Conclusions 20
6. Original publication and data availability 21
7. Acknowledgements 21
8. Tables 22
9. Figures 23
10. Supplemental figures 27
11. References 31

Chapter 2: Oxygenation of offshore Southern California marine basins through the Holocene

Abstract 36
1. Introduction 37
   1.1. Marine oxygenation in the past and present 37
   1.2. Southern California modern and paleoceanography 38
   1.3. Benthic foraminiferal assemblages as a metric of past oxygenation and organic matter export 40
2. Methods 42
   2.1. Study Site 42
   2.2. Sediment cores 42
   2.3. Radiocarbon dating and age model development 43

2.4. Stable Isotope Analysis 44
2.5. Benthic Foraminiferal Assemblages 45
2.6. Foraminiferal morphometrics 45
2.7. Metazoan microfossil assemblages 46
2.8. Benthic foraminiferal oxygenation index 46
2.9. Statistical analysis 46
2.10. Modern oxygenation data 47
3. Results 47
3.1. Age Model Development 47
3.2. Stable isotope record 47
3.3. Benthic foraminiferal assemblages 48
3.4. Metazoan microfossil analysis 49
3.5. Shell morphometrics 50
3.6. Modern oxygenation in the Southern California Borderlands 50
4. Discussion 50
4.1. Benthic foraminiferal assemblages as paleo-oxygenation proxy 50
4.2. Oxygenation and ventilation change in individual basins through the Holocene 52
4.2.1. Assemblage and environmental change through time in Tanner Basin 52
4.2.2. Assemblage and environmental change through time in San Nicolas Basin 54
4.2.3. Assemblage and environmental change through time in San Clemente Basin 55
4.3. Intermediate water change and basinal processes in Southern California Borderlands 56
5. Conclusions 58
6. Tables 60
7. Figures 61
8. Supplemental Figures 65
9. Supplemental Tables 70
10. References 71

Chapter 3: A systematic review of Holocene climate and oceanography of the coastal Western United States and Northeast Pacific

Abstract 76
1. Introduction 77
1.1. Overview of Holocene Climate 77
1.2. Modern climate and oceanography of Western North America 78
2. Methodology 81
3. Results and discussion 84
3.1. Early Holocene (11.75-8.2 ka) 84
3.1.1. Regional synthesis 84
3.1.2. Terrestrial climate 85
3.1.3. Marine conditions 87
3.1.4. 8.2 ka Event 88
3.1.5. Ecological responses to change 88
3.1.6. Human-environment interactions 90
3.2. Mid-Holocene (8.2-4.2 ka) 90
3.2.1. Regional synthesis 90
3.2.2. Terrestrial climate 92
3.2.3. Marine conditions 94
3.2.4. Ecological responses to change 95
3.2.5. Human-environment interactions 96
3.3. Late Holocene (4.2 ka-present) 97

3.3.1. Regional synthesis 97
3.3.2. Terrestrial climate 98
3.3.3. Marine conditions 101
3.3.4. Ecological responses to change 103
3.3.5. Human-environment interactions 104
3.4. Medieval Climate Anomaly and Little Ice Age 106
3.5. Era of Colonization 106
4. Conclusions 109
5. Acknowledgements 112
6. Figures 113
7. References 120

Appendices

Appendix 1 135
Appendix 2 141
Appendix 3 144
Appendix 4 146
Appendix 5 150
Appendix 6 153

Abstract

Anthropogenic climate change is altering global biogeochemical cycles and climate processes with critical implications for marine and terrestrial ecosystems and human communities. Investigation of climate records from the Holocene (11.75 ka to present) provides critical insights into contextualizing modern climate change and understanding biogeochemical and ecosystem responses to environmental change. Here, I investigated changes in marine oxygenation along the Southern California margin and explored Northeast Pacific marine-terrestrial interactions throughout the Holocene. Through investigation of marine sediment archives, specifically benthic foraminifera, I quantitatively refined oxygenation proxies, examined changes in the oxygen minimum zone (OMZ) in past 1.5 ka, and reconstructed oxygenation of waters below 1000 m throughout the Holocene. In the first chapter, I conducted paired spatial and temporal analysis of benthic foraminiferal assemblages across a modern oxygen gradient on the San Diego margin. Results show that modern oxygenation gradients structure foraminiferal species distributions, shell size, and diversity. Centennial-scale variability in the upper margin of the OMZ occurred in the past 1.5 ka, while the core of the OMZ and below the OMZ remained stable. A recent expansion of the OMZ and decline in oxygenation at 528 m in the last 400 years on the San Diego margin is synchronous with regional records of deoxygenation. In the second chapter, I analyzed oxygen and carbon stable isotope records from planktic and benthic foraminifera and benthic foraminiferal assemblages from three silled basins in the Southern California Borderlands through the Holocene to constrain timing and implications of oxygenation and ventilation change across depth. Reconstructed oxygenation at depth (from 1100-1800m) was consistently within a range of intermediate hypoxia (0.5-1.5 ml L^{-1} $[O_2]$) through the Holocene and had reduced variability relative to shallower basins. To contextualize these marine changes within a linked marine-terrestrial system, in my third chapter I conducted a systematic review of Holocene climate and oceanography of Western North America and the Northeast Pacific. Findings reveal that the early Holocene is characterized by warming relative to pre-Holocene conditions, including warm sea surface conditions, a warm and dry Pacific

Northwest, a warm and wet Southwest, and overall spatial and temporal stability. In the mid Holocene, these patterns reverse; this interval is characterized by cool sea surface temperatures, a cool and wet Pacific Northwest and warm and dry Southwest. The late Holocene is the most variable interval spatially and temporally, and a new spatial trend appears characterized by warmer coastal areas and cooler inland areas. This synthesis of climate and oceanographic processes and resultant impacts on ecosystems and human communities provides a window into understanding modern patterns of climate and environmental change in Western North America.

Acknowledgements

Throughout my academic journey, I received tremendous support and guidance from my professional and personal communities, and the successful completion of my doctoral degree would not have been possible without this support. I would like to thank my dissertation advisor, Tessa Hill for her outstanding mentorship, trust, and leadership. I would like to thank the members of the Oceans and Climate Lab past and present for their support, guidance, and collaboration. I would like to acknowledge the Earth and Planetary Sciences and Bodega Marine Laboratory communities that have provided me with intellectual, professional, and personal support. I thank each of my students and mentees who taught me so much more than I could hope to teach them. I would like to acknowledge the open spaces across California on which I have had the opportunity to step away from my research and gain clarity. I am grateful for all my friends who have supported me through this endeavor and who continually remind me of the many joys in life. I would like to thank my family for their encouragement, steadfast support, and belief in my potential. Finally, I would like to acknowledge the endless support of my partner Carl who throughout this journey has helped me to make every day a great day.

Chapter 1

Southern California margin benthic foraminiferal assemblages record recent centennial-scale changes in oxygen minimum zone

Abstract

Microfossil assemblages provide valuable records to investigate variability in continental margin biogeochemical cycles, including dynamics of the oxygen minimum zone (OMZ). Analyses of modern assemblages across environmental gradients are necessary to understand relationships between assemblage characteristics and environmental factors. Five cores were analyzed from the San Diego margin (32°42'00"N, 117°30'00"W, 300-1175 m water depth) for core top benthic foraminiferal assemblages to understand relationships between community assemblages and spatial hydrographic gradients and for down core benthic foraminiferal assemblages to identify changes in the OMZ through time. Comparisons of benthic foraminiferal assemblages from two size fractions (63-150 and >150 μm) exhibit similar trends across the spatial/environmental gradient, or in some cases exhibit more pronounced spatial trends in the >150 μm fraction. A range of species diversity exists within the modern OMZ (1.910-2.586 H, Shannon Index), suggesting that diversity is not driven by oxygenation alone. We identify two hypoxic associated species (*B. spissa* and *U. peregrina*), one oxic associated species (*G. subglobosa*) and one OMZ edge-associated species (*B. argentea*). Down core analysis of indicator species reveal variability in the upper margin of the OMZ (528 m water depth) while the core of the OMZ (800 m) and below the OMZ (1175 m) remained stable in the last 1.5 ka. We document expansion of the upper margin of the OMZ beginning 400 ybp on the San Diego margin that is synchronous with other regional records of oxygenation.

1 Introduction

Ocean oxygenation is declining globally; rising ocean temperatures decrease oxygen solubility at the sea surface and increased stratification inhibits ventilation, leading to decreased oxygen at depth (Breitburg et al., 2018; Levin et al., 2009; Stramma et al., 2010). Expansions of oxygen minimum zones (OMZ) have already been documented and further expansions are predicted (Bograd et al., 2008; Schmidtko et al., 2017; Stramma et al., 2010). Within the California Current system, a decline in dissolved oxygen (DO) concentration, shoaling of the hypoxic boundary, and decreased pH have been documented (Bakun, 2017; Bograd et al., 2008). The intensity and geographic extent of the CA margin OMZ has oscillated in response to past changes in climate and ocean temperatures on millennial timescales – weakening during cool periods and strengthening during warm periods (Cannariato and Kennett, 1999; Jaccard et al., 2014; Moffitt et al., 2014, 2015a; Ohkushi et al., 2013). Determination of timing and drivers of past expansions and contractions of OMZs is critical to developing accurate predictions of future change (Jaccard et al., 2014).

Continental margin biogeochemical dynamics structure shelf ecosystems across space and time (Levin et al., 2009; Levin and Dayton, 2009). In particular, oxygenation is a key determinant of benthic zonation; seafloor ecosystems are subject to major turnover in response to relatively minor inferred changes in oxygenation (Levin, 2003; Levin and Dayton, 2009; Moffitt et al., 2015b). Areas of low oxygen availability typically contain low abundance and diversity of organisms (Levin, 2003; Levin and Dayton, 2009). However, several species of benthic foraminifera are adapted to survive in low-oxygen conditions and are thus present, and often abundant, in such environments (Bernhard and Gupta, 1999; Gooday et al., 2000; Kaiho, 1994, 1999; Keating-Bitonti and Payne, 2016).

1.1 Benthic foraminifera record changes in coastal margin biogeochemistry

Microfossil records from the Southern California Borderlands are a critical tool for understanding changes in productivity (Cannariato and Kennett, 1999; Emmer and Thunell, 2000; Stott et al., 2000),

orbital and millennial scale climate changes (Hendy, 2010; Hendy and Kennett, 2000; Taylor et al., 2015), and climate change through the Holocene (Balmaki et al., 2019; Fisler and Hendy, 2008; Friddell et al., 2003; Roark et al., 2003). Benthic foraminiferal assemblages are widely used as a proxy for changes in oxygenation through time (Balestra et al., 2018; Bernhard et al., 1997; Bernhard and Gupta, 1999; Cannariato and Kennett, 1999; Gooday, 2003; Jorissen et al., 2007; Moffitt et al., 2014; Ohkushi et al., 2013; Shibahara et al., 2007; Tetard et al., 2017). Previous work (through analysis of benthic foraminifera along environmental depth gradients and in laboratory culturing studies) documented relationships between benthic foraminiferal taxa and water depth, oxygen concentration, sediment substrate, position in the sediment matrix, nitrate availability, and organic matter availability (Bernhard et al., 1997; Bernhard and Bowser, 1999; Bernhard and Gupta, 1999; Cardich et al., 2019; Caulle et al., 2014; Douglas, 1981; Douglas and Heitman, 1979; Erdem et al., 2019; Jorissen et al., 2007; Kaiho, 1994, 1999; Mallon et al., 2012; Mazumder and Nigam, 2014; Mullins et al., 1985).

Generally, low oxygen environments contain high abundance and low diversity of benthic foraminifera; in these settings, infaunal, elongate, thin-walled species with high porosity dominate over porcelaneous and epifaunal taxa (Bernhard et al., 1997; Douglas, 1981; Jorissen et al., 1995, 2007; Kaiho, 1994, 1999; Mazumder and Nigam, 2014). Further work has explored the relationship between foraminiferal size and oxygenation; generally volume to surface area ratios of foraminiferal tests are positively correlated with dissolved oxygen, yet studies of individual taxa on the Southern California margin do not consistently show this relationship (Keating-Bitonti and Payne, 2016; Keating-Bitonti and Payne, 2017; Rathburn et al., 2018). Often, individual taxa of foraminifera are classified into groups based on oxygen affinity or individually identified as oxygen indicator taxa (Jorissen et al., 1995; Kaiho, 1999; Moffitt et al., 2014). In particular, bolivinid taxa are noted as low oxygen indicator taxa (Cardich et al., 2015; Caulle et al., 2014; Mallon et al., 2012; Mullins et al., 1985). However, these relationships between foraminiferal assemblages and environmental metrics are regionally defined and cannot be applied globally; regional calibrations of the benthic foraminifera oxygen proxy are required for accurate paleoceanographic

analyses (Bernhard et al., 1997; Caulle et al., 2014; Kaiho, 1999; Mallon et al., 2012; Mazumder and Nigam, 2014). Similarly, the classification of oxygenation levels varies among paleoceanographic studies (Balestra et al., 2018; Kaiho, 1994; Moffitt et al., 2015a). This study uses the following classification: oxic ($[O_2]$ >1.5 ml/L), intermediate hypoxia/suboxic ($[O_2]$ 1.5-0.5 ml/L), and severe hypoxia/dysoxic ($[O_2]$ <0.5 ml/L) (Moffitt et al., 2015a). Although oxygenation is a dominant driver of ecosystem zonation in marginal environments, sediment substrate, organic matter availability, and nitrate availability also play important roles in structuring benthic foraminiferal assemblages. Further analysis of the interacting environmental factors along depth/environmental gradients is needed (Jorissen et al., 1995, 2007; Mullins et al., 1985; Venturelli et al., 2018).

Previous studies of oxygenation change over time from the Southern California margin focus largely on the Santa Barbara and Santa Monica Basins, due to their high sedimentation rates and regular laminations (Balestra et al., 2018; Cannariato and Kennett, 1999; Christensen et al., 1994; Kaiho, 1999; Moffitt et al., 2014; Schimmelmann et al., 2013). Significantly fewer studies in the Northeast Pacific investigate sediments outside of those basin environments (McGann, 2002). Further analysis is therefore needed to constrain relationships between benthic foraminifera and environmental conditions in the open continental margin where biological and chemical gradients are more variable and to identify decadal to centennial changes in OMZ dynamics.

1.2 Regional Setting

The California margin is a well-studied system characterized by southward flow of the California Current, a strong seasonal upwelling regime bringing cold, nutrient rich waters to the surface, high coastal productivity, and a large OMZ occurring at intermediate water depths (Checkley and Barth, 2009). The San Diego margin is dominated by two surface currents: the southward flowing California Current and the seasonal, northward flowing surface Davidson Current (Checkley and Barth, 2009).

An important feature of California margin coastal oceanography is the presence of a large, intermediate depth OMZ and carbon maximum zone (CMZ), from approximately 500 to 1000 m water depth (Helly and Levin, 2004; Stramma et al., 2010). The intensity and spatial extent of the modern California margin OMZ is driven by physical mixing of well-oxygenated surface water, biological activity at the surface and at depth, and intrusion of lower oxygen bottom waters (Gilly et al., 2013). Both physical processes (temperature-dependent diffusion from atmosphere, mixing, stratification, deep water circulation) and biological processes (primary productivity at the surface and respiration at depth) control the intensity and extent of OMZs (Gilly et al., 2013; Helly and Levin, 2004).

Here we utilize the spatial variability of the continental margin as a natural laboratory to analyze relationships between core top, modern benthic foraminiferal assemblages and *in situ* measurements of environmental parameters (temperature, oxygenation, carbonate chemistry). We then quantify benthic foraminiferal assemblages down core to understand past environmental change.

2 Methods

2.1 Study site

The San Diego margin is located in the Southern California Borderlands in the Eastern North Pacific (Fig. 1). The margin slopes downward to a depth of approximately 1200 m at a distance of 30 km normal to shore (Fig. 1) and is bounded by a bathymetric rise (600 m water depth) to the west. All hydrographic data and sediment cores used in this study were collected by the San Diego Coastal Expedition aboard the R/V *Melville* in December 2012 by a team from the Scripps Institution of Oceanography.

2.2 Oceanographic data collection

Bottom water temperature, salinity, and dissolved oxygen concentration were collected at each coring location using a Seabird CTD (SBE9), with a dissolved oxygen probe (Seabird Electronics Sensor SBE43). Carbonate chemistry was completed using *in situ* bottle sampling for pH and total dissolved

inorganic carbon (DIC) and were previously published (Nam et al., 2015; Takeshita et al., 2015). Bottom depths were measured acoustically at each site.

2.3 Sediment cores

Five sediment cores collected along a depth transect from 300 to 1175 m depth were selected for use in this study (Figure 1; Table 1). Short (15-31cm) surface sediment cores were collected along the coastal margin using a deep-sea multicore with 9 cm diameter cores. Each core was divided into 1 cm intervals aboard the ship and immediately frozen. Sediments were not stained upon retrieval; thus, we could not carry out an analysis of live vs. dead or depth habitat of these species. Total organic matter of core top sediments was measured as percent ash-free dry weight and previously published in Grupe et al. 2015 (Grupe et al., 2015). Subsamples were each disaggregated in deionized water, washed over a 63 μm sieve and oven dried at 50° C.

2.3 Foraminiferal assemblages

Assemblages were counted from the > 150 μm and 63 - 150 μm fraction for comparison between the size fractions. Sediments were split using a sediment splitter and dry sieved; a minimum of 300 foraminifera per sediment sample (in the >150 μm fraction) were identified and counted for all core top samples to provide a representative assemblage, unless fewer than 300 specimens were present in the entire sample. Identification of benthic foraminiferal taxa was based on previously published descriptions and images of benthic foraminifera (see Supplemental Figures, Figure S4 for images of dominant taxa and taxonomic reference list) (Balestra et al., 2018; Erdem and Schönfeld, 2017; Keating-Bitonti and Payne, 2017; Moffitt et al., 2014; Setoyama and Kaminski, 2015). Assemblages in the 63-150 μm fraction were quantified from the same sediment fraction as the > 150 μm to allow for comparison of abundance between the two groups. Down core assemblages were quantified in the > 150 μm size fraction (see discussion below) and a minimum of 150 foraminifera per sediment sample were counted in all down core samples unless fewer than 150 specimens were present in the sample (Mallon et al., 2012).

Assemblage counts are standardized to the volume (63.62 cm^3) of the sampled cylinder of the sediment (core). Core top sediment (0-1, 1-2 cm) calcareous benthic foraminiferal assemblages were described for all cores. Complete down-core records of benthic foraminiferal assemblages were examined at 1 or 2 cm intervals for cores MV1217-2-3 (0-18 cm, sampled at 1 cm interval, 528 m water depth), MV1217-1-3 (0-10 cm, sampled at 1 cm interval; 10-20 cm, sampled at 2 cm interval, 800 m water depth). In order to build a longer temporal record at 1175 m we combine two multi cores; core MV1217-4-3 (0-10 cm, sampled at 1 cm interval) and MV1217-4-1 (sampled at 10-16 cm, 2 cm interval, 1175 m water depth).

Shannon Index of diversity was used to describe foraminiferal diversity (Peet, 1974). Analysis of variance (ANOVA) was used to determine differences between assemblages in two size fractions > 150 μm and 63 – 150 μm. Distance-based redundancy analysis (dbRDA) with Bray–Curtis distances was used to ordinate core top assemblages and examine relationship to environmental variables. Non-metric multidimensional scaling ordination, using square root transformation of assemblage species counts and Bray-Curtis similarities, were completed to identify relatedness between assemblages through time. All multivariate analyses were completed using the Vegan R package (Myhre et al., 2017; Oksanen et al., 2013).

2.4 Radiocarbon based chronology

Cores from two sites (528 m water depth, MV1217-2-3, 1175 m water depth, MV1217-4-1 and MV1217-4-3) were selected for radiocarbon (^{14}C) dating using mixed planktonic foraminifera. Core MV1217-2-3 (528 m) was sampled at three 1-cm intervals (11-12 cm, 16-17 cm, 25-26 cm). To generate an age model for the multicores at 1175m water depth, core MV1217-4-3 (1175 m) was sampled at one 1-cm interval (5-6 cm) and core MV1217-4-1 (1175 m) was sampled at two 1-cm intervals (10-11 cm, 20-21 cm) (Table 2). Radiocarbon analysis was completed at the Lawrence Livermore National Laboratory using $\delta^{13}C$ assumed values following the convention of Stuiver and Polach 1977 (Stuiver and Polach, 1977). The quoted age was given in radiocarbon years using the Libby half-life of 5568 years. The Calib7.1

calibration program was used to calibrate ages using a reservoir age of 220.0 +/- 40.0 (Ingram and Southon, 1996; Stuiver and Polach, 1977).

3.0 Results

3.1 Vertical profiles, sediment characterization of San Diego margin

Across the depth profile, bottom water temperature decreased steadily with depth (300 m to 1175 m) ranging from 8.6ºC (300 m) to 3.8ºC (1175 m) (Figure 2, Table 1). Salinity (not plotted here) had a mean of 34.4 psu ranging from 34.1 to 34.5 psu. Water column DO measurements collected directly above each coring site show oxic conditions at 300 m (1.54 ml/L) above the OMZ, intermediate hypoxia at 1175 m (0.58 ml/L) below the OMZ, and severe hypoxia at 528 m (0.35 ml/L) at the upper edge of the OMZ, and within the OMZ at 700 m (0.26 ml/L) and 800 m (0.29 ml/L). Although not greatly variable, a pH minimum occurs at 700 m (7.55) and is higher at 300 m (7.65) and 1175 m, (7.59) (Figure 2, Table 1). Total organic matter increased with depth (6.8-14.7% AFDW, Table 1). These results are consistent with previous analyses of the California margin OMZ/CMZ (Helly and Levin, 2004).

3.2 Benthic foraminiferal assemblage across modern environmental gradient

Relative abundance of benthic foraminifera was quantified for all sites in the 0-1 and 1-2 cm intervals. We compared the 0-1 cm interval to the 1-2 cm interval to assess if depth habitat of any species determined their relative abundance in the core top assemblage. Specimens were not Rose Bengal stained, thus their presence in any interval does not indicate that they were living at the time of collection. We do not identify any significant relationship between relative abundance of a species and depth interval (ANOVA; in all cases $p>0.05$ or r^2 is <0.001). Foraminiferal abundance is low (<100 individuals) in some of the samples from 0-1 cm. Thus, in order to utilize sufficient numbers of individuals and because there were no significant differences in abundance of species between 0-1 cm and 1-2 cm, for the rest of the discussion we refer to the 0-2 cm fraction as the core top material (Figure 2 and 3). Calcareous taxa dominated the assemblage at every site; agglutinated foraminifera made up 0 (300 m) to 21% (700 m) of

the assemblage. Due to their propensity for degradation and to remain consistent with other regional studies, we exclude agglutinated taxa and all values are reported as percent of total calcareous taxa for the remainder of the text (Balestra et al., 2018; Kaiho, 1994; Moffitt et al., 2014; Venturelli et al., 2018).

Total abundance of foraminifera decreases with depth (Figure 2). Core top assemblages were dominated by *Bolivina argentea, Epistominella* sp.*, Uvigerina peregrina, Globocassidulina subglobosa, Cassidulina carinata,* and *Bolivina spissa,* in order of decreasing abundance (see Figure S4 for images of dominant taxa). These dominant taxa make up 80% of all calcareous foraminifera counted across all core top samples. All other species each represent less than four percent of the total assemblage across all core tops. The following taxa are found at all five water depths: *Bolivina argentea, Bolivina spissa, Bulimina* spp., *Cibicidoides* sp.*, Epistominella* sp.*, Globobulimina pacifica, Globocassidulina subglobosa, Globobulimina ovata, Nonionella stella, Quinqueloculina* sp. and *Uvigerina peregrina.*

First, we report the benthic foraminiferal assemblage from the >63 μm size fraction; we then report on a comparison between the 63 - 150 μm and >150 μm size fractions. The assemblage at 300 m is dominated by *G. subglobosa* (28%), *B. argentea* (25%), *U. peregrina* (10%), *Epistominella* sp. (8%), and *Bolivina spissa* (6%); species richness is 24 and diversity (H) is 2.133. The assemblage at 528 m is dominated by *B. argentea* (37%), *U. peregrina* (23%), *Epistominella* sp. (15%), *C. carinata* (6%) and *G. subglobosa* (5%); species richness is 25 and diversity (H) is 1.910. The assemblage at 700 m is dominated by *Epistominella* sp. (29%), *C. carinata* (15%), *U. peregrina* (13%), *G. subglobosa* (11%), *B. argentea* (10%), and *B. spissa* (7%); species richness is 23 and diversity (H) is 2.249. The assemblage at 800 m is dominated by *B. spissa* (16%)*, U. peregrina* (16%)*, Epistominella* sp. (13%), *C. carinata* (10%), *Cibicidoides* sp. (10%)*,* and *Globobulimina ovata* (13%); species richness is 25 and diversity (H) is 2.586. The assemblage at 1175 m is dominated by *C. carinata* (25%), *Epistominella* sp. (20%), *G. subglobosa* (8%), *B. spissa* (6%); species richness is 25 and diversity (H) is 2.389 (Figure 2).

3.3 Comparison of benthic foraminifera in two size fractions

Comparison of foraminiferal abundance between the 63-150 μm and >150 μm shows higher abundance in the small fraction at 300 m, 700 m and 1175 m, and higher abundance in the large size fraction at 528 m and 800 m. Several taxa are found in both size fractions at all five water depths: *Globocassidulina subglobosa* and *Epistominella* sp. Four species have significantly different relative abundances between size classes; three are more likely to be found in the 63-150 μm (*C. carinata, Epistominella* sp. and *G. subglobosa*) and one species (*U. peregrina)* is significantly more likely to be found in the 150 μm size fraction (ANOVA, $p<0.05$ for all, Figure 3).

In the >150 μm size fraction, species diversity (H) ranges from 1.316–2.700; minimum diversity (H) is found at 528 m (1.316) and maximum diversity (H) is found at 1175 m (2.700). In comparison, in the 63-150 μm size fraction, species diversity (H) ranges from 1.710–2.042; minimum diversity (H) is found at 700 m (1.710) and maximum diversity (H) is found at 800 m (2.042) (Figure 2). Species diversity is greater in the >150 μm size fraction relative to the 63-150 μm size fraction at all sites except the site at 528 m (Figure 2).

When we consider the complete assemblage (>63μm) we can classify the most abundant species into four groups based on their trends relative to the OMZ (Figure 3). Two species are more abundant within the OMZ: *B. spissa,* and *U. peregrina*; we identify these species as dysoxic indicator species. One species is less abundant within the OMZ relative to sites outside of the range of the OMZ: *G. subglobosa*; we identify this species as an oxic indicator species (Kaiho, 1999). Two species increase in abundance with water depth: *C. carinata* and *Epistominella* sp. One species is most abundant near the uppermost edge of the OMZ: *B. argentea*; this species may be edge-associated (Mullins et al., 1985). Importantly, when we consider only the >150 μm size fraction, we observe the same trends: high abundance in OMZ (*B. spissa, U. peregrina*), low abundance in OMZ (*G. subglobosa*), increased abundance with depth (*C. carinata* and *Epistominella* sp.), and OMZ edge-associated (*B. argentea*) (Figure 3). Generally, we find that trends

across depth are similar between the complete (>63 μm) and large size fraction (>150 μm) or are more pronounced in the >150 μm size fraction compared to the 63-150 μm size fraction (Figure 3). In some taxa, trends in both size fractions are similar across depth (*B. spissa, Epistominella* sp., *G. subglobosa, C. carinata*) (Figure 3). For other taxa, we observe a low relative abundance of a species in the (63-150 μm) fraction throughout all water depths, while for the same species in the >150 μm size fraction, we observe a pronounced trend through depth (*U. peregrina*, *B. argentea*) (Figure 3).

To further analyze these trends, we completed pairwise analysis of relative abundances of benthic foraminifera and environmental parameters. DO concentrations and pH are correlated at all water depths; here we chose to compare foraminiferal abundances to dissolved oxygen, yet we acknowledge that these affiliations may be driven by the combined effect of the OMZ/CMZ. When we analyze the complete assemblage (>63 μm) we identify a significant positive correlation between *G. subglobosa* and dissolved oxygen (r^2=0.76, p<0.05) and temperature (r^2=0.64, p<0.05) and a significant negative correlation between *G. subglobosa* and total organic matter (r^2=-0.72, p<0.05). If we analyze the >150 μm size fraction only, we identify the same significant positive correlation between DO and *G. subglobosa* (r^2=0.96, p<0.05) and also identify a positive correlation between *C. carinata* and water depth; abundance of this species increases with depth (r^2=0.93, p<0.05). When we analyze the 63-150 μm size fraction alone, we identify the same trends as observed in the >150 μm fraction: a significant positive correlation between *G. subglobosa* and dissolved oxygen (r^2=0.90, p<0.05). and a significant positive correlation between *C. carinata* and water depth (r^2=0.88, p<0.05). In the 63-150 μm fraction we also identify a significant negative correlation between *U. peregrina* and water depth (r^2=-0.95, p<0.05). We do not identify significant correlations between any other taxa and environmental parameter.

3.4 Multivariate analyses of benthic foraminiferal assemblage

Multivariate statistical analysis (using distance-based redundancy analysis) of core top assemblages identifies several taxa that contribute most strongly to the ordination of the assemblages (*G. subglobosa,*

U. peregrina, B. argentea) (Figure S1). Oxygenation operates on an axis - separating sites at 300 m and 1175 m from the three OMZ sites 528 m, 700 m, and 800 m. Temperature operates on a second axis (Figure S1). Our findings support previous work that identify *G. subglobosa* with higher oxygen environments and *B. argentea* and *U. peregrina* with lower oxygen environments (Bernhard et al., 1997; Kaiho, 1994, 1999; Moffitt et al., 2014).

3.5 Age model development

Radiocarbon dating of two cores yielded variable sedimentation rates, from 6.1 to 42.2 cm/ka (error of +/- 11.3, see Table 2). An age model was developed for each core based on linear interpolation between radiocarbon dates (Figure S2). Core MV1217-3-3 (800 m water depth) was not radiocarbon dated; for this core we apply an average sedimentation rate (19.6 cm/ka) generated from the core above (528 m) and below (1175 m) this core. All following results will be discussed in age (years before present).

3.6 Temporal change in benthic foraminiferal assemblages

Down core assemblages were quantified in three cores (from 528, 800, and 1175 m water depth) in the >150 μm size fraction only, following results from core top analysis (see section 4.1). Down core assemblages contained similar species to core tops. Down core assemblages were dominated by (in descending order) *Uvigerina peregrina, Bolivina spissa, Bolivina argentea, Globobulimina* sp*., Cibicidoides* sp*.,* and *Epistominella* sp.. These dominant taxa make up more than 75% of all foraminifera counted across all cores and subsamples. All other species each account for less than 5% of total assemblage across all cores and depths. The total number of species in each sample ranged from 11 to 26, comparable to the number of species found in the core tops.

Multivariate statistical analysis (using non-metric multidimensional scaling) of down core assemblages and core top assemblages shows that, through time, assemblage similarity within sites exceeds similarity to assemblages at any other site (Figure S3). In multivariate space, the difference between sites across

space is greater than within any one site through time. For this reason, we subsequently discuss change in assemblage through time at each site independently.

At 528 m water depth, foraminiferal assemblages vary through time, with a notable shift occurring at 400 ybp. Diversity decreases from 400 ybp to present, which is concurrent with a decrease in oxic indicator taxa *G. subglobosa*, an increase in dysoxic indicator *U. peregrina*, and a major increase in the proportion of *B. argentea* (Figure 4).

At 800 m water depth, we do not document a significant shift in relative abundance of oxic indicators or dysoxic indicators over time, or a significant change in diversity over the interval examined (Figure 4). We interpret these assemblages to reflect environmental stability over the past 1.5ka (Figure 4). At 1175 m water depth, we document little change in relative abundance of oxic and dysoxic indicator species from 200-800 ybp. Beginning at 200 ybp, we document an increase in *B. spissa*, but no change in *U. peregrina* (Figure 4).

4 Discussion

4.1 Benthic foraminiferal assemblages across modern environmental gradient

Analysis of benthic foraminifera from two size fractions (63-150 μm and >150 μm) across a modern environmental gradient improves our understanding of benthic foraminifera as a proxy for past change. Total number of foraminifera in each size class varies with depth (Figure 2). A range of species diversity exists within the OMZ, suggesting that diversity is not driven by oxygenation alone (Figure 2).

In most cases, trends of relative abundance of benthic foraminifera across space are either similar between the complete assemblage (>63μm) and the >150 μm size fraction or trends in the >150 μm size fraction are more pronounced than in the complete assemblage (Figure 3). Trends across the OMZ gradient are similar in both size fractions (63-150 μm and >150 μm) in *G. subglobosa, Epistominella* sp., and *C.*

carinata. If one were to interpret the combined assemblage or the >150 μm assemblage in these species, the results would be similar, despite these species being higher in abundance in the small size fraction. Two species (*B. argentea* and *U. peregrina*) are present in the 63-150 μm size fraction in all sites in similar (low) relative abundance, while in the >150 μm fraction, we document distinct trends in relative abundance of these two species across space (Figure 3). This is noteworthy as it may indicate that these species are able to tolerate a range of environmental conditions, and thus are present in small numbers and small shell sizes at all sites, but that in certain environments, these species are able to thrive and out-compete other species, thus allowing them to grow to larger sizes (De Villiers, 2004; Gooday, 2003; Levin et al., 2010). This is supported by previous work showing that environmental conditions do not play a role in determining volume of benthic foraminiferal proloculus (skeletal remains of initial cell), while volume and volume to surface area ratio of adult benthic foraminifera are controlled by dissolved oxygen within low oxygen environments (Keating-Bitonti and Payne, 2018).

In the Southern California Borderlands, the disciplinary convention has largely been to focus on the >150 μm size fraction, therefore quantifying this fraction is necessary for comparison to previously published studies (Balestra et al., 2018; Cannariato and Kennett, 1999; Moffitt et al., 2014). Our findings show that spatial trends in the >150 μm size fraction generally reflect those found in the >63 μm size fraction or are muted by the inclusion of the 63-150 μm (Figure 3). Results from a similar study in the Arabian Sea OMZ showed that assemblages were similar within the 63 – 125 μm fraction and >125 μm fraction and interpretation of the larger fraction was more useful to compare results to most paleoceanographic studies (Caulle et al., 2014). Thus, we recommend that workers utilize the >150 μm size fraction for analysis when targeting indicator taxa such as *B. argentea, B. spissa, U. peregrina, G. subglobosa* or when assessing trends across the OMZ gradient. However, it is useful to quantify the complete >63μm assemblage in a subset of samples to ascertain whether there are important species or trends being missed. If the target of a project is to quantify changes in the ecology of a site or in specific metrics such as diversity, shell size, or shell weight, we recommend the inclusion of the complete assemblage (>63 μm).

We acknowledge that the identification of microfossils as a tool for paleoceanographic interpretation contains inherent uncertainty due to variability in identification of species between observers and within single observers (Al-Sabouni et al., 2018; Fox et al., 2018; Hsiang et al., 2019). Further, it has been shown that there is a correlation between size of specimen and accuracy of identification, meaning that the inclusion of the smaller specimens in the >63 μm fraction may reduce the accuracy of identification (Fox et al., 2018). Given this uncertainty, in subsequent text we focus only on spatial/environmental trends that change by a minimum of 10% relative abundance across the depth transect or through time.

In order to better compare to other similar studies from the Southern California Borderlands, for the remainder of the discussion we analyze the >150 μm fraction only. We identify two hypoxic-associated species (*B. spissa* and *U. peregrina*), one oxic-associated species (*G. subglobosa*) and one OMZ edge-associated species (*B. argentea*). These trends are shown in both the >150 μm assemblage and in the complete assemblage (>63 μm) (Figure 3). Not surprisingly, these taxa are commonly used as indicator species in previous studies (Balestra et al., 2018; Cannariato and Kennett, 1999; Moffitt et al., 2014). The species we identify as dysoxic and edge-associated (*B. spissa, U. peregrina*, and *B. argentea*) are elongated in shape and are infaunal species. In comparison, *G. subglobosa* is more abundant in higher oxygen environments and is a spherical, epifaunal species. This supports previous findings that infaunal vs. epifaunal habitat preference impacts the species distribution across the oxygenation gradient and that species in low oxygen zones have lower volume to surface area ratios relative to those in well oxygenated areas (Kaiho, 1999; Keating-Bitonti and Payne, 2016, 2018; Venturelli et al., 2018). In general, infaunal species are more common within the OMZ, while epifaunal are more common in well-oxygenated areas (Kaiho, 1999).

Previous studies have categorized benthic foraminifera into categories of oxygenation based upon similar work combining *in situ* environmental conditions and assemblage data (Cannariato and Kennett, 1999; Douglas and Heitman, 1979; Kaiho, 1994; Moffitt et al., 2014). Our findings indicate that region (or

environment) specific oxygen species associations may be necessary, as our findings do not align directly with previous categorization of species. Several species that were previously recognized as low-oxygen indicators (*B. argentea, B. spissa,* and *U. peregrina*) were found at all water depths in this study, but we find only very low abundances of two well-documented low-oxygen indicator species, *Nonionella stella* and *Bolivina tumida* (Bernhard et al., 1997; Bernhard and Gupta, 1999; Cannariato and Kennett, 1999; Moffitt et al., 2014). These taxa have documented adaptations to extreme environments; *B. tumida* is associated with methane seep environments (Hill et al., 2003) and *N. stella* is known to sequester symbionts or plastids in extreme conditions (Bernhard and Bowser, 1999). We hypothesize that the marginal environment studied here does not reach the extreme hypoxic to anoxic conditions that are suitable for *B. tumida* or *N. stella.* Several species of documented oxic indicators (*Cibicidoides* sp. and *Quinqueloculina* sp. are found across all depths (300-1175 m) and oxygenation environments (0.26-1.54 ml/L) in the San Diego margin. Many past categorizations of these species were generated using species from very low oxygen basins (e.g., Santa Barbara Basin) where seasonal anoxia is present. The presence of oxic indicator species across all water depths on the San Diego margin may provide evidence for periodic flushing of high oxygen water or a selection for species that can tolerate a range of environmental conditions rather than a specific threshold of oxygenation. Alternatively, these species may be able to tolerate lower dissolved oxygen than previously thought if other environmental conditions (including substrate) are favorable or they may be able to tolerate short periods of low oxygen conditions (Burkett et al., 2016; Keating-Bitonti and Payne, 2018; Venturelli et al., 2018) (Figure 3). Further, habitat heterogeneity, including grain size (not measured here), may play a role in the determination of species assemblages at this site, particularly in low-oxygen areas in which the nature of the sediment matrix determines oxygenation of sediment porewater (Levin et al., 2010; Venturelli et al., 2018).

We document the presence of members of the *Bolivina* genera at all water depths and in some intervals described here, bolivinids make up more than fifty percent of the total assemblage. Therefore, any changes in abundance of this genus alone can drive changes in the assemblages as a whole. Within-

species variation of morphologic traits have been correlated with affinities for certain environmental conditions (Lutze, 1964), yet congeneric gradations such as those observed here in the bolivinid genera merit further investigation. While bolivinids are widely accepted as low-oxygen dwelling species, *Bolivina argentea* specifically has been utilized as a low-oxygen indicator taxon and analysis of their abundance and distribution requires careful scrutiny (Cardich et al., 2015; Caulle et al., 2014; Mallon et al., 2012).

We identify an anomalous assemblage at 528 m water depth; this assemblage is the least diverse (H=1.316, in >150 μm size fraction). Importantly, the low diversity at this site is driven by the dominance of a single species, *B. argentea*. We observe the dominance of *B. argentea* at 528 m water depth, near the modern upper margin of the OMZ and a lower relative abundance of this species at 700 and 800 m water depth, in the heart of the OMZ (Figure 3). This pattern of *B. argentea* at high abundances near the upper margin of the OMZ has been previously observed (Douglas, 1981; Mullins et al., 1985) and these species are often used as indicators of dysoxic environments (Bernhard et al., 1997; Kaiho, 1999). We attribute some of the unexpected variability in benthic communities that does not correlate with bottom water oxygenation to "edge effects" of the OMZ. Specifically, there is more biologically available nitrate and nitrifying bacteria at the edges of the OMZ as compared to the center, and thus we expect greater nutrient concentrations and larger food availability in these zones (Mullins et al., 1985). Multiple species of benthic foraminifera respire nitrate in low oxygen environments; in particular, *B. argentea* is particularly effective in utilizing nitrate as an alternative electron acceptor and this may contribute to its dominance at the upper edge of the OMZ (Bernhard et al., 2012; Glock et al., 2019; Kuhnt et al., 2013). Additionally, seasonal or annual variability in oxygenation of the upper margin of the OMZ causing a variable oxygenation regime at 528 m may drive selection for species that can tolerate a range of environmental conditions rather than a specific threshold of oxygenation. Further, environmental and ecological factors may combine to drive assemblage diversity; the interactive effects of competition and environmental adaptation may promote habitat specialization at this water depth (Fine et al., 2004). While the sites

measured here document changes in the upper margin of the OMZ (528 m site), they may exclude the lower margin of the OMZ due to sampling depths of coring sites.

4.2 Temporal change in benthic foraminiferal assemblages record environmental change through time

Following results of analysis across modern core tops, all down core benthic foraminiferal assemblages were collected from the >150 μm size fraction. The combination of analysis from three distinct modern environments (upper margin of the OMZ (528 m), the center of the OMZ (800 m) and below the OMZ (1175 m)) allows for reconstruction of oceanographic change through the water column. We acknowledge that the environment is more variable than we can describe given the record available. Oxygenation varies on seasonal, annual, and decadal timescales - yet each interval of sediment analyzed represents >35 years, thus we are capturing a time-averaged signal. Further, several factors complicate our ability to interpret benthic assemblage records: relative preservation of various shell types, post-depositional changes in sediment, dominant fauna within some assemblages that dominate responses, and high frequency variability not captured in the record. Yet, we are still able to analyze benthic foraminiferal assemblages to identify environmental changes through the time interval described here.

Integrating analysis of cores from multiple depths reveals decadal to centennial variability in oxygenation at the upper margin of the OMZ (528 m) during the last 1.5 ka, but little to no change in the oxygenation at the center of the OMZ (800 m) or below the OMZ (1175 m) (Figure 4). The change in assemblage at 528 m beginning at 400 ybp indicates a transition to the OMZ 'edge' environment in which *B. argentea* and *U. peregrina* species dominate in the modern. The formation of an assemblage that is similar to modern at 400 ybp implies the onset of modern conditions at this site which would include relatively low oxygen with variable oxygenation on seasonal to yearly timescales. We interpret the transition in assemblage as a decrease in oxygenation at this depth and a shoaling of the upper margin of the OMZ beginning at 400 ybp and continuing to present. The combined suite of foraminiferal assemblages reveals

shoaling of the upper margin of the OMZ in the last 400 years, while the center of the OMZ and below the OMZ remained stable (Figure 4). As such, we document an expansion of the upper margin of the OMZ beginning ~ 1600 CE and continuing to the present.

Our findings are consistent with observations from other regional records of oxygenation, including those from well-resolved records in nearby basins. Santa Monica Basin (SMB) and Santa Barbara Basin (SBB) are silled basins that experience periodic flushing; changes in the strength or oxygen content of North Pacific Intermediate Water, stratification or surface productivity can lead to changes in oxygenation within each basin (Balestra et al., 2018; Cannariato and Kennett, 1999; Schimmelmann et al., 2013). Marine sediment records from Santa Monica Basin show non-annual laminations (indicating a hypoxic to anoxic environment) beginning 400 ybp and document shoaling of the low-oxygen zone within the basin from 400 ybp to present (Christensen et al., 1994). Santa Barbara Basin has well-documented sediment laminations through most of the Holocene indicating persistent low oxygen, but also shows gradual intensification of the OMZ within SBB since 1850 CE (Wang et al., 2017).

The synchronous decrease in oxygenation in Santa Monica Basin (Christensen et al., 1994) and San Diego margin (this study) from 400 ybp to present indicates that this deoxygenation is not driven by basinal changes alone; rather it is likely driven by regional scale phenomena. The decrease in oxygenation across the Southern California margin since 400 ybp could be attributed to 1) a change in oxygenation or strength of North Pacific Intermediate Water, 2) an increase in organic carbon flux from sea surface to depth driven by changes in surface productivity, or 3) decrease in bottom water mixing or ventilation as a result of changes in surface water temperatures. We note that within the San Diego margin and Santa Monica Basin records, deoxygenation trends begin ~400 ybp but continue or intensify in the last 200 years. In the last 150 years, deoxygenation is synchronous across SBB, SMB and SDM. In this interval, decreases in oxygenation may be due to an increase in organic carbon supply from terrestrial sources due to human land use change in the Southern CA region which has documented impacts on nearby benthic

ecosystems (Tomasovych and Kidwell, 2017; Wang et al., 2017). Investigation of oxygenation change over time requires further research to identify forcing mechanisms for changes in the upper margin of the OMZ and to discern the relative impact of human and natural forcing in changing oxygenation across the last few centuries.

5 Conclusions

This spatial and temporal analysis of benthic foraminifera assemblages across a modern oxygen gradient on the San Diego margin improves our understanding of the relationship between assemblages and their environment. Comparison of the relative abundance of benthic foraminifera in two size fractions (63-150 and >150 μm) across the modern OMZ shows that trends are either similar in both size fractions or are more pronounced in the larger size fraction. As a result, we conclude that analysis of the >150 μm assemblage for this site provides the most useful record for interpreting benthic foraminifera as a proxy for past change. We identify two hypoxic associated species (*B. spissa,* and *U. peregrina*), one oxic associated species (*G. subglobosa*) and one OMZ edge-associated species (*B. argentea*). Down core analysis of indicator species reveals variability in the upper margin of the OMZ while the center of the OMZ remained stable in the last 1.5ka. At 528 m, benthic foraminiferal assemblages indicate a decrease in oxygenation at this depth and a shoaling of the upper margin of the OMZ beginning at 400 ybp and continuing to present. Expansion of the upper margin of OMZ beginning 400 ybp is synchronous with regional records of oxygenation.

6 Original publication and data availability

This chapter is reproduced from the original publication: Palmer, H. M., Hill, T. M., Roopnarine, P. D., Myhre, S. E., Reyes, K. R., and Donnenfield, J. T.: Southern California margin benthic foraminiferal assemblages record recent centennial-scale changes in oxygen minimum zone, 17, 2923–2937, https://doi.org/10.5194/bg-17-2923-2020, 2020. All data collected for this paper is electronically archived by the NOAA Paleoclimatology Database as "San Diego Margin Benthic Foraminiferal Assemblages from Late Holocene" at www.ncdc.noaa.gov/paleo-search/study/28290 (Palmer et al., 2019).

7 Acknowledgements

We would like to acknowledge the San Diego Coastal Expedition team for their work in collecting the oceanographic data and sediment cores used in this study, particularly PIs Dr. Christina Frieder and Dr. Benjamin Grupe. We thank Dr. Seth Finnegan and Sara Kahanamoku for their support in microscopy and imaging. We acknowledge NSF support to T. Hill (OCE 1444451 and OCE 1832812), and Russell J. and Dorothy S. Bilinski Fellowship at Bodega Marine Laboratory, Geological Society of America Graduate Student Research Grant, Cushman Foundation for Foraminiferal Research William V. Sliter Research Award, and UC Davis Earth and Planetary Sciences Durrell Grant for support to H. Palmer.

8 Tables

Core Name	Water Depth (m)	Latitude	Longitude	Core Length (cm)	Temperature (ºC)	Dissolved Oxygen (mL/L)	pH	Salinity (psu)	Total organic matter (% wt)
MV1217-5-2	300	32.8100166	117.468100	16	8.614	1.54	7.65	34.145	6.8
MV1217-2-3	528	32.8100333	117.416583	26	6.622	0.35	7.57	34.313	11.7
MV1217-3-3	700	32.8099666	117.450966	20	5.898	0.26	7.56	34.348	13.9
MV1217-1-3	800	32.8095166	117.506933	20	5.049	0.29	7.56	34.405	14.2
MV1217-4-3/1	1175	32.6333333	117.499883	16	3.823	0.58	7.59	34.501	14.7

Table 1: Data for cores used in this study. Temperature, dissolved oxygen, pH and salinity were measured in bottom water directly above each coring site.

Core	Sample Interval	Age (^{14}C years)	±	1 Sigma Maximum Calendar Age Range	1 Sigma Minimum Calendar Age Range	Age in Calendar Years	Sedimentation Rate (cm/ka)	±
MV1217-2-3	11-12 cm	1230	30	1403	1319	1361	16.9	1.0
MV1217-2-3	16-17 cm	2085	30	602	474	538	6.1	0.2
MV1217-2-3	25-26 cm	2405	35	237	107	172	24.6	0.1
MV1217-4-3	5-6 cm	670	35	1950	1837	1893.5	42.2	11.3
MV1217-4-1	10-11 cm	960	30	1630	1518	1574	15.6	0.2
MV1217-4-1	20-21 cm	1840	35	817	698	757.5	12.3	0.4

Table 2. Radiocarbon ages of mixed planktonic foraminifera from MV1217-2-3 (528 m water depth), MV1217-4-3 (1175 m water depth) and MV1217-4-1 (1175 m water depth).

Bolivina argentea Cushman 1926. (Figure S4)
Bolivina spissa = Bolivina subadvaena Cushman var. *spissa* Cushman 1926. (Figure S4)
Bulimina spp.* (includes *Bulimina mexicana = Bulimina inflata* Seguenza var. *mexicana* Cushman, 1922 and *Bulimina exilis = Bulimina elegans* d'Orbigny var. *exilis* Brady, 1884.)
Cassidulina carinata = Cassidulina laevigata d'Orbigny var. *carinata* Silvestri, 1896. (Figure S4)
Cibicidoides sp. **
Epistominella sp. (Figure S4)
Globobulimina pacifica Cushman, 1927.
Globobulimina ovata d'Orbigny 1846.
Globocassidulina subglobosa = Cassidulina subglobosa Brady, 1881. (Figure S4)
Nonionella stella = Nonionella miocenica Cushman var. *stella* Cushman and Moyer, 1930.
Quinqueloculina sp.**
Uvigerina peregrina (Figure S4) Cushman 1923.

Table 3. Taxonomic reference list of benthic foraminifera species included in Chapter 1. * Individuals in this genus were identified to species but considered together for the interpretations of this paper. **Due to low abundance, individuals in this genus were not identified to species level.

9 Figures

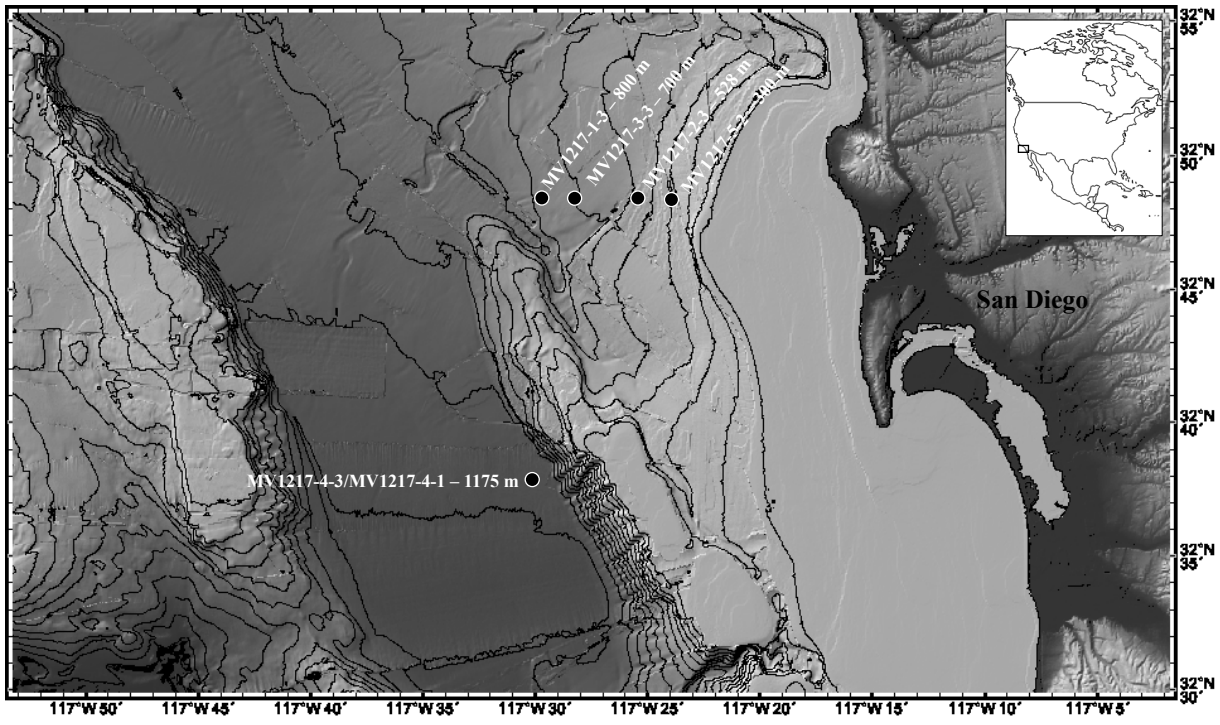

Figure 1. Map of cores used in this study. The cores were collected along a transect perpendicular to shore at the following water depths: 300, 528, 700, 800, 1175 m. Core top samples were analyzed for all cores. Cores MV1217-2-3, MV1217-1-3, and MV1217-4-3/MV1217-4-1 were analyzed down core.

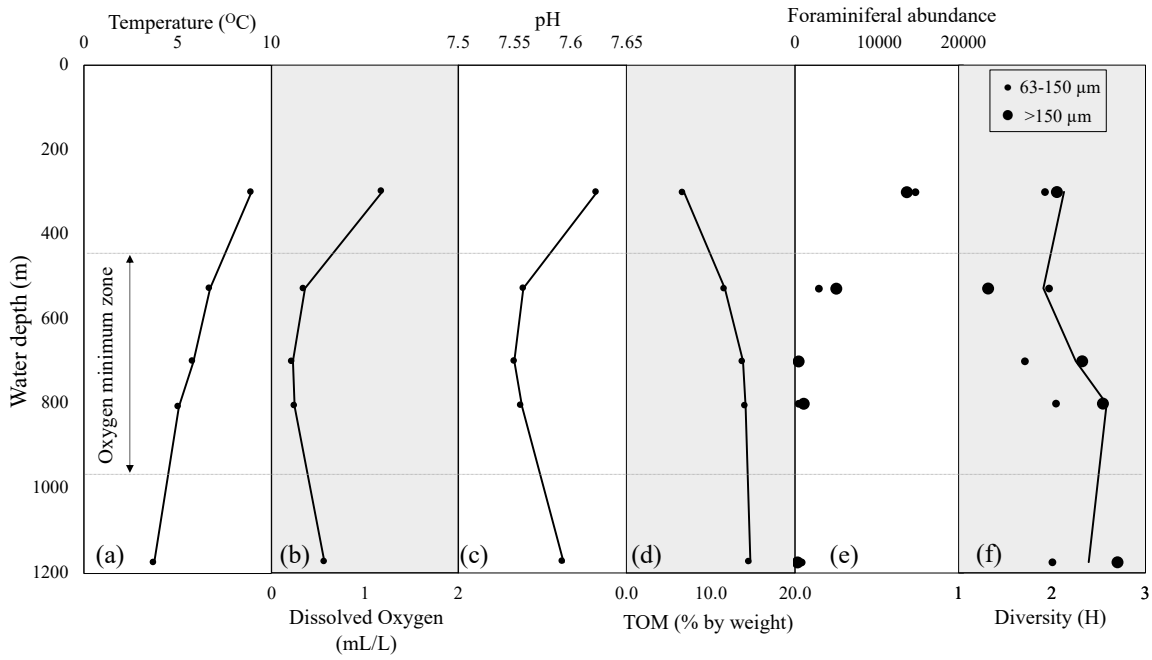

Figure 2. Profiles of temperature (a), dissolved oxygen (b), pH (c), and total organic matter (% by weight) (d) across depth transect. Foraminiferal abundance (total calcareous foraminifera) (e) and diversity (Shannon Index, H) (f) are shown for two size fractions. In panels (e) and (f), large black dots are >150 µm size fraction, small black dots are 63-150 µm and black line on diversity plot represents trends from the complete assemblage (>63 µm). Assemblage counts are standardized to the volume (63.62 cm^3) of the sampled cylinder of the sediment (core). Gray dashed line shows approximate boundaries of the oxygen minimum zone.

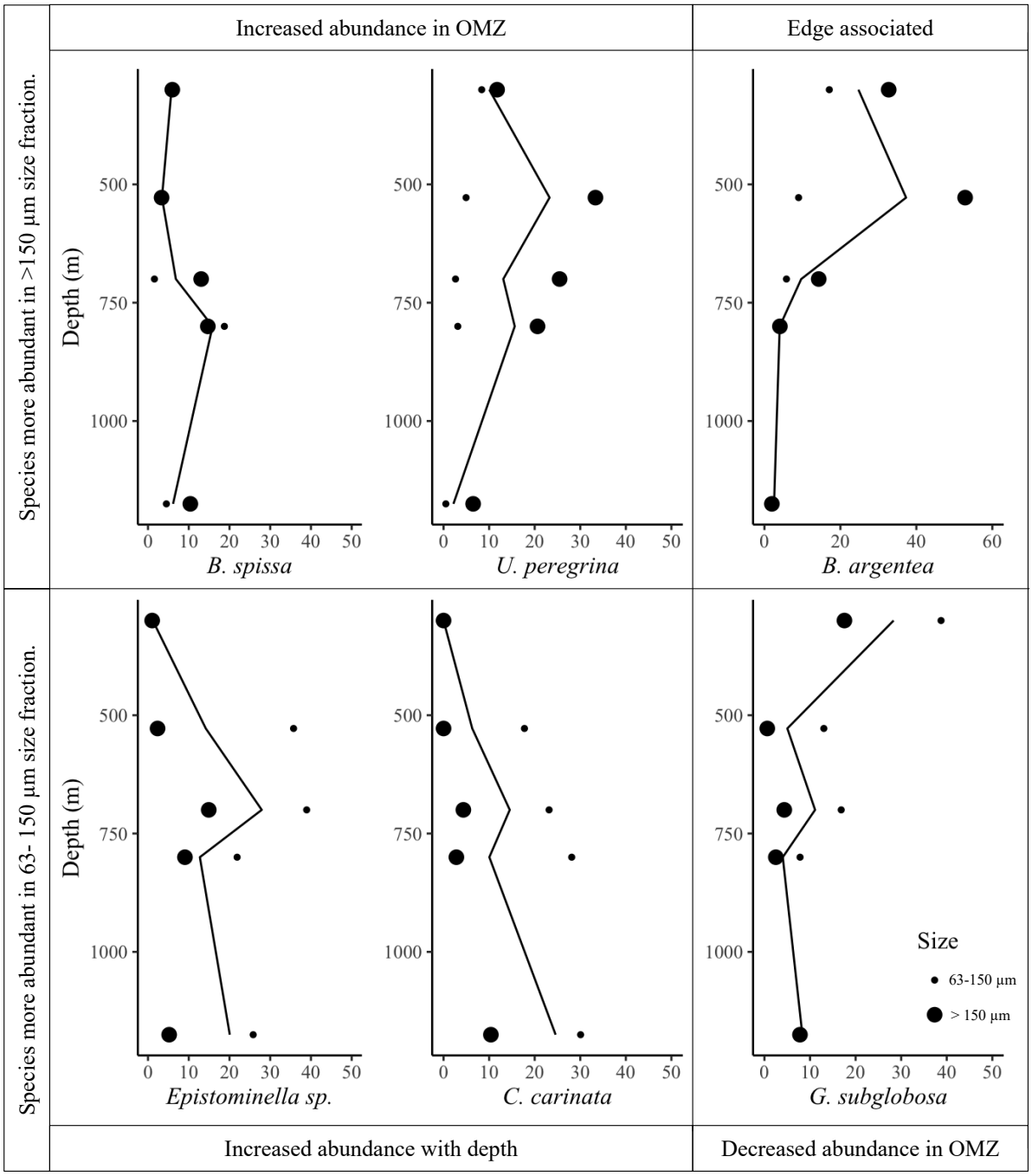

Figure 3: Relative abundance of foraminiferal species (percent of total calcareous taxa) in core top sample (0-2 cm) vs. water depth (m). Large black dots are >150 µm size fraction, small black dots are 63-150 µm size fraction and black lines represent trends considering the complete assemblage (>63 µm).

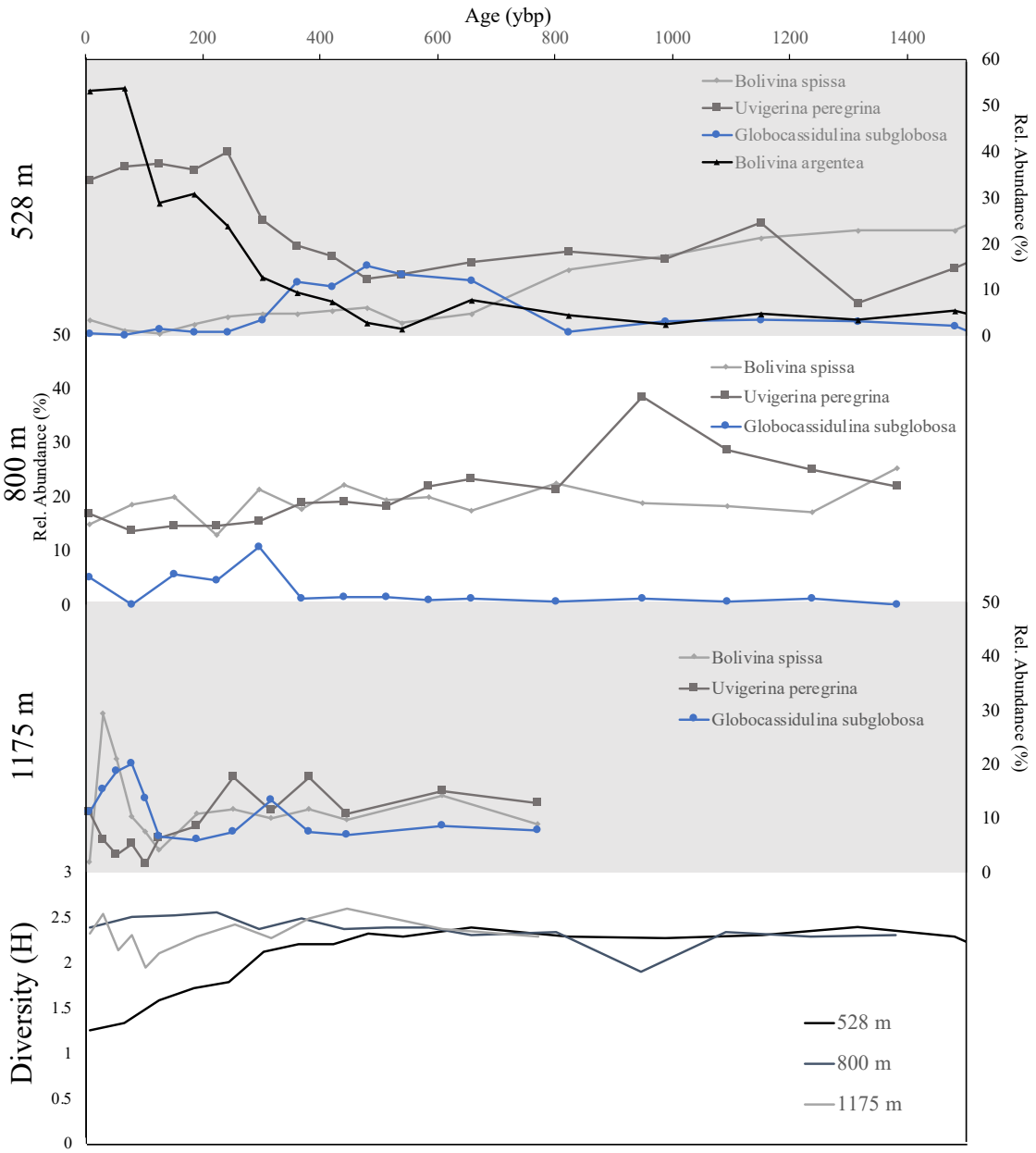

Figure 4: Top 3 panels show relative abundance of two species of hypoxia indicator foraminifera (*B. spissa* and *U. peregrina*, gray lines) and one species of oxic indicator foraminifera (*G. subglobosa*, blue lines) from the >150 µm size fraction down core through time, in years before present for cores from 3 water depths (528 m, 800 m, 1175 m). Top panel also includes relative abundance of *B. argentea* (edge-associated). Bottom panel shows diversity (Shannon's Index, H) through time for 3 cores.

10 Supplemental Figures

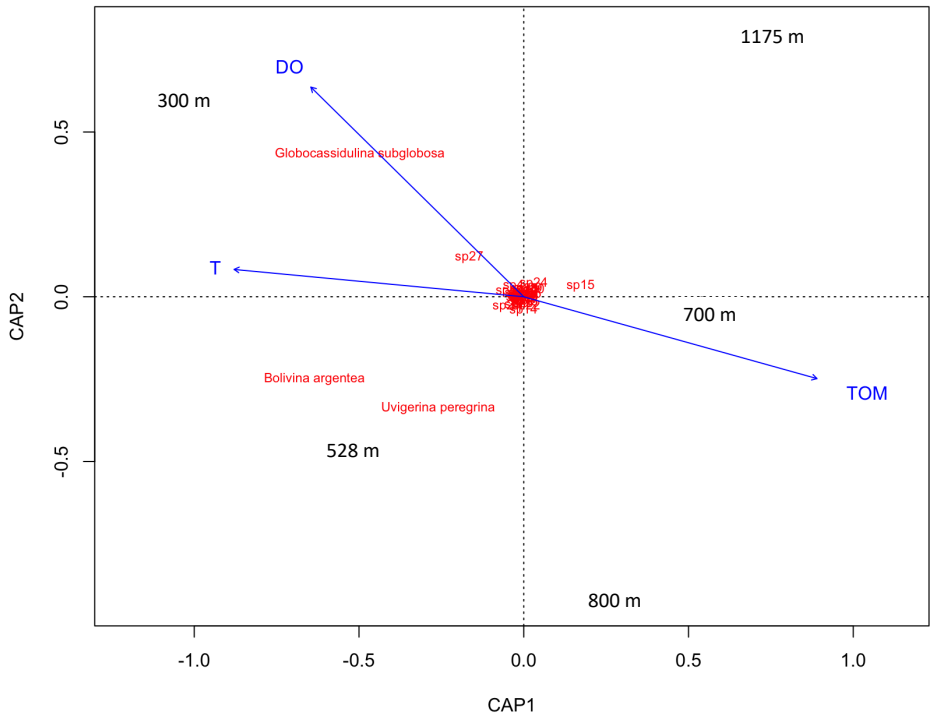

Figure S1. Distance Based Redundance Analysis of core-top benthic foraminiferal assemblages including both size fractions (>63 µm). Species are listed in red – species discussed in manuscript are labeled. Sites are listed as water depth in meters. Blue arrows show ordination of environmental factors T= temperature, DO = dissolved oxygen, TOM= total organic matter). Eigenvalues for two axes are CAP1 (0.4575) and CAP2 (0.2024).

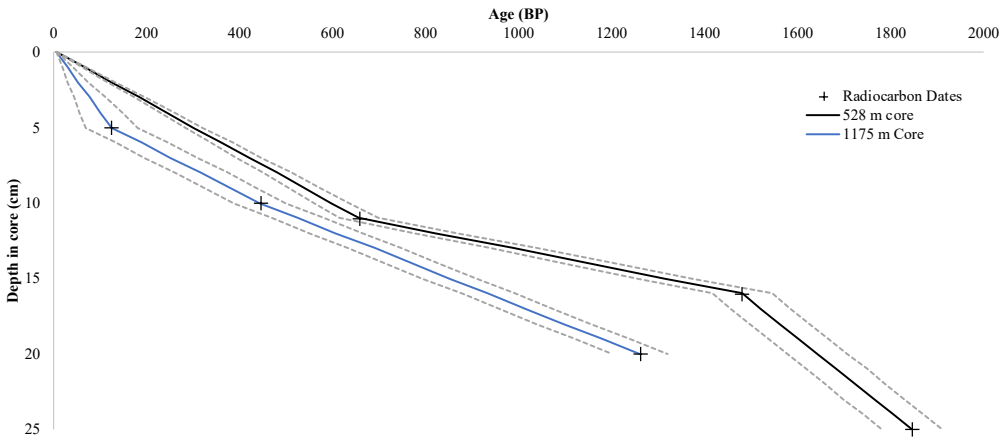

Figure S2. Age model for two cores. Age shown in years before present. Linear interpolation between radiocarbon dates (+). MV1217-2-3 (528 m water depth) is black line. MV1217-4-3 and MV1217-4-1 (1175 m) is blue line. Dashed lined represent +/- 1 sigma years.

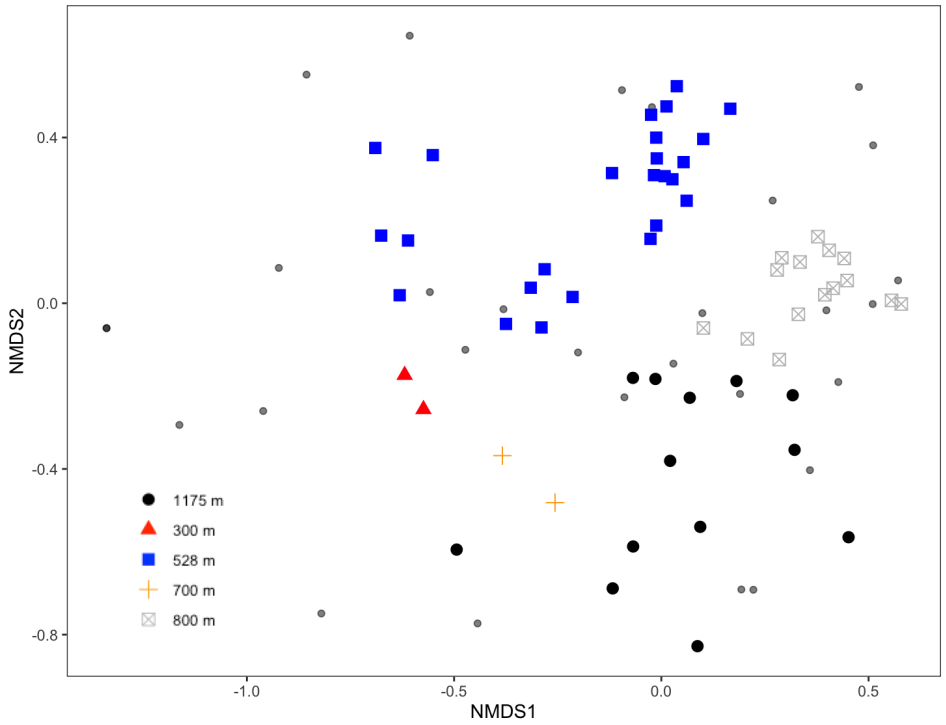

Figure S3. Non-metric multidimensional scaling plot of all benthic foraminiferal assemblages through time. Species are plotted as small gray dots. All other points represent assemblages from 1 cm intervals through time at each of the 5 cores. Legend shows which dots represent each water depth/site (Red triangle = 300 m, blue square = 528 m, orange crosshair = 700 m, Grey box with x = 800 m, black circle = 1175 m).

Figure S4: Light microscope images of benthic foraminifera (*Bolivina spissa, Uvigerina peregrina, Bolivina argentea, Epistominella* sp., *Cassidulina carinata, Globocassidulina subglobosa*) evaluated in this study. All scale bars are 100 µm.

11 References

Al-Sabouni, N., Fenton, I. S., Telford, R. J. and Kučera, M.: Reproducibility of species recognition in modern planktonic foraminifera and its implications for analyses of community structure, Journal of Micropalaeontology; Bath, 37(2), 519–534, doi:http://dx.doi.org/10.5194/jm-37-519-2018, 2018.

Bakun, A.: Climate change and ocean deoxygenation within intensified surface-driven upwelling circulations, Philos T R Soc A, 375(2102), doi:ARTN 20160327 10.1098/rsta.2016.0327, 2017.

Balestra, B., Krupinski, N. B. Q., Erohina, T., Fessenden-Rahn, J., Rahn, T. and Paytan, A.: Bottom-water oxygenation and environmental change in Santa Monica Basin, Southern California during the last 23 kyr, Palaeogeography, Palaeoclimatology, Palaeoecology, 490, 17–37, 2018.

Balmaki, B., Wigand, P. E., Frontalini, F., Shaw, T. A., Avnaim-Katav, S. and Rostami, M. A.: Late Holocene paleoenvironmental changes in the Seal Beach wetland (California, USA): A micropaleontological perspective, Quaternary International, doi:10.1016/j.quaint.2019.10.012, 2019.

Bernhard, J. M. and Bowser, S. S.: Benthic foraminifera of dysoxic sediments: chloroplast sequestration and functional morphology, Earth-Sci Rev, 46(1–4), 149–165, 1999.

Bernhard, J. M. and Gupta, B. K. S.: Foraminifera of oxygen-depleted environments, in Modern foraminifera, pp. 201–216, Springer., 1999.

Bernhard, J. M., Sen Gupta, B. K. and Borne, P. F.: Benthic foraminiferal proxy to estimate dysoxic bottom-water oxygen concentrations; Santa Barbara Basin, US Pacific continental margin, The Journal of Foraminiferal Research, 27(4), 301–310, 1997.

Bernhard, J. M., Casciotti, K. L., McIlvin, M. R., Beaudoin, D. J., Visscher, P. T. and Edgcomb, V. P.: Potential importance of physiologically diverse benthic foraminifera in sedimentary nitrate storage and respiration, Journal of Geophysical Research: Biogeosciences, 117(G3), doi:10.1029/2012JG001949, 2012.

Bograd, S. J., Castro, C. G., Di Lorenzo, E., Palacios, D. M., Bailey, H., Gilly, W. and Chavez, F. P.: Oxygen declines and the shoaling of the hypoxic boundary in the California Current, Geophysical Research Letters, 35(12), doi:Artn L12607 10.1029/2008gl034185, 2008.

Breitburg, D., Levin, L. A., Oschlies, A., Gregoire, M., Chavez, F. P., Conley, D. J., Garcon, V., Gilbert, D., Gutierrez, D., Isensee, K., Jacinto, G. S., Limburg, K. E., Montes, I., Naqvi, S. W. A., Pitcher, G. C., Rabalais, N. N., Roman, M. R., Rose, K. A., Seibel, B. A., Telszewski, M., Yasuhara, M. and Zhang, J.: Declining oxygen in the global ocean and coastal waters, Science, 359(6371), 46-+, doi:10.1126/science.aam7240, 2018.

Burkett, A. M., Rathburn, A. E., Elena Pérez, M., Levin, L. A. and Martin, J. B.: Colonization of over a thousand Cibicidoides wuellerstorfi (foraminifera: Schwager, 1866) on artificial substrates in seep and adjacent off-seep locations in dysoxic, deep-sea environments, Deep Sea Research Part I: Oceanographic Research Papers, 117, 39–50, doi:10.1016/j.dsr.2016.08.011, 2016.

Cannariato, K. G. and Kennett, J. P.: Climatically related millennial-scale fluctuations in strength of California margin oxygen-minimum zone during the past 60 k.y., Geology, 27(11), 975–978, doi:Doi 10.1130/0091-7613(1999)027<0975:Crmsfi>2.3.Co;2, 1999.

Cardich, J., Gutiérrez, D., Romero, D., Pérez, A., Quipúzcoa, L., Marquina, R., Yupanqui, W., Solís, J., Carhuapoma, W., Sifeddine, A. and Rathburn, A.: Calcareous benthic foraminifera from the upper central Peruvian margin: control of the assemblage by pore water redox and sedimentary organic matter, Marine Ecology Progress Series, 535, 63–87, doi:10.3354/meps11409, 2015.

Cardich, J., Sifeddine, A., Salvatteci, R., Romero, D., Briceño-Zuluaga, F., Graco, M., Anculle, T., Almeida, C. and Gutiérrez, D.: Multidecadal Changes in Marine Subsurface Oxygenation Off Central Peru During the Last ca. 170 Years, Front. Mar. Sci., 6, doi:10.3389/fmars.2019.00270, 2019.

Caulle, C., Koho, K. A., Mojtahid, M., Reichart, G. J. and Jorissen, F. J.: Live (Rose Bengal stained) foraminiferal faunas from the northern Arabian Sea: faunal succession within and below the OMZ, Biogeosciences, 11(4), 1155–1175, doi:10.5194/bg-11-1155-2014, 2014.
Checkley, D. M. and Barth, J. A.: Patterns and processes in the California Current System, Prog Oceanogr, 83(1–4), 49–64, doi:10.1016/j.pocean.2009.07.028, 2009.
Christensen, C. J., Gorsline, D. S., Hammond, D. E. and Lund, S. P.: Non-annual laminations and expansion of anoxic basin-floor conditions in Santa Monica Basin, California Borderland, over the past four centuries, Mar Geol, 116(3–4), 399–418, 1994.
De Villiers, S.: Optimum growth conditions as opposed to calcite saturation as a control on the calcification rate and shell-weight of marine foraminifera, Marine Biology, 144(1), 45–49, 2004.
Douglas, R.: Paleoecology of Continental Margin Basins: A modern case history from the borderland of Southern California, Depositional System of Active Continental Margin Basins- Short Course Notes, 1981.
Douglas, R. G. and Heitman, H. L.: Slope and basin benthic foraminifera of the California borderland, 1979.
Emmer, E. and Thunell, R. C.: Nitrogen isotope variations in Santa Barbara Basin sediments: Implications for denitrification in the eastern tropical North Pacific during the last 50,000 years, Paleoceanography, 15(4), 377–387, doi:Doi 10.1029/1999pa000417, 2000.
Erdem, Z. and Schönfeld, J.: Pleistocene to Holocene benthic foraminiferal assemblages from the Peruvian continental margin, Palaeontologia Electronica, doi:10.26879/764, 2017.
Erdem, Z., Schönfeld, J., Rathburn, A. E., Perez, M.-E., Cardich, J. and Glock, N.: Bottom-water deoxygenation at the Peruvian Margin during the last deglaciation recorded by benthic foraminifera, Biogeosciences Discussions, doi:https://orcid.org/0000-0002-5509-8733, 2019.
Fine, P. V. A., Mesones, I. and Coley, P. D.: Herbivores promote habitat specialization by trees in amazonian forests, Science, 305(5684), 663–665, doi:DOI 10.1126/science.1098982, 2004.
Fisler, J. and Hendy, I. L.: California Current System response to late Holocene climate cooling in southern California, Geophysical Research Letters, 35(9), doi:Artn L09702 10.1029/2008gl033902, 2008.
Fox, L., Liebrand, D., Giles Miller, C., Roseby, Z. A., Stukins, S., Taylor, B., Pearson, P. N., Wade, B. S. and Purvis, A.: Factors affecting consistency and accuracy in identifying modern macroperforate planktonic foraminifera, Journal of Micropalaeontology, 37(2), 431–443, 2018.
Friddell, J. E., Thunell, R. C., Guilderson, T. P. and Kashgarian, M.: Increased northeast Pacific climatic variability during the warm middle Holocene, Geophysical Research Letters, 30(11), 2003.
Gilly, W. F., Beman, J. M., Litvin, S. Y. and Robison, B. H.: Oceanographic and Biological Effects of Shoaling of the Oxygen Minimum Zone, Annu Rev Mar Sci, 5, 393–420, doi:10.1146/annurev-marine-120710-100849, 2013.
Glock, N., Roy, A.-S., Romero, D., Wein, T., Weissenbach, J., Revsbech, N. P., Høgslund, S., Clemens, D., Sommer, S. and Dagan, T.: Metabolic preference of nitrate over oxygen as an electron acceptor in foraminifera from the Peruvian oxygen minimum zone, PNAS, 116(8), 2860–2865, doi:10.1073/pnas.1813887116, 2019.
Gooday, A. J.: Benthic foraminifera (Protista) as tools in deep-water palaeoceanography: environmental influences on faunal characteristics, 2003.
Gooday, A. J., Bernhard, J. M., Levin, L. A. and Suhr, S. B.: Foraminifera in the Arabian Sea oxygen minimum zone and other oxygen-deficient settings: taxonomic composition, diversity, and relation to metazoan faunas, Deep Sea Research Part II: Topical Studies in Oceanography, 47(1–2), 25–54, 2000.
Grupe, B. M., Krach, M. L., Pasulka, A. L., Maloney, J. M., Levin, L. A. and Frieder, C. A.: Methane seep ecosystem functions and services from a recently discovered southern California seep, Mar Ecol-Evol Persp, 36, 91–108, doi:10.1111/maec.12243, 2015.
Helly, J. J. and Levin, L. A.: Global distribution of naturally occurring marine hypoxia on continental margins, Deep-Sea Res Pt I, 51(9), 1159–1168, doi:10.1016/j.dsr.2004.03.009, 2004.

Hendy, I. L.: The paleoclimatic response of the Southern Californian Margin to the rapid climate change of the last 60 ka: A regional overview, Quatern Int, 215(1–2), 62–73, 2010.
Hendy, I. L. and Kennett, J. P.: Dansgaard-Oeschger cycles and the California Current System: Planktonic foraminiferal response to rapid climate change in Santa Barbara Basin, Ocean Drilling Program hole 893A, Paleoceanography, 15(1), 30–42, doi:Doi 10.1029/1999pa000413, 2000.
Hill, T. M., Kennett, J. P. and Spero, H. J.: Foraminifera as indicators of methane-rich environments: a study of modern methane seeps in Santa Barbara Channel, California, Mar Micropaleontol, 49(1–2), 123–138, 2003.
Hsiang, A. Y., Brombacher, A., Rillo, M. C., Mleneck-Vautravers, M. J., Conn, S., Lordsmith, S., Jentzen, A., Henehan, M. J., Metcalfe, B., Fenton, I. S., Wade, B. S., Fox, L., Meilland, J., Davis, C. V., Baranowski, U., Groeneveld, J., Edgar, K. M., Movellan, A., Aze, T., Dowsett, H. J., Miller, C. G., Rios, N. and Hull, P. M.: Endless Forams: >34,000 Modern Planktonic Foraminiferal Images for Taxonomic Training and Automated Species Recognition Using Convolutional Neural Networks, Paleoceanography and Paleoclimatology, 34(7), 1157–1177, doi:10.1029/2019PA003612, 2019.
Ingram, B. L. and Southon, J. R.: Reservoir ages in eastern Pacific coastal and estuarine waters, Radiocarbon, 38(3), 573–582, 1996.
Jaccard, S. L., Galbraith, E. D., Frolicher, T. L. and Gruber, N.: Ocean (De)Oxygenation across the Last Deglaciation Insights for the Future, Oceanography, 27(1), 26–35, 2014.
Jorissen, F. J., de Stigter, H. C. and Widmark, J. G. V.: A conceptual model explaining benthic foraminiferal microhabitats, Marine Micropaleontology, 26(1), 3–15, doi:10.1016/0377-8398(95)00047-X, 1995.
Jorissen, F. J., Fontanier, C. and Thomas, E.: Chapter Seven Paleoceanographical Proxies Based on Deep-Sea Benthic Foraminiferal Assemblage Characteristics, in Developments in Marine Geology, vol. 1, pp. 263–325, Elsevier., 2007.
Kaiho, K.: Benthic Foraminiferal Dissolved-Oxygen Index and Dissolved-Oxygen Levels in the Modern Ocean, Geology, 22(8), 719–722, doi:Doi 10.1130/0091-7613(1994)022<0719:Bfdoia>2.3.Co;2, 1994.
Kaiho, K.: Effect of organic carbon flux and dissolved oxygen on the benthic foraminiferal oxygen index (BFOI), Mar Micropaleontol, 37(1), 67–76, doi:Doi 10.1016/S0377-8398(99)00008-0, 1999.
Keating-Bitonti, C. R. and Payne, J. L.: Physicochemical controls on biogeographic variation of benthic foraminiferal test size and shape, Paleobiology, 42(4), 595–611, 2016.
Keating-Bitonti, C. R. and Payne, J. L.: Ecophenotypic responses of benthic foraminifera to oxygen availability along an oxygen gradient in the California Borderland, Marine Ecology, 38(3), 2017.
Keating-Bitonti, C. R. and Payne, J. L.: Environmental influence on growth history in marine benthic foraminifera, Paleobiology, 44(4), 736–757, doi:10.1017/pab.2018.19, 2018.
Kuhnt, T., Friedrich, O., Schmiedl, G., Milker, Y., Mackensen, A. and Lückge, A.: Relationship between pore density in benthic foraminifera and bottom-water oxygen content, Deep Sea Research Part I: Oceanographic Research Papers, 76, 85–95, doi:10.1016/j.dsr.2012.11.013, 2013.
Levin, L. A.: Oxygen minimum zone benthos: Adaptation and community response to hypoxia, Oceanogr Mar Biol, 41, 1–45, 2003.
Levin, L. A. and Dayton, P. K.: Ecological theory and continental margins: where shallow meets deep, Trends Ecol Evol, 24(11), 606–617, doi:10.1016/j.tree.2009.04.012, 2009.
Levin, L. A., Ekau, W., Gooday, A. J., Jorissen, F., Middelburg, J. J., Naqvi, S. W. A., Neira, C., Rabalais, N. N. and Zhang, J.: Effects of natural and human-induced hypoxia on coastal benthos, Biogeosciences, 6(10), 2063–2098, doi:10.5194/bg-6-2063-2009, 2009.
Levin, L. A., Sibuet, M., Gooday, A. J., Smith, C. R. and Vanreusel, A.: The roles of habitat heterogeneity in generating and maintaining biodiversity on continental margins: an introduction, Mar Ecol-Evol Persp, 31(1), 1–5, doi:DOI 10.1111/j.1439-0485.2009.00358.x, 2010.
Lutze, G. F.: Statistical Investigations of the variability of Bolivina argentea Cushman, Contributions from te Cushman Foundation for Foraminiferal Research, XV(3), 1964.

Mallon, J., Glock, N. and Schönfeld, J.: The Response of Benthic Foraminifera to Low-Oxygen Conditions of the Peruvian Oxygen Minimum Zone, in Anoxia: Evidence for Eukaryote Survival and Paleontological Strategies, edited by A. V. Altenbach, J. M. Bernhard, and J. Seckbach, pp. 305–321, Springer Netherlands, Dordrecht., 2012.

Mazumder, A. and Nigam, R.: Bathymetric preference of four major genera of rectilinear benthic foraminifera within oxygen minimum zone in Arabian Sea off central west coast of India, J Earth Syst Sci, 123(3), 633–639, doi:10.1007/s12040-014-0419-y, 2014.

McGann, M.: Historical and modern distributions of benthic foraminifers on the continental shelf of Monterey Bay, California, Mar Geol, 181(1–3), 115–156, doi:Pii S0025-3227(01)00264-X Doi 10.1016/S0025-3227(01)00264-X, 2002.

Moffitt, S. E., Hill, T. M., Ohkushi, K., Kennett, J. P. and Behl, R. J.: Vertical oxygen minimum zone oscillations since 20 ka in Santa Barbara Basin: A benthic foraminiferal community perspective, Paleoceanography, 29(1), 44–57, doi:10.1002/2013pa002483, 2014.

Moffitt, S. E., Moffitt, R. A., Sauthoff, W., Davis, C. V., Hewett, K. and Hill, T. M.: Paleoceanographic insights on recent oxygen minimum zone expansion: lessons for modern oceanography, PLoS One, 10(1), e0115246, doi:10.1371/journal.pone.0115246, 2015a.

Moffitt, S. E., Hill, T. M., Roopnarine, P. D. and Kennett, J. P.: Response of seafloor ecosystems to abrupt global climate change, P Natl Acad Sci USA, 112(15), 4684–4689, doi:10.1073/pnas.1417130112, 2015b.

Mullins, H. T., Thompson, J. B., Mcdougall, K. and Vercoutere, T. L.: Oxygen-Minimum Zone Edge Effects - Evidence from the Central California Coastal Upwelling System, Geology, 13(7), 491–494, doi:Doi 10.1130/0091-7613(1985)13<491:Ozeeef>2.0.Co;2, 1985.

Myhre, S. E., Kroeker, K. J., Hill, T. M., Roopnarine, P. and Kennett, J. P.: Community benthic paleoecology from high-resolution climate records: Mollusca and foraminifera in post-glacial environments of the California margin, Quaternary Sci Rev, 155, 179–197, doi:10.1016/j.quascirev.2016.11.009, 2017.

Nam, S., Takeshita, Y., Frieder, C. A., Martz, T. and Ballard, J.: Seasonal advection of Pacific Equatorial Water alters oxygen and pH in the Southern California Bight, J Geophys Res-Oceans, 120(8), 5387–5399, doi:10.1002/2015jc010859, 2015.

Ohkushi, K., Kennett, J. P., Zeleski, C. M., Moffitt, S. E., Hill, T. M., Robert, C., Beaufort, L. and Behl, R. J.: Quantified intermediate water oxygenation history of the NE Pacific: A new benthic foraminiferal record from Santa Barbara basin, Paleoceanography, 28(3), 453–467, doi:10.1002/palo.20043, 2013.

Oksanen, J., Blanchet, F. G., Kindt, R., Legendre, P., Minchin, P. R., O'hara, R. B., Simpson, G. L., Solymos, P., Stevens, M. H. H. and Wagner, H.: Package 'vegan,' Community ecology package, version, 2(9), 2013.

Palmer, H.M.; Hill, T.M.; Myhre, S.E.; Roopnarine, P.R.; Reyes, K.R.; Donnenfield, J.T.: San Diego Margin Benthic Foraminiferal Assemblages from Late Holocene. NOAA Paleoclimate Database. https://www.ncdc.noaa.gov/paleo-search/study/28290, 201

Peet, R. K.: The measurement of species diversity, Annual review of ecology and systematics, 5(1), 285–307, 1974.

Rathburn, A. E., Willingham, J., Ziebis, W., Burkett, A. M. and Corliss, B. H.: A New biological proxy for deep-sea paleo-oxygen: Pores of epifaunal benthic foraminifera, Sci Rep, 8(1), 9456, doi:10.1038/s41598-018-27793-4, 2018.

Roark, E. B., Ingram, B. L., Southon, J. and Kennett, J. P.: Holocene foraminiferal radiocarbon record of paleocirculation in the Santa Barbara Basin, Geology, 31(4), 379–382, doi:Doi 10.1130/0091-7613(2003)031<0379:Hfrrop>2.0.Co;2, 2003.

Schimmelmann, A., Hendy, I. L., Dunn, L., Pak, D. K. and Lange, C. B.: Revised similar to 2000-year chronostratigraphy of partially varved marine sediment in Santa Barbara Basin, California, Gff, 135(3–4), 258–264, doi:10.1080/11035897.2013.773066, 2013.

Schmidtko, S., Stramma, L. and Visbeck, M.: Decline in global oceanic oxygen content during the past five decades, Nature, 542(7641), 335-+, doi:10.1038/nature21399, 2017.
Setoyama, E. and Kaminski, M.: Neogene Benthic Foraminifera from the southern Bering Sea (IODP Expedition 323), Palaeontologia Electronica, doi:10.26879/462, 2015.
Shibahara, A., Ohkushi, K., Kennett, J. P. and Ikehara, K.: Late Quaternary changes in intermediate water oxygenation and oxygen minimum zone, northern Japan: A benthic foraminiferal perspective, Paleoceanography, 22(3), doi:Artn Pa3213 10.1029/2005pa001234, 2007.
Stott, L. D., Neumann, M. and Hammond, D.: Intermediate water ventilation on the northeastern Pacific margin during the late Pleistocene inferred from benthic foraminiferal delta C-13, Paleoceanography, 15(2), 161–169, doi:Doi 10.1029/1999pa000375, 2000.
Stramma, L., Johnson, G. C., Firing, E. and Schmidtko, S.: Eastern Pacific oxygen minimum zones: Supply paths and multidecadal changes, Journal of Geophysical Research: Oceans, 115(C9), 2010.
Stuiver, M. and Polach, H. A.: Discussion reporting of 14 C data, Radiocarbon, 19(3), 355–363, 1977.
Takeshita, Y., Frieder, C. A., Martz, T. R., Ballard, J. R., Feely, R. A., Kram, S., Nam, S., Navarro, M. O., Price, N. N. and Smith, J. E.: Including high-frequency variability in coastal ocean acidification projections, Biogeosciences, 12(19), 5853–5870, 2015.
Taylor, M. A., Hendy, I. L. and Pak, D. K.: The California Current System as a transmitter of millennial scale climate change on the northeastern Pacific margin from 10 to 50 ka, Paleoceanography, 30(9), 1168–1182, doi:10.1002/2014pa002738, 2015.
Tetard, M., Licari, L. and Beaufort, L.: Oxygen history off Baja California over the last 80 kyr: A new foraminiferal-based record, Paleoceanography, 32(3), 246–264, doi:10.1002/2016PA003034, 2017.
Tomasovych, A. and Kidwell, S. M.: Nineteenth-century collapse of a benthic marine ecosystem on the open continental shelf, P Roy Soc B-Biol Sci, 284(1856), doi:ARTN 20170328 10.1098/rspb.2017.0328, 2017.
Venturelli, R. A., Rathburn, A., Burkett, A. and Ziebis, W.: Epifaunal Foraminifera in an Infaunal World: Insights Into the Influence of Heterogeneity on the Benthic Ecology of Oxygen-Poor, Deep-Sea Habitats, Frontiers in Marine Science, 5, 344, 2018.
Wang, Y., Hendy, I. and Napier, T. J.: Climate and Anthropogenic Controls of Coastal Deoxygenation on Interannual to Centennial Timescales, Geophysical Research Letters, 2017.

Chapter 2

Oxygenation of offshore Southern California marine basins through the Holocene

Abstract

In the face of global marine deoxygenation, understanding the timescales and drivers of past oxygenation change is of critical importance. Marine sediment cores from tiered silled basins, such as the Southern California Borderlands, provide a natural laboratory in which we can constrain timing and implications of changes in oxygenation and ventilation across multiple depths. Benthic foraminiferal assemblages can be utilized as a proxy for past change using known environmental associations, including oxygen affinity, and examined ecologically in conjunction with geochemical environmental reconstructions. Here, we quantified benthic foraminiferal assemblages in three sediment cores, EW 9504-09PC (Tanner Basin, 1194 m water depth), EW 9504-08PC (San Nicolas Basin, 1442 m water depth), and EW 9504-05PC (San Clemente Basin, 1818 m water depth) to assess changes in oxygenation over time in each basin and across the Southern California Borderlands. We also generate new, higher resolution carbon and oxygen isotope records from planktonic foraminifera *Globigerina bulloides* and benthic foraminifera *Cibicides mckannai* from Tanner Basin. We combine analysis of indicator taxa, community ecological metrics, and an oxygenation transfer function to reconstruct past environmental conditions using benthic foraminiferal assemblages. Early to mid-Holocene (11.2-4.7 ka) assemblage records from San Clemente Basin (1815 m) and San Nicolas Basin (1442 m) indicate oxygenation below 1400 m was constant in the Southern CA Borderlands and likely driven by a consistent source of intermediate waters. In the mid to late Holocene, San Nicolas experienced a multi-centennial oxygenation episode from 4.7-4.2 ka and oxygenation increased in Tanner Basin (1194 m) gradually from 5.5-1.9 ka. Ventilation and oxygenation of these offshore basins is synchronous with an increase in oxygenation in Santa Barbara Basin beginning around 6 ka and may be due to the increasing oxygenation of North Pacific Intermediate Water. Yet across all three depths and time intervals studied, the seafloor environment is consistently within a range of

intermediate hypoxia, from 0.5-1.5 ml L^{-1} [O_2], indicating stability in the environment through time. Reconstructed Holocene-scale changes in marine oxygenation below 1000 m are within the range of modern decadal variability and exhibit reduced variability relative to shallower basins.

1. Introduction

1.1 Marine oxygenation in the past and present

At present, global marine oxygenation is declining due to anthropogenic climate change, with important implications for benthic and pelagic ecosystems (Schmidtko et al., 2017; Breitburg et al., 2018; Oschlies et al., 2018). Ocean oxygenation, particularly at depth, is an important driver of ecosystem zonation, and expansion of oxygen minimum zones (OMZ) is a current threat to global marine ecosystems (Helly and Levin, 2004; Stramma et al., 2010b; Breitburg et al., 2018). Deoxygenation at depth can be driven by several processes: increased export of organic matter from surface to depth leading to increased respiration below the photic zone, increased stratification (often due to surface warming) reducing ventilation at depth, warming surface temperatures reducing rates of diffusion of atmospheric oxygen into surface waters, and changes in the source, current velocity, or oxygenation of intermediate waters (Levin et al., 2009; Stramma et al., 2010b; Oschlies et al., 2018).

Understanding drivers and timescales of changes to marine oxygenation is critical for understanding and predicting future change (Jaccard et al., 2014). Paleorecords provide an important archive to investigate temporal and spatial scales of changes to marine oxygenation. In general, warm intervals during the late Quaternary are associated with decreased global ocean oxygenation and cool intervals are associated with increased oxygenation (Cannariato and Kennett, 1999; Jaccard et al., 2014; Praetorius et al., 2015; Cardich et al., 2019; Erdem et al., 2019). The Holocene is an ideal epoch to investigate changes in marine oxygenation because it has well documented intervals of oceanographic change and provides an opportunity to investigate ecological response to stress, including changes to temperature, oxygenation, carbon cycling and ocean circulation (Barron et al., 2003; Fisler and Hendy, 2008; Moffitt et al., 2015;

Praetorius et al., 2015; Addison et al., 2017). Significant work has documented paleoceanographic change over millennial timescales in coastal basins and within the bounds of the modern OMZ (Cannariato and Kennett, 1999; Moffitt et al., 2014; Taylor et al., 2015; Balestra et al., 2018), yet additional work is needed to constrain the timing and extent of oxygenation change below 1000 m, the relative impacts of surface processes and source waters on seafloor oxygenation, and how oxygenation at these depths responds to global and regional environmental change.

1.2 Southern California modern and paleoceanography

In the modern Northeast Pacific eastern boundary upwelling system, an OMZ exists at approximately 500 – 1000 m water depth and is an important driver of ecosystem zonation (Helly and Levin, 2004; Stramma et al., 2010a). The combination of high productivity, high export of organic matter, and the age of water masses entering the North Pacific at depth make this a particularly thick and laterally extensive OMZ (Bograd et al., 2008, 2019; Evans et al., 2020). The California Margin OMZ is expanding in intensity (decreases in dissolved oxygen), horizontal extent, and vertical thickness (shoaling) (Stramma et al., 2010a; Schmidtko et al., 2017) due to reduction in oxygenation of source water and decreased vertical ventilation due to surface warming and stratification (Bograd et al., 2008; Evans et al., 2020). Off the coast of California, dissolved oxygen decreased at a rate of up to 2.1 μmol/kg/year from 1984-2006 in the upper 500 m of the water column and continues to decrease (Bograd et al., 2008), and 81% of deoxygenation in the Southern California Current System observed from 1993-2018 can be attributed to changes in oxygenation of source waters even within the upper 400 m of the water column (Evans et al., 2020).

In the modern system, Southern California Borderlands surface water flow is driven by the southward flowing California Current and the Southern California Eddy that moves water northward via the California Countercurrent and Davidson Current. At depth, the California Undercurrent flows south to north and is comprised of a mix of Southern Component Intermediate Water from the eastern tropical

Pacific and northerly sourced North Pacific Intermediate Water (Talley, 1993; Stott et al., 2000; Checkley and Barth, 2009; Balestra et al., 2018; Bograd et al., 2019). Offshore Southern California, a series of submarine basins, generally deepening from north to south, structure intermediate and deep-water flow (Berelson, 1991; Berelson and Stott, 2003). Oxygenation in basinal environments such as these is impacted by the export of organic matter from overlying surface waters, advection of intermediate and deep waters that spill into the basin, and within basin processes, including sediment and pelagic biogeochemical cycles.

The California margin OMZ fluctuated throughout the Holocene (Christensen et al., 1994; McGann, 2011; Moffitt et al., 2014; Balestra et al., 2018; Palmer et al., 2020). Previous analyses of marine sediment cores from the Santa Barbara Basin (SBB) document intervals of hypoxia in the early Holocene (11.5-10 ka) followed by oscillations in the strength of the OMZ from 10-6 ka with several intervals of hypoxia (less than 0.5 ml L^{-1} [O_2]) and an increase in oxygenation in the last 6 ka within SBB (Ohkushi et al., 2013; Moffitt et al., 2014; Wang et al., 2020). In Santa Monica Basin (SMB), severe hypoxia (less than 0.3 ml L^{-1} [O_2]) was present from the start of the Holocene to 9 ka, and the mid to late Holocene (9-0 ka) had weaker hypoxia (0.3-1.5 ml L^{-1} [O_2]) than the early Holocene (Balestra et al., 2018). The modern OMZ developed in the mid to late Holocene (by 6-4 ka) across the broader North Pacific (McGann, 2011; Ohkushi et al., 2013; Praetorius et al., 2015; Addison et al., 2017). Previous analysis of ecosystem responses (benthic foraminiferal and invertebrate) to change through the Holocene from SBB indicate that intervals within the Holocene exhibit distinct phases of ecosystems that do not repeat or overlap, as the oxygen minimum zone and carbon maximum zone fluctuate (Moffitt et al., 2015; Myhre et al., 2017).

Here, we utilize records from three offshore basins to constrain changes in ocean oxygenation through the Holocene and resultant impacts on benthic ecosystems. Silled basins provide a unique opportunity to examine both local changes within each basin and to compare oxygenation history across depths when records overlap temporally. Combining a series of silled basins allows for the examination of change

through time at multiple water depths and sill depths to investigate the relative impact of surface processes and intermediate water changes in determining oxygenation at depth (Moffitt et al., 2014; Balestra et al., 2018; Wang et al., 2020).

1.3 Benthic foraminiferal assemblages as a metric of past oxygenation and organic matter export

Benthic foraminiferal assemblages are an effective and established metric to quantify past changes in marine oxygenation (Kaiho, 1994; Bernhard and Gupta, 1999; Murgese and De Deckker, 2005; De and Gupta, 2010; Ohkushi et al., 2013; Caulle et al., 2014; Moffitt et al., 2014; Cardich et al., 2015, 2019; Praetorius et al., 2015; Balestra et al., 2018; Belanger et al., 2020). Benthic foraminiferal assemblages are sensitive to changes in oxygenation in the North Pacific, even in suboxic environments, not only across biological threshold anoxic or sulfidic conditions (Sharon et al., 2021). Multiple methodologies are used to interpret past environmental change from benthic foraminiferal assemblages, which we introduce and review below.

Quantifying absolute and relative abundance of benthic foraminiferal species is an established and foundational method; typically, studies quantify species downcore and interpret trends through time using observational or statistical approaches (e.g. Moffitt et al., 2014; McGann, 2011; Gardner et al., 1988). Studies of modern benthic foraminifera from multiple depositional environments and oxygenation regimes have identified oxygenation affinity of benthic foraminiferal species that can be used as indicator species of change through time; this method is most useful to reconstruct relative oxygenation or to identify past oxygenation thresholds (e.g. Cannariato and Kennett, 1999; Palmer et al., 2020; Balestra et al., 2018; Bernhard and Gupta, 1999).

While these approaches provide relative oxygenation history, transfer functions are used to translate whole or partial benthic species assemblages into absolute oxygenation values (Kaiho, 1994, 1999; Behl and Kennett, 1996; McGann, 2011; Ohkushi et al., 2013; Moffitt et al., 2014; Sharon et al., 2021). Multi-

species transfer functions including the Kaiho Benthic Foraminiferal Oxygenation Index, Behl Dissolved Oxygen Index, Schmidel Dissolved Oxygen Index, and Sharon-Behl Dissolved Oxygen Index are used to generate absolute values of past oxygenation by transforming the relative abundance of species into ml L^{-1} [O_2] (Kaiho, 1994; Ohkushi et al., 2013; Sharon et al., 2021). Transfer functions have typically been constructed using case studies from very low oxygen environments (such as Santa Barbara Basin) or by using the lowest known oxygen tolerance for a species (Kaiho, 1994; Ohkushi et al., 2013; Sharon et al., 2021). This approach generates inherently conservative predictions of oxygenation. Categorization of species into oxic, intermediate hypoxic, and anoxic environments used in both transfer functions and as indicator species varies by author (Kaiho, 1994; Cannariato and Kennett, 1999; Moffitt et al., 2014; Praetorius et al., 2015; Palmer et al., 2020). Here we follow the convention: oxic ([O_2] >1.5 ml L^{-1}), intermediate hypoxic/suboxic ([O_2] 1.5-0.5 ml L^{-1}), and severe hypoxic/dysoxic ([O_2] <0.5 ml L^{-1}) (Moffitt et al., 2014; Palmer et al., 2020; Tetard et al., 2021).

Recent work on paleoecological assemblages, including benthic foraminiferal assemblages, incorporating methodology from community ecology, including analysis of diversity, richness, and multidimensional statistical analysis, has expanded our breadth of understanding of how oxygenation impacts seafloor ecosystems (Myhre et al., 2017; Belanger et al., 2020; Sharon et al., 2021). Ecological analysis provides community-scale assessments of environmental change over time and often complements analysis of indicator taxa or transfer function calculations (Myhre et al., 2017; Belanger et al., 2020; Sharon et al., 2021). In addition to taxonomic evaluation of benthic foraminifera, studies are increasingly relying on morphometrics to assess past environments. These studies are predicated on biological morphological response or adaptation to oxygenation such as pore density, size, and shape (i.e., roundedness) and are used in both taxon-specific and taxon-independent analyses (Keating-Bitonti and Payne, 2016, 2018; Keating-Bitonti and Payne, 2017; Rathburn et al., 2018; Tetard et al., 2021). Typically, smaller, thin-walled, elongate species are indicative of low oxygen environments in which high-surface area to volume

ratio is advantageous to absorb oxygen and while in well oxygenated environments, larger, thick-walled and porcelaneous taxa with rounded shapes are dominant (Tetard et al., 2021).

Food availability, driven by the timing (pulsed vs. constant) and amount of export of organic matter, and water depth play an important role in structuring seafloor ecosystems, including benthic foraminiferal assemblages (Kaiho, 1999; Belanger et al., 2012, 2020; Venturelli et al., 2018). Here we employ multiple assemblage analyses to investigate cores from three silled basins in the Southern California Borderlands. By combining approaches listed above, we quantify changes in oxygenation below 1000 m, deconstruct surface vs. advective processes as drivers of change, and investigate changes in source waters. This multi-site, multi-faceted approach allows us to reconstruct change over time in each basin and to assess regional scale oxygenation and ventilation history of the Southern California Borderlands through the Holocene.

2 Methods

2.1 Study site

Cores were collected from three silled basins within the Southern California Borderlands (Figure 1). Tanner Basin is located west of the Channel Islands and is the farthest offshore. The basin has a sill depth of 1160 m and a bottom depth of approximately 1500 m (Figure 1). San Nicolas Island is located south of San Nicolas Island and west of San Clemente Island. The basin has a sill depth of 1100 m and a bottom depth of approximately 1800 m (Figure 1). San Clemente Basin is located south of San Clemente Island and is the deepest site explored here. The basin has a sill depth of 1815 m and a bottom depth of approximately 1950 m (Figure 1). The water depth of each core was assessed at time of core collection and bottom depths of each basin were measured using GeoMapApp.

2.2 Sediment cores

We investigate three piston cores collected from the Southern California Borderlands on the Maurice Ewing Cruise 9504 in May - June 1995: EW 9504-09PC from Tanner Basin at 1194 m water depth, EW

9504-08PC from San Nicolas Basin at 1442 m water depth, and EW 9504-05 from San Clemente Basin at 1818 m water depth. All cores have 10.16 cm inner diameter. Cores were split on board the ship and were sampled at 2 cm intervals. All intervals here describe sediments with initial volume of 162.15 cm^3. Sediments from the working half of the core were disaggregated in sodium hexametaphosphate washed over a 63 μm sieve (see Stott et al. 2000). Sediments were dried and stored in glass vials at the University of Southern California until they were processed for this study. EW 9504-09PC (Tanner Basin) was examined from 0-40 cm at 2 cm intervals; intervals below 40 cm were not available for analysis. EW 9504-08PC (San Nicolas Basin) was examined at 2 cm intervals from 0-22 cm and every 6 cm from 24-64 cm. EW 9504-05 (San Clemente Basin) was examined at 2 cm intervals from 30-52 cm; intervals from 0-30 cm in EW9504-05 did not have sufficient foraminifera for robust analysis (see below) and were thus excluded from analysis.

2.3 Radiocarbon dating and age model development

Radiocarbon based age models were developed for each core using a combination of previously published and newly generated planktic radiocarbon ages (Table 1, Supplemental Figure 1). Five age dates within the Holocene (1 San Clemente, 1 Tanner, 2 San Nicolas) were previously measured (Stott et al., 2000). These AMS ^{14}C ages were completed using bulk planktonic foraminifera (weight ~3-5 mg) analyzed at the Lawrence Livermore National Laboratory (Stott et al., 2000). Three additional radiocarbon dates (1 San Clemente, 2 Tanner, 1 San Nicolas) from bulk planktic foraminifera were analyzed in this study. All samples for radiocarbon analysis were prepared by picking shell material from the >150 μm fraction, rinsing shells in methanol, sonicating in methanol for 5-10 seconds, and rinsing twice with deionized water. Shells were then dried in a $60^{O}C$ drying oven. Radiocarbon analysis was completed at the Lawrence Livermore National Laboratory using $\delta^{13}C$ assumed values following the convention of Stuiver and Polach (1977). The reported age is given in radiocarbon years using the Libby half-life of 5568 years. The Calib7.1 calibration program was used to calibrate ages using a reservoir age of 220.0 +/- 40.0

(Stuiver and Polach, 1977; Ingram and Southon, 1996). The age model for each core was generated using liner interpolation between radiocarbon age dates (Table 1, Supplemental Figure 1).

2.4 Stable Isotope Analysis

Stable isotope analyses from planktic and benthic foraminifera from EW9504-09 (Tanner Basin) were conducted on *Globigerina bulloides* planktic foraminifera and *Cibicides mckannai* benthic foraminifera from 0-40 cm at 2 cm intervals. Samples were prepared by picking from the >150 μm size fraction (2-5 individual *C. mckannai* per interval, 15-25 *G. bulloides* per interval), rinsing in methanol, sonicating in methanol for 5-10 seconds, and rinsing twice with deionized water. Planktic foraminifera were analyzed for $\delta^{18}O$ and $\delta^{13}C$ at the UC Davis Stable Isotope Laboratory and benthic foraminifera were analyzed at the UC Santa Cruz Stable Isotope Laboratory.

Planktic carbon and oxygen isotope samples were analyzed using a GasBench II system interfaced with a Delta V Plus Isotope Ratio Mass Spectrometer at the UC Davis Stable Isotope Laboratory using standard UCD-SM92 (-1.94 for $\delta^{18}O$ and 2.08‰ $\delta^{13}C$) (Ostermann 2000). Values for $\delta^{13}C$ and $\delta^{18}O$ are expressed in per mil (‰) relative to Vienna Pee Dee Belemnite, and values are corrected for changes in linearity and instrumental drift. Benthic carbon and oxygen isotope samples were analyzed at the UC Santa Cruz Stable Isotope Laboratory by acid digestion using an individual vial acid drop Themo Scientific Kiel IV carbonate device interfaced to Thermo Scientific MAT 253 dual-inlet isotope ratio mass spectrometer (iRMS). All samples were measured with several replicates of the externally calibrated Carrera Marble in-house standard reference material 'CM12' and the NBS-18 limestone international standard reference material. Values for $\delta^{13}C$ and $\delta^{18}O$ are expressed in per mil (‰) relative to Vienna Pee Dee Belemnite, and values are corrected for changes in linearity and instrumental drift. Data were combined with previously published records of planktic oxygen isotopes and benthic oxygen and carbon isotopes from the same core examined here (EW9504-09) to increase replicates in the late Holocene and to extend the

record through the entire Holocene (Stott et al., 2000). As such, isotope records reflect analyses from three different laboratories.

2.5 Benthic Foraminiferal Assemblages

Samples were dry sieved over a 150 μm sieve and picked for benthic foraminiferal microfossils. Foraminifera greater than 150 μm have been documented to capture the range of environmental variability in paleoceanographic reconstructions as well as assemblages containing smaller foraminifera and the use of larger specimens results in reduced error in identification (Cannariato and Kennett, 1999; Caulle et al., 2014; Fenton et al., 2018; Palmer et al., 2020; Sharon et al., 2021). Individual foraminifera were picked and identified from each interval to obtain >100 individuals per sample (Kemp et al., 2020), yet two samples with 90 and 93 individuals available were included, as sample sizes as low as 58 have been shown to have stable assemblages (Forcino et al., 2015; Belanger et al., 2020). The average number of individual foraminifera identified in each interval was 230, with a range of 90-665. Samples were mounted on micropaleontology slides using gum tragacanth at time of identification and are archived in the Ocean Climate Laboratory at the UC Davis Bodega Marine Laboratory. Cores were not laminated; thus, bioturbation is expected and may have had an averaging effect on assemblages.

2.6 Foraminiferal morphometrics

Morphometrics of benthic foraminifera, including length, width, and surface area were measured using ImageJ software. Length and width of each individual was measured to the longest and widest margins of the shell. Three species were selected for analysis to represent a gradient of oxygenation affinity: *Quinqueloculina* sp. is weakly hypoxic to oxic and *B. spissa* and *U. peregrina* are categorized as suboxic (Supplemental Table 1). Measurements of *Quinqueloculina* sp. and *B. spissa* were quantified in Tanner Basin at 2 cm intervals from 0-40 cm, measurements of *Quinqueloculina* sp. and *U. peregrina* were quantified in San Clemente Basin at 2 cm intervals from 30-44 cm. From each interval, 5-25 individual shells were measured (based on availability of taxa). Results of morphometric analysis were compared to

morphometric data (collected using the same methodology) from five open coastal margin sites (300-1175m) near San Diego (Palmer unpublished data), see Palmer et al., 2020 for further explanation of the open margin study site.

2.7 Metazoan microfossil assemblages

In addition to picking and identifying benthic foraminifera, ostracods (Arthropoda - Ostracoda) and urchin spines (Echinodermata) were picked from the 150 μm sediment fraction at all intervals examined. Samples were mounted on micropaleontology slides using gum tragacanth at time of identification and are archived in the Ocean Climate Laboratory at the UC Davis Bodega Marine Laboratory. Due to low abundances, presence/absence is recorded, rather than relative abundance.

2.8 Benthic foraminiferal oxygenation index

Oxygenation was reconstructed using two modified benthic foraminiferal oxygenation indices: Sharon-Behl and Schmidel. Using a combination of paleo and modern samples, Sharon et al., 2021 modified the Behl Dissolved Oxygen Index to allow for the inclusion of more species, thus allowing for its application in a broader range of seafloor environments (Sharon et al., 2021). Here we further modified each by adding ten additional species to the Sharon-Behl Dissolved Oxygen Index list of species using previously published oxygenation affiliations and morphometric/taxonomic similarities (Supplemental Table 1). Oxygenation reconstructions were calculated using two equations: Sharon-Behl DO index = ((dysoxic % * 0.1) + (suboxic % * 0.5) + (weakly suboxic/oxic % * 1.5))/100 and Schmidel index = ((weakly suboxic/oxic %)/(weakly suboxic/oxic % + hypoxic %) + diversity (H`)) * 0.5 (Ohkushi et al., 2013).

2.9 Statistical analysis

Diversity of each interval of each core was calculated using Shannon Index (H). Richness was calculated by tabulating the number of distinct species present in an interval. Non-metric multidimensional scaling ordination, using square root transformation of assemblage species counts and Bray-Curtis similarities,

and cluster analysis were completed to identify relatedness between assemblages through time. All multivariate analyses were completed using the Vegan R package (Oksanen et al., 2013; Myhre et al., 2017). We used a single factor ANOVA to determine if there were significant differences among mean morphometrics (length, width, surface area) and diversity between basins. If results of ANOVA were significant, we performed Tukey's Test to determine where differences in means occurred.

2.10 Modern oxygenation data

Modern oxygen data were sourced from the California Cooperative Oceanic Fisheries Investigations for the years 1986-2019. Data were included from all sites in the CalCOFI sampling grid with oxygenation data below 1000 m to maximize data availability. Oxygenation was calculated using Winkler Titration of bottle samples at the Scripps Institution of Oceanography (Bograd and Lynn, 2003; Bograd et al., 2003).

3 Results

3.1 Age Model Development

An age model was developed for each core based on linear interpolation between radiocarbon dates. Sedimentation rates were similar between basins and remained relatively constant through the Holocene: Tanner Basin sedimentation rate was 10.7 cm/kyr from 5.5 ka-1.9 ka, San Nicolas sedimentation rate was 10.3 cm/kyr from 11.9 ka- 5.4 ka and 8.9 cm/kyr from 5.4-2.9 ka, and San Clemente sedimentation rate was 5.3 cm/kyr from 12.7-1.4 ka (see Table 1 for radiocarbon ages and error and Supplemental Figure 1). Sedimentation rate decreased with water depth, as expected. Coherence of age model within each core and between cores supports use of this age model (Supplemental Figure 1). All following results will be discussed as age in thousands of years before present (ka).

3.2 Stable isotope record

Stable isotope records from Tanner Basin varied slightly through time (Figure 3). Analysis of planktic oxygen and carbon isotopes from *G. bulloides* yielded the following: $\delta^{13}C$ mean is -0.59 ($\pm$ 1σ = 0.25),

range -0.92 to -0.05, $\delta^{18}O$ mean is 0.22 (± 1σ = 0.31), range is -0.15 to 1.08 (Figure 3). Analysis of benthic oxygen and carbon isotopes from *C. mckannai* yielded the following: $\delta^{13}C$ mean is -0.03 (± 1σ =0.07), range -0.13 to 0.10, $\delta^{18}O$ mean is 2.53 (± 1σ = 0.17), range is 2.29 to 2.73 (Figure 3).

3.3 Benthic foraminiferal assemblages

Benthic foraminiferal assemblages were quantified down core on each core in which sufficient benthic foraminifera were present (Tanner Basin 0-40 cm at 2 cm intervals, San Nicolas Basin 0-22 cm at 2 cm intervals, 24-66 at 6 cm intervals, San Clemente Basin 30-54 cm at 2 cm intervals). The total number of species (richness) in each sample ranged from 15 to 24 and species diversity (Shannon Index, H) ranged from 2.12 to 2.68, with a mean of 2.40 (± 1σ = 0.15) across all three basins. Species diversity (H) is significantly higher in Tanner Basin (mean=2.51, ± 0.11), relative to San Nicolas Basin (mean=2.30, ± 1σ = 0.11) and San Clemente Basin (mean=2.37, ± 1σ = 0.10) (ANOVA, Tukey Test $p<0.05$) (Supplemental Figure 4). Comparison of diversity through time in individual basins using 0.5 or 1 ka time bins shows that diversity (H) is not statistically different through time in Tanner ($p>0.05$), San Nicolas ($p>0.05$), and San Clemente ($p>0.05$) basins. Multivariate statistical analysis (using nonmetric multidimensional scaling) of down-core assemblages shows that, through time, assemblage similarity within sites exceeds similarity to assemblages at any other site (Supplemental Figure 2).

In Tanner Basin, the most common species (in descending order) are *B. spissa, G. subglobosa, H. soldanii, Quinqueloculina* sp., and *P. murrhina* (Figure 2). Species diversity (H) ranged from 2.12-2.68 with a mean of 2.51 (± 1σ = 0.11) (Supplemental Figure 4); diversity did not change significantly through time when considered at 0.5 or 1 ka time intervals (ANOVA, $p>0.05$). The benthic foraminiferal assemblage gradually changed from 5.5 – 1.9 ka. Cluster analysis with 50% similarity identifies two cohorts of benthic assemblages in Tanner Basin separated in time from 5.5 – 4.0 ka and 4.0 – 1.9 ka (Supplemental Figure 2). Comparison of NMDS with cluster analysis and individual species plot shows this shift is largely driven by a gradual increase in *Hansenisca soldanii* (previously *Gyroidina soldanii*)

and decrease in *B. spissa* and *U. peregrina* from 5.5 to 1.9 ka (Figure 2 and Supplemental Figure 2). *G. subglobosa* and *Quinqueloculina* sp consistently make up 10-20% of the assemblage through time (Figure 2).

In San Nicolas Basin, the most common species (in descending order) are *U. peregrina, E. pacifica, C. mckannai, B. spissa,* and *Uvigerina* sp (Figure 2). Species diversity (H) ranges from 2.12-2.56 with a mean of 2.30 (± 0.11) (Supplemental Figure 4); diversity did not change significantly through time when considered at 0.5 or 1 ka time intervals (ANOVA, $p>0.05$). The assemblage in San Nicolas Basin exhibits little change through time from 10.1-4.7 ka, and *U. peregrina* makes up 15-45% of the assemblage at this time. From 4.7-4.2 ka, there is a sharp decline in *U. peregrina* and a sharp increase in *C. mckannai* (Figure 2). From 4.0-1.9 ka, the trend reverses, and the assemblage is very similar to the assemblage from 10.1-4.7 ka. NMDS and cluster analysis (with 50% similarity) identify an anomalous period in San Nicolas Basin from 4.7-4.2 ka that is different from the time points before and after this period (Figure 2 and Supplemental Figure 2).

In San Clemente Basin, the most common species (in descending order) are *U. peregrina, C. mckannai, E. pacifica, Quinqueloculina* sp., and *Uvigerina* sp (Figure 2). Species diversity (H) ranges from 2.17-2.51 with a mean of 2.37 (± 0.10) (Supplemental Figure 4); diversity did not change significantly through time when considered at 0.5 or 1 ka time intervals (ANOVA, $p>0.05$). In San Clemente Basin, relative abundance of benthic foraminifera exhibits little change over time from 11.2-7.1 ka as shown by both individual species analysis and NMDS. Cluster analysis shows the assemblage is 50% similar through all time intervals examined (Figure 2 and Supplemental Figure 2).

3.4 Metazoan microfossil analysis

Urchin spines and ostracods were present in the Tanner Basin core, but do not present a coeval trend; urchins are present in 13 of 19 intervals, ostracods are present in 5 of 19 samples. Urchin spines and

ostracods were scarce in sediments from San Nicolas Basin: urchin spines are present in 6 of 17 and ostracods are present in 2 of 17 intervals. Ostracods and urchin spines were nearly ubiquitous (present in every interval except one) in San Clemente Basin (Supplemental Figure 5).

3.5 Shell morphometrics

Shell size, measured as length, width, and surface area of three taxa (*U. peregrina, Quinqueloculina* sp., and *B. spissa*) was compared across the three cores examined here and compared to unpublished size data from a suite of cores from the San Diego Margin. Shell size of *U. peregrina* is statistically significantly larger in coastal sites ($p<0.05$) relative to San Clemente basin. Shell size of *B. spissa* is statistically significantly larger in coastal sites ($p<0.05$) relative to Tanner basin (Supplemental Figure 3). Shell size of *B. spissa* and *Quinqueloculina* from Tanner Basin show relatively little variability through time (5.5-1.9 ka) (Supplemental Figure 3). As all metrics of shell size (length, width, and surface area) show the same trends, further discussion uses only shell surface area as a metric of whole shell size.

3.6 Modern oxygenation in the Southern California Borderlands

Modern oxygenation decreases linearly with depth from 1000 to 2000 m in this region, from approximately 0.5 ml L^{-1} to 1.78 ml L^{-1} [O_2]. Modern values near 1194 m (depth of Tanner Basin core) are approximately 0.75 ml L^{-1} [O_2]; modern values near 1442 m (depth of San Nicolas Basin core) are approximately 1 ml L^{-1} [O_2]; modern values near 1818 m (depth of San Clemente Basin core) are approximately 1.5 ml L^{-1} [O_2] (Figure 4).

4 Discussion

4.1 Benthic foraminiferal assemblages as paleo-oxygenation proxy

By analyzing the complete assemblage from each basin, we interpret a gradual shift in relative abundance of taxa in Tanner Basin, multi-centennial shifts in the assemblage at San Nicolas Basin, and stability in the assemblage in San Clemente Basin. Examining indicator taxa, we identify a decrease in hypoxic

taxon *B. spissa* and a decrease in *U. peregrina* coeval with an increase in oxic indicator *Hansenisca* sp. in Tanner Basin from 5.5 to 1.9 ka. In San Nicolas Basin, we observe a short period of divergence from the mean assemblage driven by an increase in the oxic-associated taxon *C. mckannai* and a sharp decline in *U. peregrina* from 4.7-4.2 ka. We observe little change over time in the relative abundance of these indicator taxa in San Clemente Basin.

Reconstructed oxygen concentration differs between the two transfer functions compared here. Reconstructed dissolved oxygen using Sharon-Behl Index for all three cores yields values (0.59-1.12 ml L^{-1} [O_2]) within "intermediate hypoxia" as defined by Moffitt et al., 2014 and "suboxic" as defined by Cannariato and Kennett 1999 and Kaiho 1994. Reconstructed values using the Sharon-Behl Index are similar to the range of modern values for bottom water oxygenation with notable exceptions discussed below (Figure 4). In comparison, the Schmidel Index output is higher (1.37-1.83 ml L^{-1} [O_2]) than the Sharon-Behl Index by approximately 0.5 ml L^{-1} [O_2], and it does not capture the variability seen in the full assemblage (Supplemental Figure 4). We posit that this is due to the fact that diversity and oxygenation are not necessarily inversely correlated, particularly in intermediate hypoxia environments, yet the Schmidel Index is based on diversity. Across taxa and faunal size, diversity is typically low within oxygen minimum zones (Levin, 2003). For benthic foraminifera in dysoxic basins specifically, typically density is high, and diversity is low (Levin, 2003; Moffitt et al., 2014). Yet, other parameters such as proximity to the margin of the OMZ, sediment grain size, and organic matter availability also play important roles in structuring foraminiferal diversity. Further, oxygenation plays a more dominant role in structuring diversity across biological thresholds (such as below 0.5 ml L^{-1} [O_2]) than across oxygen gradients that do not cross biological thresholds (McGann, 2011; Venturelli et al., 2018; Palmer et al., 2020; Sharon et al., 2021). Thus, we utilize the modified Sharon-Behl Index to reconstruct absolute values of paleo-oxygenation (Figure 3).

Community-level changes are tracked by diversity and multi-dimensional community metrics. Diversity varied little between basins and through time within each basin. Shannon Index of diversity (H) ranged from 2.12 to 2.68 across all sites and points in time, and diversity did not significantly change through time at any site across this interval (ANOVA, $p>0.05$) (Supplemental Figure 4). We hypothesize that the stability in diversity indicates that environmental conditions were also relatively stable through this interval. This evidence aligns with results of oxygenation reconstruction in the suboxic/intermediate hypoxic category from the Sharon-Behl Index throughout all records examined here (Figure 3). Results of multi-dimensional analysis show species assemblages are distinct in each basin; non-metric multi-dimensional scaling and 50% similarity analysis demonstrates that at any time point, assemblages are more similar to other time points from the same basin than to any other time point from an adjacent basin (Supplemental Figure 2). This demonstrates that each basinal environment is unique and the analysis of benthic foraminifera as environmental indicators must consider local factors.

Changes in benthic foraminifera morphology can reflect environmental variations that are missed by community-based analyses. Comparison of two species (*U. peregrina*, *B. spissa*) between basins (studied here) and open margin sediments (San Diego Margin, see Palmer et al., 2020) shows that both species are larger in the nearshore environment relative to offshore basins (Supplemental Figure 3). At this scale, we interpret the size difference to be representative of higher relative organic matter input at coastal margin sites in comparison to offshore basins.

4.2 Oxygenation and ventilation change in individual basins through the Holocene

4.2.1 Assemblage and environmental change through time in Tanner Basin

Planktic $\delta^{18}O$ records from Tanner Basin indicate constant sea surface conditions (salinity/temperature) through most of the Holocene (11.75 – 2.3 ka) and a decrease in sea surface temperature or increase in salinity from 2.3 – 1.9 ka relative to the rest of the Holocene (Figure 3). Benthic $\delta^{18}O$ and $\delta^{13}C$ exhibit little change through the Holocene (Figure 4). In contrast, the benthic foraminiferal assemblage gradually

shifts from more hypoxic to more oxic associated taxa from 5.5ka to 1.9 ka (Figures 2, 3). Cluster analysis indicates two distinct cohorts (each with 50% similarity in species) at 5.5-3.6 ka and 3.6-1.9 ka. This shift is largely driven by the increase in *Hansenisca soldanii* (previously *Gyroidina soldanii*) and decrease in *B. spissa* and *U. peregrina* (Figure 2). *Hansenisca soldanii* has been documented in well oxygenated, oligotrophic, cold deep water with pulsed food supply (De and Gupta, 2010), and both *B. spissa* and *U. peregrina* are well documented indicators of low oxygen. Using the modified Sharon-Behl Index, reconstructed oxygenation increases from 0.58 to 1.12 ml L^{-1} $[O_2]$across this interval (Figure 3). Thus, we interpret this assemblage shift as an indication of a gradual increase in oxygenation of this site from 5.5 to 1.9 ka.

Downcore morphometric analysis shows that neither relative abundance nor surface area of *Quinqueloculina* sp. (an oxic indicator species) changes through time. Although *B. spissa* decreases in relative abundance from 5.5-1.9 ka, shell size (surface area) does not change through time (Supplemental Figure 3). Stability in shell size concurrent with changes in relative abundance may indicate an interaction of factors including oxygen and organic matter influx in determining lethal vs. sublethal effects on *B. spissa*. Further, the lack of changes in shell size of *B. spissa* and *Quinqueloculina* across this interval may indicate a consistent supply of surface -exported organic matter, the main food resource for these benthic foraminifera.

Ostracod and echinoderm presence are not correlated with increase in dissolved oxygen at this site (Supplemental Figure 5). We hypothesize that the shift identified in the benthic foraminiferal assemblage is in response to a relatively small change in oxygenation (less than 1 ml L^{-1} $[O_2]$) and does not represent fluctuations across biologically important thresholds for metazoan taxa (oxygenation was never below 0.4 ml $L^{-1}[O_2]$, Figure 3). When compared to modern CalCOFI data, reconstructed oxygenation (using the Sharon-Behl Index) is equal to modern (Figure 4), except for the interval from 3 – 1.9 ka in which reconstructed oxygen is higher than modern by 0.3 ml $L^{-1}[O_2]$ (Figure 4). Combining assemblage,

oxygenation index, and isotopic history of Tanner Basin, we identify a gradual increase in oxygenation in the basin from 5.5-1.9 ka that is not correlated with changes in the oxygen or carbon isotope records and that is largely within the modern range of dissolved oxygen. This increase in oxygenation is coeval with a decrease in the strength of the OMZ in the last 6 ka in Santa Barbara Basin, which has been shown to be driven by an increase in the oxygenation of North Pacific Intermediate Water formation and ventilation relative to the early Holocene (Wang et al., 2020). We hypothesize that the increase in oxygenation in Tanner Basin during the late Holocene is driven by an increase in oxygenation of North Pacific Intermediate Water. Further, our data show that the changes in Tanner Basin dissolved oxygen are minor when compared to changes in oxygenation in nearby shallow basins still within the OMZ (Moffitt et al., 2014; Balestra et al., 2018; Palmer et al., 2020; Wang et al., 2020).

4.2.2 Assemblage and environmental change through time in San Nicolas Basin

In San Nicolas Basin, low oxygen associated benthic foraminiferal taxa dominate from 10.0 to 4.7 ka. A short period of anomalous assemblage driven by an increase in *C. mckannai,* an oxic-associated taxon, and a sharp decline in *U. peregrina*, an intermediate hypoxia-associated taxon, occurs at 4.7-4.2 ka and is interpreted as an interval of increased oxygenation. This interval is clear in both species-specific records as well as through cluster analysis of the complete assemblage. Using the modified Sharon-Behl Index, reconstructed oxygenation increases from 0.59 ml L^{-1} [O_2] before the interval to a maximum of 1.03 ml L^{-1} [O_2] during the oxygenation interval (Figure 3). Oxygenation returned to pre-event levels of dissolved oxygen after 4.2 ka and pre and post event assemblages are similar, indicating an absence of a legacy effect of the event on the community (Figure 2). Metazoan invertebrate microfossils (ostracods and urchin spines) are scarce in this core and changes in presence/absence of metazoans do not correlate with shifts in benthic foraminiferal assemblages (Supplemental Figure 5). Modern studies of circulation in San Nicolas Basin indicate that residence time for bottom waters in the basin are 9 ± 2 months (Berelson, 1991). As such, we hypothesize that the assemblage response recorded here represents persistent oxygenation or repeated ventilation on a decadal-to centennial scale, rather than a single episode of

ventilation. Yet, the absolute change in oxygenation is relatively minor and still within a threshold of intermediate hypoxia and within the range of modern values (Figure 3, 4).

When compared to modern CalCOFI data, reconstructed oxygenation in San Nicolas Basin is slightly lower than modern through most of the Holocene, yet reconstructed oxygenation during the oxygenation interval is equal to modern oxygenation. Further, reconstructed oxygenation in periods outside the event is similar to modern oxygenation at the sill depth of San Nicolas Basin (1100m, see Figure 4). The scale of change in reconstructed dissolved oxygen, relative abundance of species, and species diversity in San Nicolas Basin across this interval of change is minor when compared to intervals of change in nearby basins across the deglacial and in comparison to Holocene changes within basins that experienced shifts between anoxic and oxic conditions, such as the Macoma Event in the Santa Barbara Basin (Cannariato and Kennett, 1999; Schimmelmann et al., 2013; Moffitt et al., 2015; Praetorius et al., 2015; Balestra et al., 2018).

4.2.3 Assemblage and environmental change through time in San Clemente Basin

Environmental conditions remained relatively constant in San Clemente Basin from 11.2-7.1 ka ka as demonstrated by the lack of variability in the benthic foraminiferal assemblages. Species diversity does not change significantly through time (Supplemental Figure 5). Reconstructed oxygenation from the modified Sharon-Behl Index ranges from 0.67 to 0.96 ml L^{-1} [O_2] across this interval; this variability is reduced relative to Tanner and San Nicolas Basins (Figure 3). The assemblage at this depth is distinct from coastal margin environments and other, shallower basins (Moffitt et al., 2014; Balestra et al., 2018; Palmer et al., 2020). Ostracods and urchin spines are present in every interval (except one) examined here, indicating a well-oxygenated seafloor environment that supported metazoan life and motile organisms (Supplemental Figure 5) (Moffitt et al., 2015). Ecological differences between the shallow sill basins (San Nicolas and Tanner) vs. the deep sill basin (San Clemente) documented here are mirrored in previously documented seafloor metazoan assemblages (France, 1994). We hypothesize that at 1815 m

water depth, this site was not impacted by changes in the oxygen minimum zone during the Holocene and that intermediate and deep water reaching this site had a consistent source from 11.2-7.1 ka.

In comparison to modern CalCOFI data, reconstructed dissolved oxygen in the early and mid-Holocene is 0.5 ml L^{-1} [O_2] less than modern (Figure 4). We propose three potentially overlapping hypotheses for this difference. First, this may be an artifact of the Sharon-Behl Index, which uses lowest known thresholds of oxygenation and thus may predict the minima of dissolved oxygen concentrations. Second, in the early Holocene, sea level was lower than modern (by approximately 70 m) thus, this site may have been less well oxygenated simply due to being at a shallower depth, but this would not explain the entire difference from modern (Figure 4) (Fleming et al., 1998; Moffitt et al., 2014). Finally, the lower oxygenation may have been lower than modern, a pattern that is reflected in Santa Monica and Santa Barbara Basins at this time (Balestra et al., 2018; Wang et al., 2020).

4.3 Intermediate water change and basinal processes in Southern California Borderlands

In the early to mid-Holocene (11.2-4.7 ka), seafloor oxygenation below 1400 m was stable in the Southern CA Borderlands, evidenced by stability in assemblage records from San Clemente Basin (1815 m) and San Nicolas Basin (1442 m), and was likely driven by consistent source and composition of intermediate waters. Benthic foraminiferal assemblage records from the Santa Lucia Slope (ODP 1017, 955 m) offshore Point Conception indicate a stable suboxic environment through the early and mid-Holocene and are similar in taxonomic composition to our records from San Nicolas and San Clemente Basins (Cannariato and Kennett, 1999). Synchrony in stability and assemblages across San Nicolas Basin (1442 m), San Clemente Basin (1818 m), and the Santa Lucia Slope (955 m) contrasts with evidence of fluctuations in age of North Pacific Intermediate Water entering SBB (as recorded by benthic-planktic radiocarbon age differences) at 9 ka (Roark et al., 2003), expansion of the OMZ in SBB in the early Holocene (Wang et al., 2020), and a turning point from hypoxic to suboxic conditions at 9 ka in Santa Monica Basin (indicated by benthic foraminiferal assemblages and geochemical records) (Balestra et al.,

2018). Differences between sites can be explained by differences across water depth. We propose that changes in the source and strength of NPIW impacted sites at 400-1000m water depth (SBB, SMB) (Roark et al., 2003; Balestra et al., 2018; Wang et al., 2020), but had less of an effect on the water column below 1000 m.

In the mid to late Holocene, San Nicolas Basin experienced a multi-centennial oxygenation interval from 4.7-4.2 ka and oxygenation increased in Tanner Basin gradually from 5.0-1.9 ka. The interval of increased oxygen in San Nicolas Basin and the increasing oxygenation in Tanner Basin from 5.0-4.0 ka may be due to the same driver because their sill depths of each are similar, 1100 m and 1160 m respectively. Ventilation and oxygenation of these offshore basins is coeval with an increase in oxygenation in Santa Barbara Basin beginning around 6 ka that is attributed to the increasing strength and oxygenation of North Pacific Intermediate Water (Wang et al., 2020). Wang et al., 2020 identify sea ice formation and brine rejection in the North Pacific as the driver of increased oxygenation after 6 ka. We posit that the slight increase in oxygenation in both San Nicolas and Tanner basins may be due to increased oxygenation of North Pacific Intermediate Water entering both basins. After 4.0 ka, the trends diverge, and San Nicolas Basin returns to lower oxygenation levels. The difference in the two basins can be explained by basinal processes occurring at depth, a change in source or strength of influx of intermediate waters to San Nicolas Basin, or differences in surface water productivity due distinct overlying surface current processes. We present two hypotheses: first, both basins may have experienced “indirect” ventilation through diffusion of dissolved oxygen from overlying waters, rather than “direct” ventilation due to advection, thus explaining why increased oxygen is persistent in Tanner Basin but not San Nicolas Basin (Talley, 1993), or basinal processes due to the different shapes and depths of each basin may have impacted the oxygenation of each.

Although oxygenation does vary across the Holocene in Tanner, San Nicolas, and San Clemente basins, all variability is within 1 ml L^{-1} [O_2]and does not cross critical biological thresholds below 0.5 ml L^{-1} [O_2]

or above 1.5 ml L^{-1} [O_2] in any basin. As such, variability in oxygenation and ventilation of San Nicolas, Tanner, and San Clemente basins is reduced relative to shallower sites, including Santa Barbara Basin and Santa Monica Basin, across the entire Holocene (Ohkushi et al., 2013; Moffitt et al., 2014; Balestra et al., 2018). Additionally, Holocene-scale oxygenation changes (presented here) are reduced relative to glacial/interglacial changes in oxygenation in the basins examined here and in the nearby Santa Lucia Slope (Cannariato and Kennett, 1999; Stott et al., 2000). This indicates that Holocene-scale climate changes driving oxygenation change shallower than 1000 m are not impacting waters below 1000 m and that climate changes within the Holocene do not significantly impact oxygenation below 1000 m, despite changes in the intensity and extent of the OMZ shallower than 1000 m. As such, we hypothesize that deoxygenation due to anthropogenic climate change will also have a greater impact on the water column above 1000 m and that source water oxygenation is a dominant driver of oxygenation at depth and must be considered when predicting future oxygenation change.

5 Conclusions

Reconstruction of past oxygenation using analysis of benthic microfaunal communities (foraminiferal and metazoan) is optimized by combining multiple approaches including analysis of indicator taxa, reconstruction of oxygenation using multi-taxa indices, and community scale-analysis such as multidimensional analysis and diversity. Here we demonstrate the utility of combined approaches, and we expand the use of the Sharon-Behl Index for paleo-oxygenation reconstruction. Analysis of benthic foraminiferal assemblages from three silled basins (Tanner, San Nicolas, San Clemente) in the Southern California Borderlands combined with benthic and planktic stable isotope analysis from Tanner Basin show a gradual increase (0.5 ml L^{-1} [O_2]) in oxygenation in Tanner Basin from 5.5-1.9 ka, multi-centennial variability in oxygenation (on the scale of 0.5 ml L^{-1} [O_2]) in San Nicolas Basin, and stability in the seafloor environment in San Clemente Basin. Holocene scale climate changes did not drive significant changes (> 1 ml L^{-1} [O_2]) in marine oxygenation below 1000 m in the Southern California Borderlands. In the context of modern oxygenation changes, findings from this analysis show that

Holocene-scale changes in seafloor oxygenation of the Southern California Borderlands below 1000 m has remined relatively stable and is similar to modern throughout the Holocene. As such, we expect that future changes to marine oxygenation will be greater at depths above 1000 m relative to deeper waters and note that if anthropogenic climate change induced changes in oxygenation do cause shifts in dissolved oxygen greater than > 1 ml L^{-1} [O_2] below 1000 m, it will represent a divergence from scales of variability over the last 11 ka.

6 Tables

Basin	**Core**	**Sample Interval**	**Source**	**Age** (^{14}C years)	**±**	**1σ minimum calendar age**	**1σ maximum calendar age**	**Age** (years before present)	**Sed rate** (cm kyr^{-1})
Tanner	EW95 04-09	8-10 cm	Stott et al., 2000	1950	50	2619	2712	2666	10.67
Tanner	EW95 04-09	38- 40 cm	This paper	5290	30	5433	5521	5477	10.25
Tanner	EW95 05-09	104-106 cm	Stott et al., 2000	10790	60	11778	12051	11915	
San Nicolas	EW95 04-08	38-40 cm	Stott et al., 2000	6780	50	7062	7198	7130	8.89
San Nicolas	EW95 04-08	74-76 cm	This paper	10330	35	11130	11225	11178	16.48
San Nicolas	EW95 04-08	76-78 cm	Stott et al., 2000	10460	70	11200	11359	11280	16.48
San Nicolas	EW95 04-08	120-122 cm	Stott et al., 2000	12870	160	13193	14603	13898	
San Clemente	EW95 04-08	40-42 cm	Stott et al., 2000	8550	60	8882	9039	8960	5.29
San Clemente	EW95 04-08	60-62 cm	Stott et al., 2000	11430	40	12690	12789	12739	7.21
San Clemente	EW95 04-08	108-110 cm	Stott et al., 2000	16650	50	19575	19207	19391	

Table 1. Radiocarbon ages and age model for all three cores examined here.

7 Figures

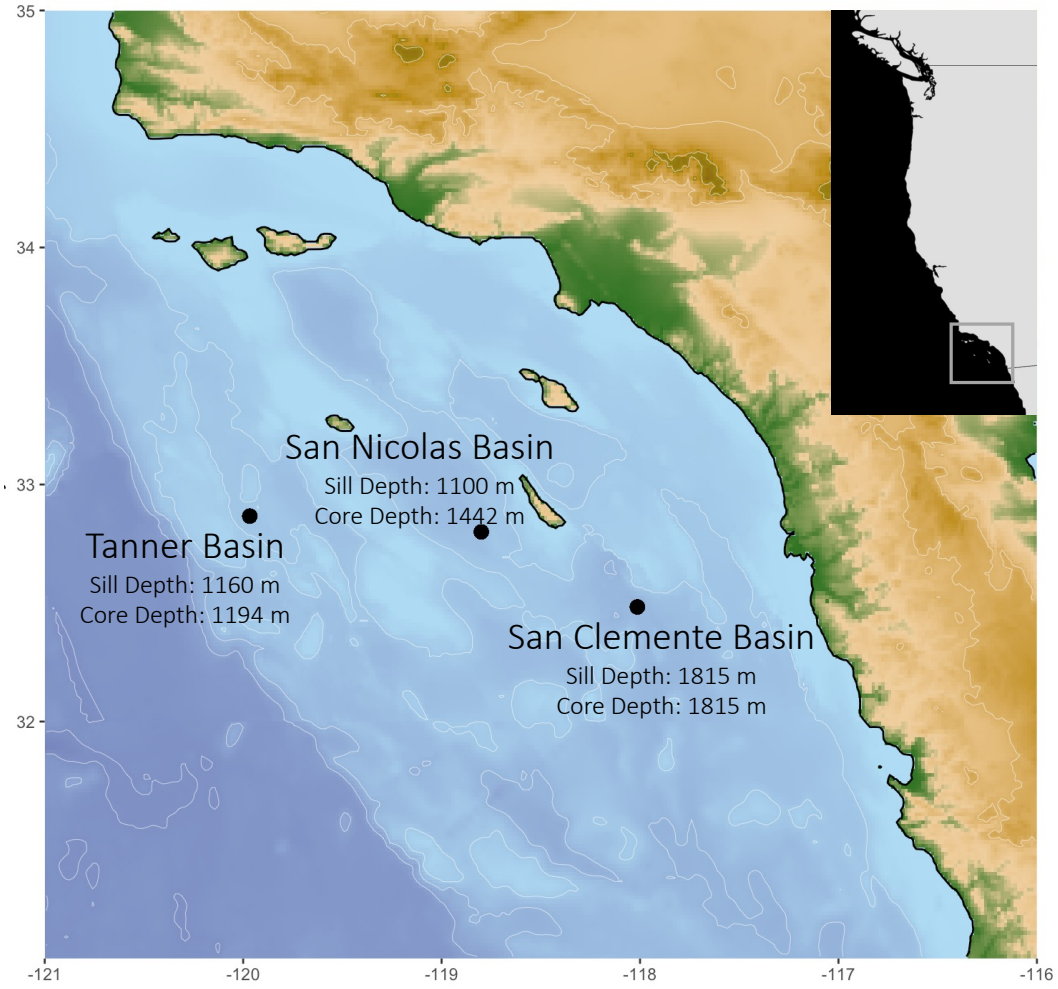

Figure 1: Map of the locations of the three cores used in this study. The sill depth and core collection depth for each core is reported in meters.

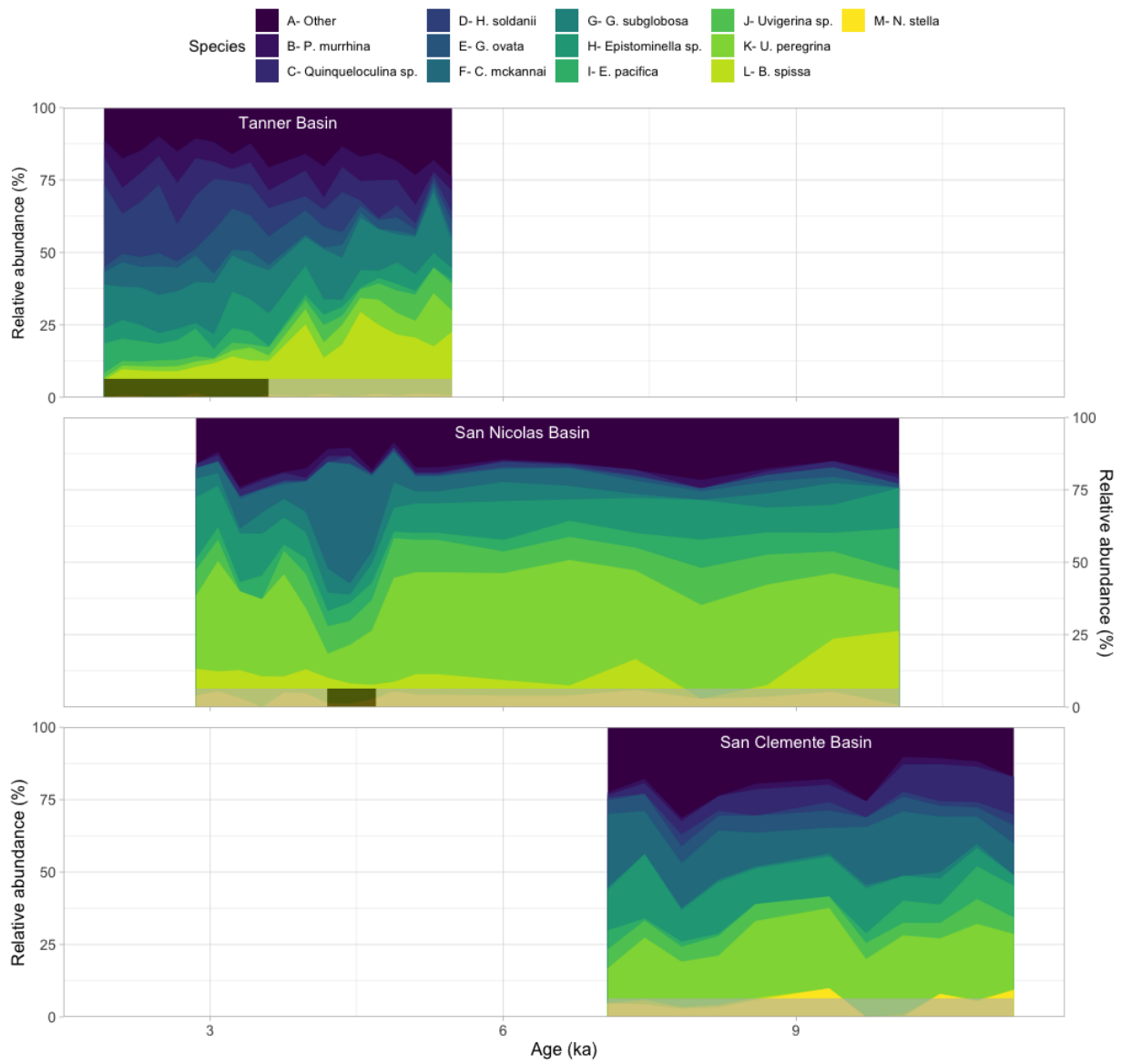

Figure 2: Relative abundance of benthic foraminifera vs. age in thousands of years before present for three cores examine here: Tanner (top), San Nicolas (middle), and San Clemente (bottom). Ten most abundant species are shown; all other species grouped as "other." Each color represents a taxonomic group (species, genus, or other). See legend at top of plot for color of each. Taxa colors are ordered (A-M) from oxic indicator taxa (blue, top of plot) to dysoxic indicator taxa (yellow, bottom of plot). Color bars across bottom of each plot represent cohorts with 50% similarity following NMDS and cluster analysis for each individual basin (see Supplemental Figure 2).

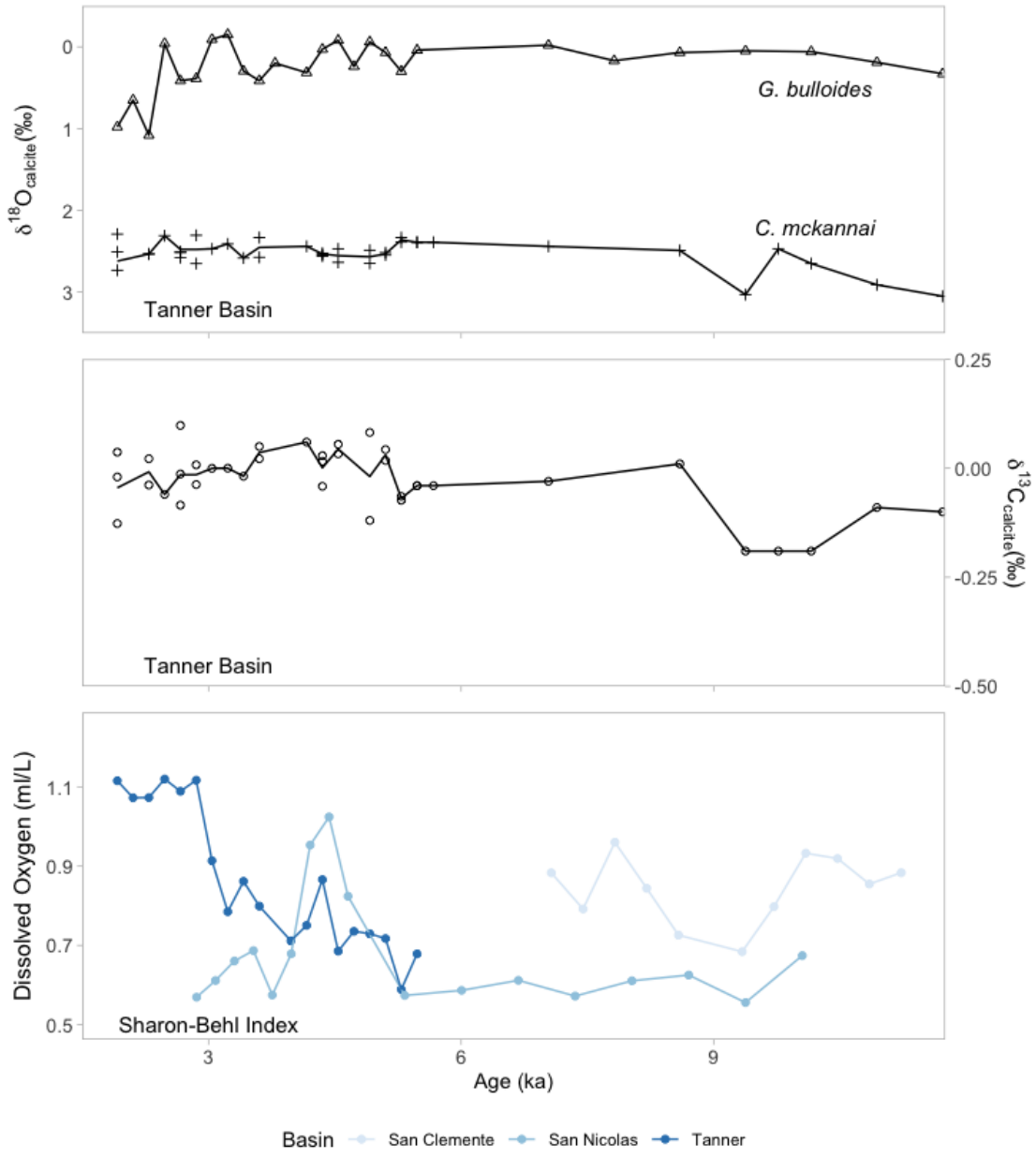

Figure 3: Oxygen isotopes of planktic foraminifera *G. bulloides* from this study and Stott et al., 2000 indicated as triangles (top). Oxygen and carbon isotopes of benthic foraminifera *C. mckannai* from this study and Stott et al., 2000 indicated as + (middle). In both isotope figures, data from 5.5-1.9 ka includes both data from Stott et al., 2000 and this study, data from 11.7-5.5 from Stott et al., 2000. Reconstructed dissolved oxygen content in each basin (Tanner, San Nicolas, San Clemente) using modified Sharon-Behl Dissolved Oxygen Index (bottom). Oxygen in ml L^{-1} [O_2].

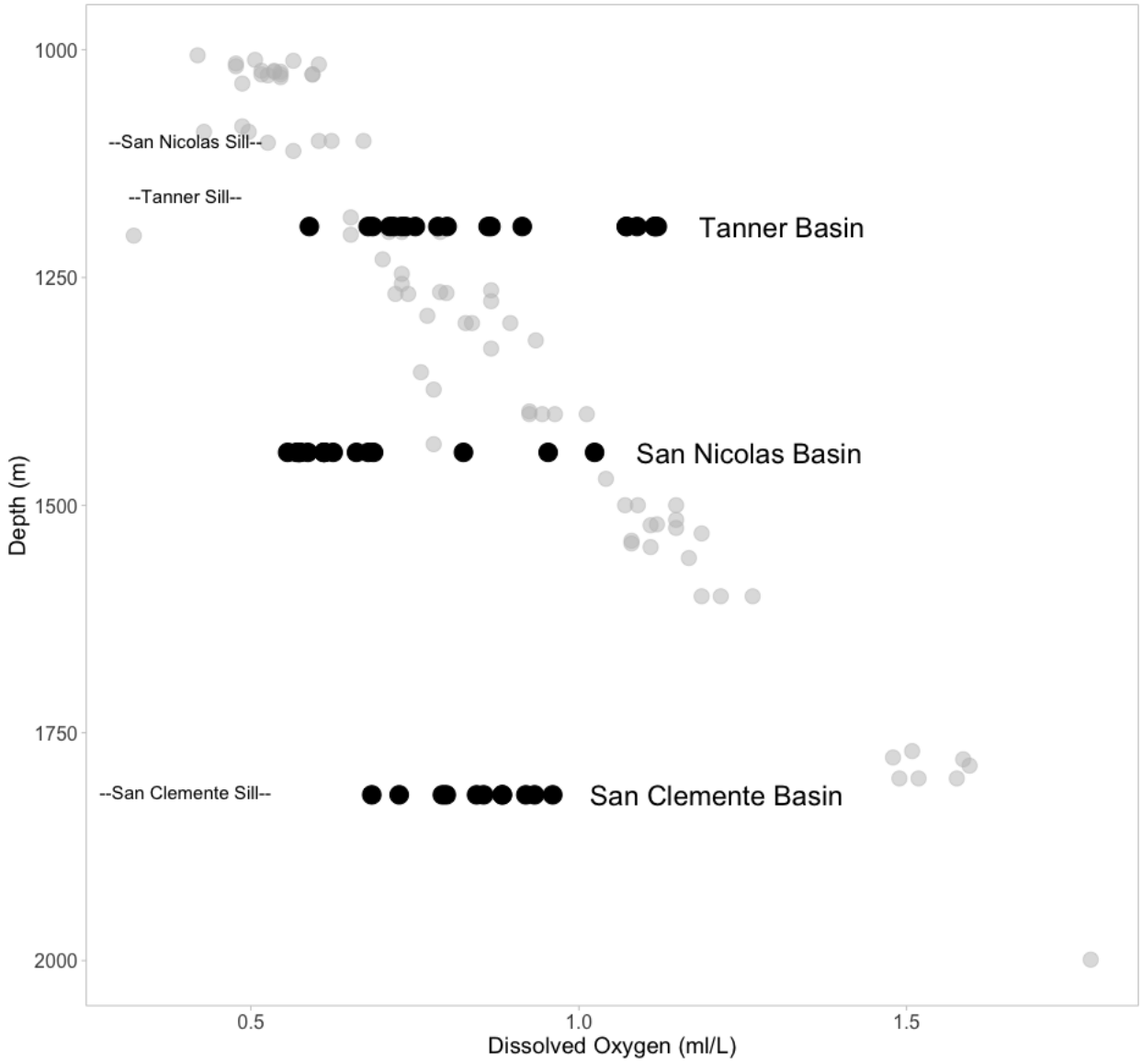

Figure 4: Reconstructed dissolved oxygen concentration (ml L^{-1} $[O_2]$) from Tanner, San Nicolas, and San Clemente Basin (black dots) compared with modern dissolved oxygen concentration (ml L^{-1} $[O_2]$) from CALCOFI bottle sampling (1986-2019) (gray dots). Depth of sill of each basin is labeled.

8 Supplemental Figures

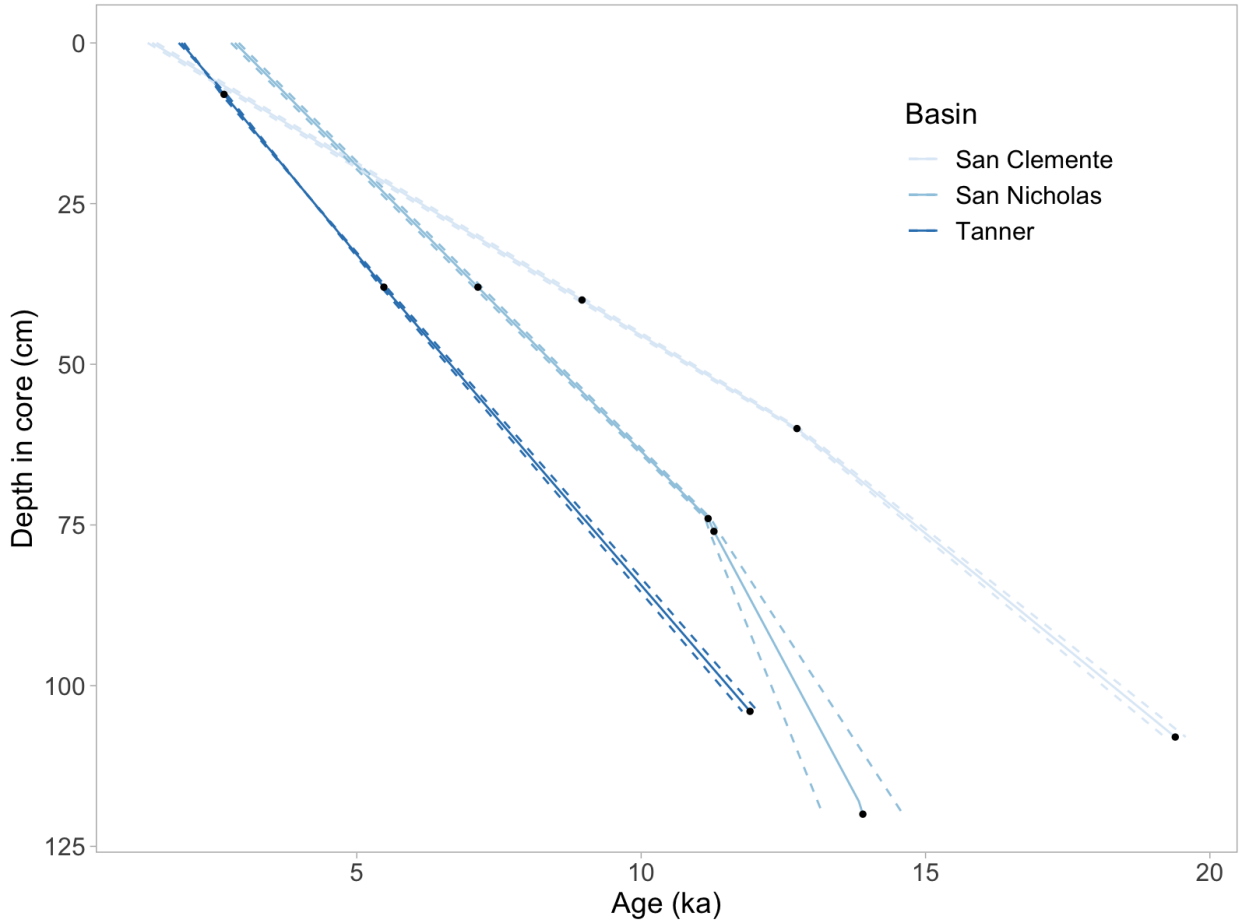

Supplemental Figure 1: Radiocarbon-based age model for three cores. Age shown in thousands of years before present. Linear interpolation between radiocarbon dates (black dots). Line color indicates basin: Tanner= dark blue, San Nicolas = medium blue, San Clemente=light blue. Dashed lined represent +/- 1 sigma years.

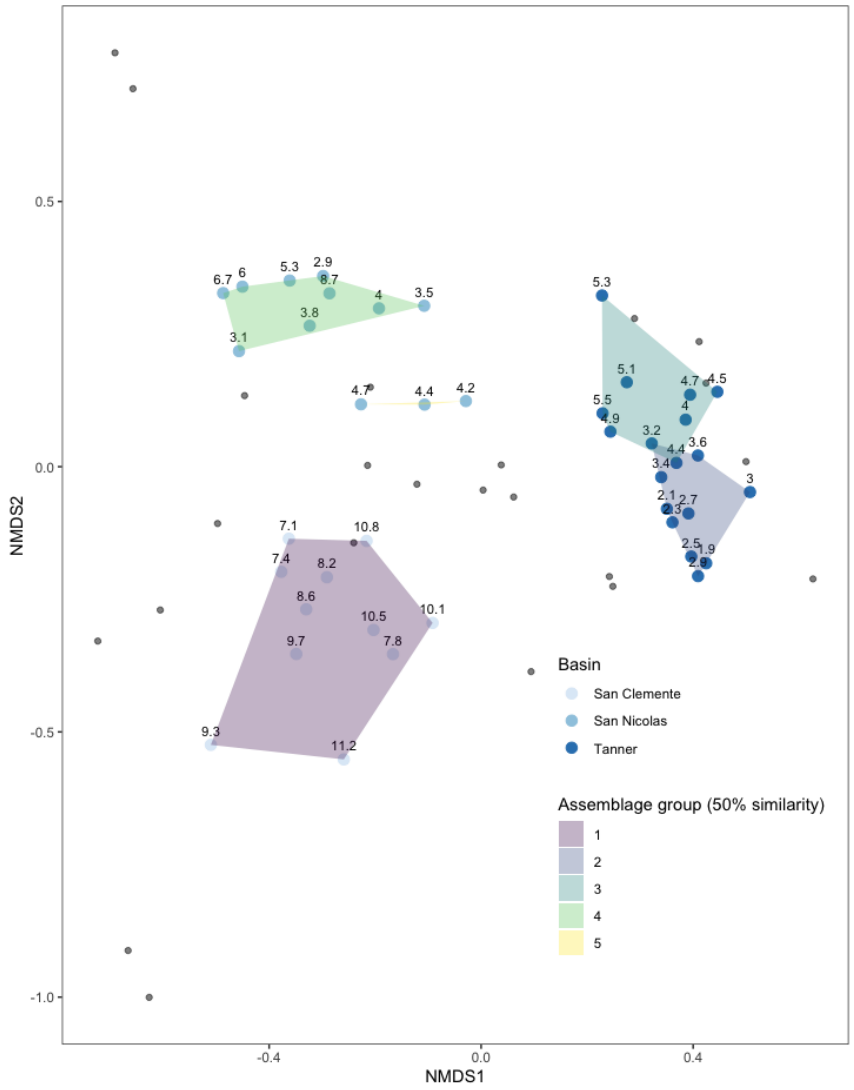

Supplemental Figure 2: Non-metric multidimensional scaling plot of all benthic foraminiferal assemblages through time from three cores. Species are plotted as small gray dots. All other points represent assemblages from 2 cm intervals through time at each of the three cores, label is age in thousands of years before present. Colored dots represent each basin: Tanner= dark blue, San Nicolas = medium blue, San Clemente=light blue. Clusters show assemblages with 50% similarity, calculated using cluster analysis; five clusters are represented.

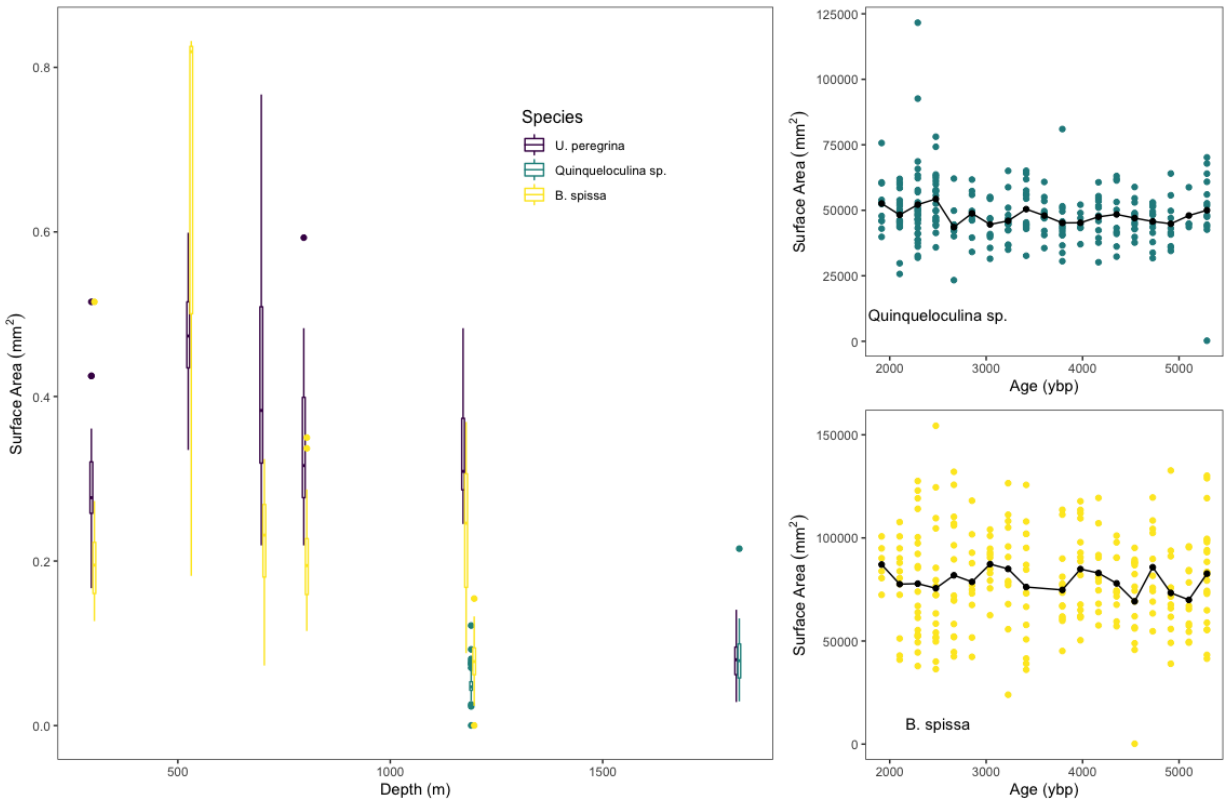

Supplemental Figure 3: Shell surface area (mm^2) vs. water depth (m) at all points in time (A). Data shown here indicate all points in time from each water depth. Colors represent species: *U. peregrina* = purple, *Quinqueloculina* sp. = green, *B. spissa* = yellow. Surface area of *Quinqueloculina* sp. (B.) and *B. spissa* (C.) vs. time in years before present from Tanner Basin.

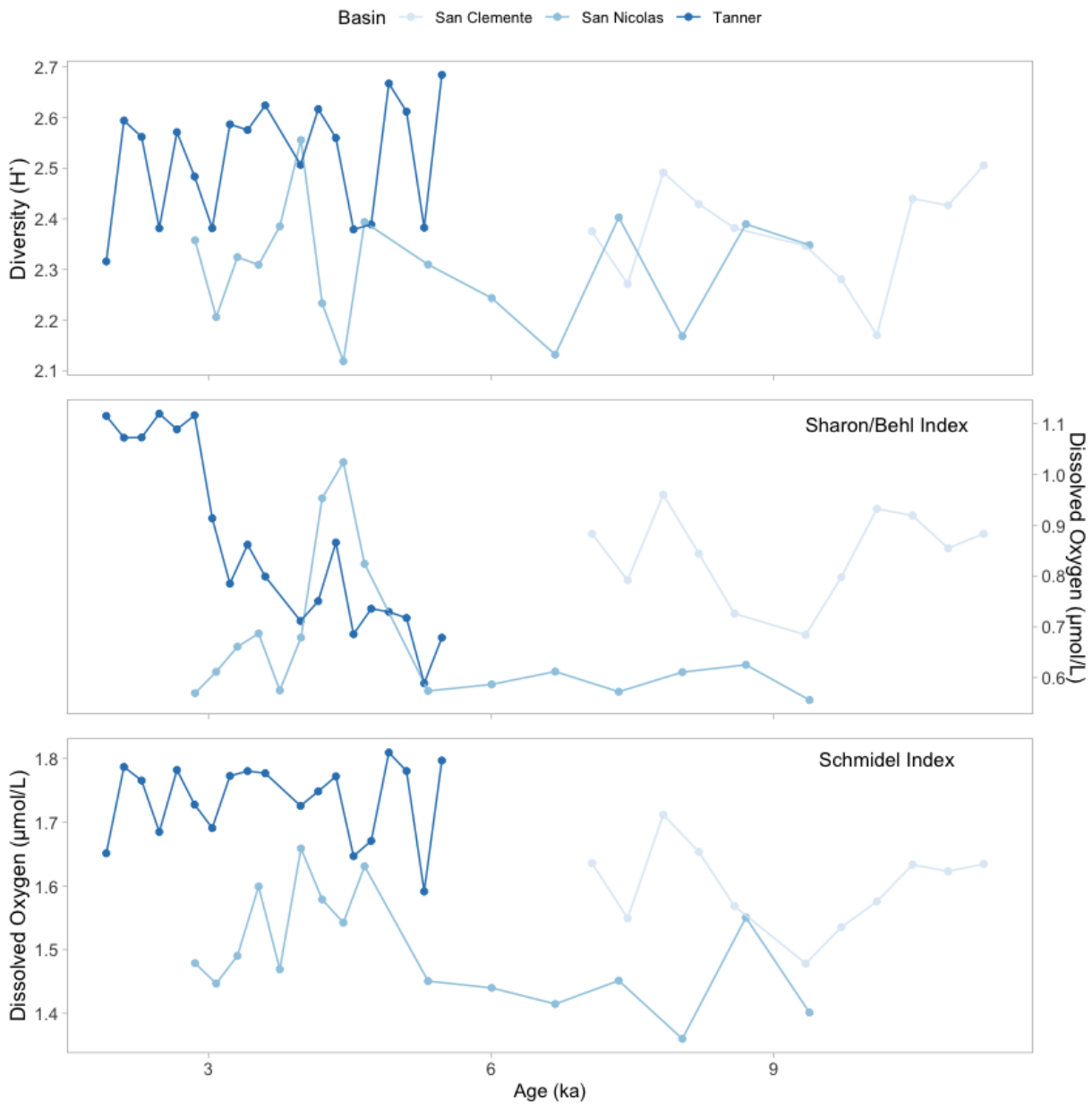

Supplemental Figure 4: Diversity (Shannon Index, top), reconstructed dissolved oxygen concentration using Sharon-Behl (middle), reconstructed dissolved oxygen concentration using Schmidel Index (bottom) for three cores: Tanner= dark blue, San Nicolas = medium blue, San Clemente = light blue vs. age in thousands of years before present.

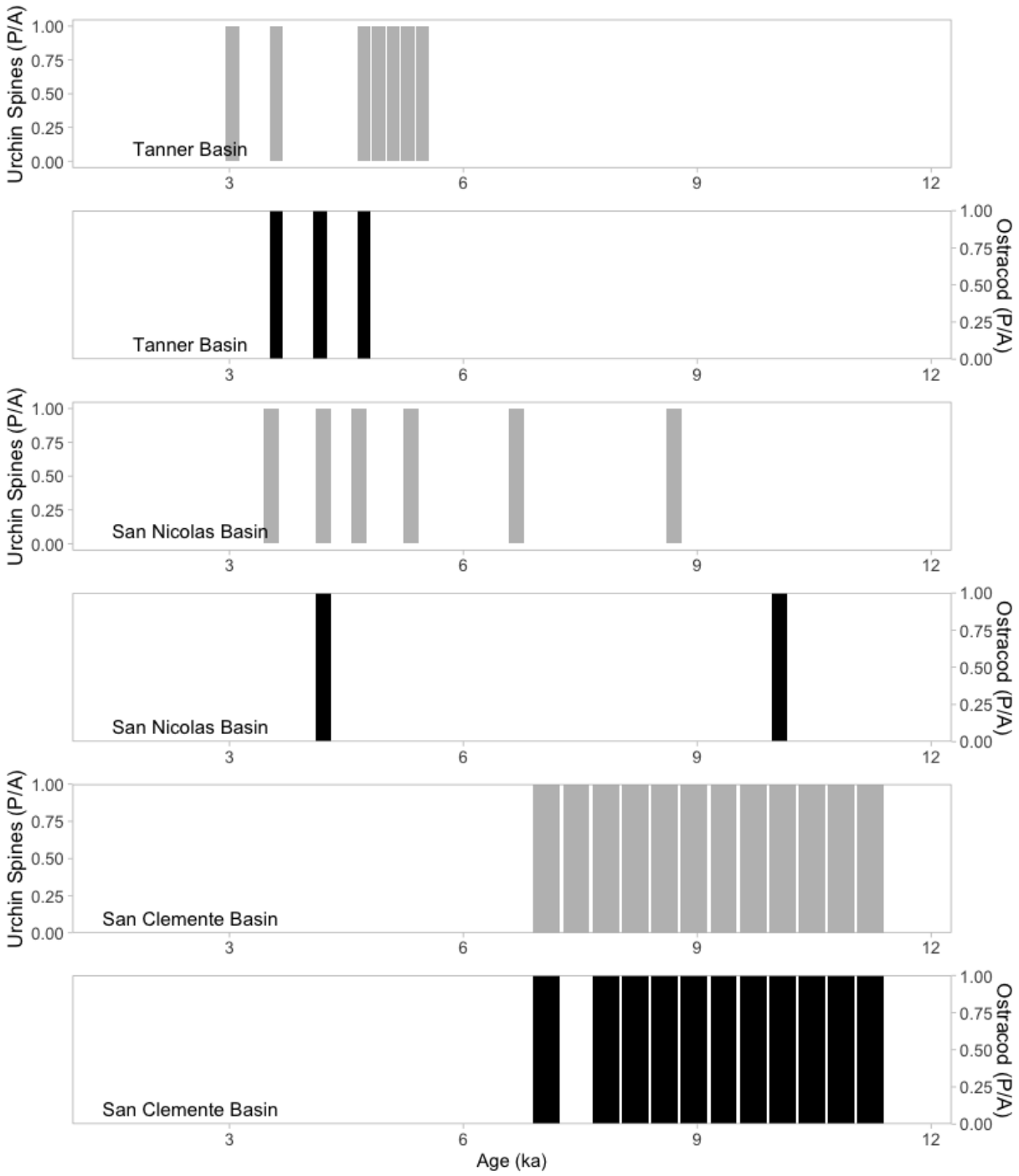

Supplemental Figure 5: Presence and absence of metazoan microfossils: urchin spines and ostracods.

Presence represented as 1, absence represented as 0.

9 Supplemental Tables

Species	Oxygen Classification	Modified from Sharon-Behl	Citation for oxygenation affinity
Bolivina argentea	Suboxic		Sharon et al., 2021
Bolivina pseudoberyethes	Dysoxic		Sharon et al., 2021
Bolivina spissa	Suboxic		Sharon et al., 2021
Bulimina tenuata	Dysoxic		Sharon et al., 2021
Cassidulina sp.	Suboxic		Sharon et al., 2021
Chlistomella ovoidea	Suboxic		Sharon et al., 2021
Cibicides mckannai	Weakly hypoxic to oxic	*	Kaiho 1994
Cibicides sp.	Weakly hypoxic to oxic	*	Kaiho 1994
Elphidium sp.	Weakly hypoxic to oxic		Sharon et al., 2021
Epistominella exigua	Suboxic		Sharon et al., 2021
Epistominella pacifica	Weakly hypoxic to oxic	*	Cannarito and Kennett 1999
Fursenkoina sp.	Suboxic	*	Kaiho 1994
Globobulimina barbata	Suboxic	*	Ohkushi et al., 2013
Globobulimina ovata1	Suboxic	*	Ohkushi et al., 2013
Globobulimina ovata2	Suboxic	*	Ohkushi et al., 2013
Globobulimina pacifica	Suboxic	*	Ohkushi et al., 2013
Globocassidulina sp.	Suboxic		Sharon et al., 2021
Globocassidulina subglobosa	Suboxic		Sharon et al., 2021
Hansenisca soldanii	Weakly hypoxic to oxic	*	De and Gupta 2010
Hansenisca sp.	Weakly hypoxic to oxic		Sharon et al., 2021
Melonis affinis	Suboxic	*	Kaiho 1994
Nonionella stella	Dysoxic		Sharon et al., 2021
Oridorsalis umbonatus	Suboxic		Sharon et al., 2021
Other			
Pyrgo murrhina	Weakly hypoxic to oxic		Sharon et al., 2021
Quinqueloculina sp.	Weakly hypoxic to oxic		Sharon et al., 2021
Quinqueloculina sp2.	Weakly hypoxic to oxic		Sharon et al., 2021
Uvigerina peregrina	Suboxic		Sharon et al., 2021
Uvigerina proboscoidea	Suboxic		Sharon et al., 2021
Uvigerina sp.	Suboxic		Sharon et al., 2021

Supplemental Table 1: Oxygen affinity for all species examined here and utilized in oxygen transfer functions.

10 References

Addison, J. A., Barron, J., Finney, B., Kusler, J., Bukry, D., Heusser, L. E., and Alexander, C. R.: A Holocene record of ocean productivity and upwelling from the northern California continental slope, Quatern Int, 2017.

Balestra, B., Krupinski, N. B. Q., Erohina, T., Fessenden-Rahn, J., Rahn, T., and Paytan, A.: Bottom-water oxygenation and environmental change in Santa Monica Basin, Southern California during the last 23 kyr, 490, 17–37, 2018.

Barron, J. A., Heusser, L., Herbert, T., and Lyle, M.: High-resolution climatic evolution of coastal northern California during the past 16,000 years, Paleoceanography, 18, 2003.

Behl, R. J. and Kennett, J. P.: Brief interstadial events in the Santa Barbara basin, NE Pacific, during the past 60 kyr, Nature, 379, 243–246, https://doi.org/DOI 10.1038/379243a0, 1996.

Belanger, C. L., Jablonski, D., Roy, K., Berke, S. K., Krug, A. Z., and Valentine, J. W.: Global environmental predictors of benthic marine biogeographic structure, Proceedings of the National Academy of Sciences, 109, 14046–14051, https://doi.org/10.1073/pnas.1212381109, 2012.

Belanger, C. L., Sharon, Du, J., Payne, C. R., and Mix, A. C.: North Pacific deep-sea ecosystem responses reflect post-glacial switch to pulsed export productivity, deoxygenation, and destratification, Deep Sea Research Part I: Oceanographic Research Papers, 164, 103341, https://doi.org/10.1016/j.dsr.2020.103341, 2020.

Berelson, W. M.: The flushing of two deep-sea basins, southern California borderland, 36, 1150–1166, https://doi.org/10.4319/lo.1991.36.6.1150, 1991.

Berelson, W. M. and Stott, L. D.: Productivity and organic carbon rain to the California margin seafloor: Modern and paleoceanographic perspectives, 18, 2-1-2–15, https://doi.org/10.1029/2001PA000672, 2003.

Bernhard, J. M. and Gupta, B. K. S.: Foraminifera of oxygen-depleted environments, in: Modern foraminifera, Springer, 201–216, 1999.

Bograd, S. J. and Lynn, R. J.: Long-term variability in the Southern California Current System, Deep Sea Research Part II: Topical Studies in Oceanography, 50, 2355–2370, https://doi.org/10.1016/S0967-0645(03)00131-0, 2003.

Bograd, S. J., Checkley, D. A., and Wooster, W. S.: CalCOFI: a half century of physical, chemical, and biological research in the California Current System, Deep Sea Research Part II: Topical Studies in Oceanography, 50, 2349–2353, https://doi.org/10.1016/S0967-0645(03)00122-X, 2003.

Bograd, S. J., Castro, C. G., Di Lorenzo, E., Palacios, D. M., Bailey, H., Gilly, W., and Chavez, F. P.: Oxygen declines and the shoaling of the hypoxic boundary in the California Current, 35, https://doi.org/Artn L12607 10.1029/2008gl034185, 2008.

Bograd, S. J., Schroeder, I. D., and Jacox, M. G.: A water mass history of the Southern California current system, 46, 6690–6698, https://doi.org/10.1029/2019GL082685, 2019.

Breitburg, D., Levin, L. A., Oschlies, A., Gregoire, M., Chavez, F. P., Conley, D. J., Garcon, V., Gilbert, D., Gutierrez, D., Isensee, K., Jacinto, G. S., Limburg, K. E., Montes, I., Naqvi, S. W. A., Pitcher, G. C., Rabalais, N. N., Roman, M. R., Rose, K. A., Seibel, B. A., Telszewski, M., Yasuhara, M., and Zhang, J.: Declining oxygen in the global ocean and coastal waters, 359, 46-+, https://doi.org/10.1126/science.aam7240, 2018.

Cannariato, K. G. and Kennett, J. P.: Climatically related millennial-scale fluctuations in strength of California margin oxygen-minimum zone during the past 60 k.y., Geology, 27, 975–978, https://doi.org/Doi 10.1130/0091-7613(1999)027<0975:Crmsfi>2.3.Co;2, 1999.

Cardich, J., Gutiérrez, D., Romero, D., Pérez, A., Quipúzcoa, L., Marquina, R., Yupanqui, W., Solís, J., Carhuapoma, W., Sifeddine, A., and Rathburn, A.: Calcareous benthic foraminifera from the upper central Peruvian margin: control of the assemblage by pore water redox and sedimentary organic matter, 535, 63–87, https://doi.org/10.3354/meps11409, 2015.

Cardich, J., Sifeddine, A., Salvatteci, R., Romero, D., Briceño-Zuluaga, F., Graco, M., Anculle, T., Almeida, C., and Gutiérrez, D.: Multidecadal Changes in Marine Subsurface Oxygenation Off Central Peru During the Last ca. 170 Years, Front. Mar. Sci., 6, https://doi.org/10.3389/fmars.2019.00270, 2019.

Caulle, C., Koho, K. A., Mojtahid, M., Reichart, G. J., and Jorissen, F. J.: Live (Rose Bengal stained) foraminiferal faunas from the northern Arabian Sea: faunal succession within and below the OMZ, Biogeosciences, 11, 1155–1175, https://doi.org/10.5194/bg-11-1155-2014, 2014.

Checkley, D. M. and Barth, J. A.: Patterns and processes in the California Current System, Prog Oceanogr, 83, 49–64, https://doi.org/10.1016/j.pocean.2009.07.028, 2009.

Christensen, C. J., Gorsline, D. S., Hammond, D. E., and Lund, S. P.: Non-annual laminations and expansion of anoxic basin-floor conditions in Santa Monica Basin, California Borderland, over the past four centuries, Mar Geol, 116, 399–418, 1994.

De, S. and Gupta, A. K.: Deep-sea faunal provinces and their inferred environments in the Indian Ocean based on distribution of Recent benthic foraminifera, Palaeogeography, Palaeoclimatology, Palaeoecology, 291, 429–442, https://doi.org/10.1016/j.palaeo.2010.03.012, 2010.

Erdem, Z., Schönfeld, J., Rathburn, A. E., Perez, M.-E., Cardich, J., and Glock, N.: Bottom-water deoxygenation at the Peruvian Margin during the last deglaciation recorded by benthic foraminifera, https://orcid.org/0000-0002-5509-8733, 2019.

Evans, N., Schroeder, I. D., Buil, M. P., Jacox, M. G., and Bograd, S. J.: Drivers of Subsurface Deoxygenation in the Southern California Current System, 47, e2020GL089274, https://doi.org/10.1029/2020GL089274, 2020.

Fenton, I. S., Baranowski, U., Boscolo-Galazzo, F., Cheales, H., Fox, L., King, D. J., Larkin, C., Latas, M., Liebrand, D., Miller, C. G., Nilsson-Kerr, K., Piga, E., Pugh, H., Remmelzwaal, S., Roseby, Z. A., Smith, Y. M., Stukins, S., Taylor, B., Woodhouse, A., Worne, S., Pearson, P. N., Poole, C. R., Wade, B. S., and Purvis, A.: Factors affecting consistency and accuracy in identifying modern macroperforate planktonic foraminifera, 37, 431–443, https://doi.org/10.5194/jm-37-431-2018, 2018.

Fisler, J. and Hendy, I. L.: California Current System response to late Holocene climate cooling in southern California, 35, https://doi.org/Artn L09702 10.1029/2008gl033902, 2008.

Fleming, K., Johnston, P., Zwartz, D., Yokoyama, Y., Lambeck, K., and Chappell, J.: Refining the eustatic sea-level curve since the Last Glacial Maximum using far- and intermediate-field sites, Earth and Planetary Science Letters, 163, 327–342, https://doi.org/10.1016/S0012-821X(98)00198-8, 1998.

Forcino, F. L., Leighton, L. R., Twerdy, P., and Cahill, J. F.: Reexamining Sample Size Requirements for Multivariate, Abundance-Based Community Research: When Resources are Limited, the Research Does Not Have to Be, PLOS ONE, 10, e0128379, https://doi.org/10.1371/journal.pone.0128379, 2015.

France, S. C.: Genetic population structure and gene flow among deep-sea amphipods,Abyssorchomene spp., from six California Continental Borderland basins, Mar. Biol., 118, 67–77, https://doi.org/10.1007/BF00699220, 1994.

Gardner, J. V., Heusser, L. E., Quinterno, P. J., Stone, S. M., Barron, J. A., and Poore, R. Z.: Clear Lake record vs. the adjacent marine record; A correlation of their past 20,000 years of paleoclimatic and paleoceanographic responses, in: Geological Society of America Special Papers, vol. 214, Geological Society of America, 171–182, https://doi.org/10.1130/SPE214-p171, 1988.

Helly, J. J. and Levin, L. A.: Global distribution of naturally occurring marine hypoxia on continental margins, Deep-Sea Res Pt I, 51, 1159–1168, https://doi.org/10.1016/j.dsr.2004.03.009, 2004.

Ingram, B. L. and Southon, J. R.: Reservoir ages in eastern Pacific coastal and estuarine waters, 38, 573–582, 1996.

Jaccard, S. L., Galbraith, E. D., Frolicher, T. L., and Gruber, N.: Ocean (De)Oxygenation across the Last Deglaciation Insights for the Future, Oceanography, 27, 26–35, 2014.

Kaiho, K.: Benthic Foraminiferal Dissolved-Oxygen Index and Dissolved-Oxygen Levels in the Modern Ocean, Geology, 22, 719–722, https://doi.org/Doi 10.1130/0091-7613(1994)022<0719:Bfdoia>2.3.Co;2, 1994.

Kaiho, K.: Effect of organic carbon flux and dissolved oxygen on the benthic foraminiferal oxygen index (BFOI), Mar Micropaleontol, 37, 67–76, https://doi.org/Doi 10.1016/S0377-8398(99)00008-0, 1999.

Keating-Bitonti, C. R. and Payne, J. L.: Physicochemical controls on biogeographic variation of benthic foraminiferal test size and shape, Paleobiology, 42, 595–611, 2016.

Keating-Bitonti, C. R. and Payne, J. L.: Ecophenotypic responses of benthic foraminifera to oxygen availability along an oxygen gradient in the California Borderland, 38, 2017.

Keating-Bitonti, C. R. and Payne, J. L.: Environmental influence on growth history in marine benthic foraminifera, 44, 736–757, https://doi.org/10.1017/pab.2018.19, 2018.

Kemp, A. C., Wright, A. J., and Cahill, N.: Enough is Enough, or More is More? Testing the Influence of Foraminiferal Count Size on Reconstructions of Paleo-Marsh Elevation, Journal of Foraminiferal Research, 50, 266–278, https://doi.org/10.2113/gsjfr.50.3.266, 2020.

Levin, L. A.: Oxygen minimum zone benthos: Adaptation and community response to hypoxia, Oceanogr Mar Biol, 41, 1–45, 2003.

Levin, L. A., Ekau, W., Gooday, A. J., Jorissen, F., Middelburg, J. J., Naqvi, S. W. A., Neira, C., Rabalais, N. N., and Zhang, J.: Effects of natural and human-induced hypoxia on coastal benthos, Biogeosciences, 6, 2063–2098, https://doi.org/10.5194/bg-6-2063-2009, 2009.

McGann, M.: Paleoceanographic changes on the Farallon Escarpment off central California during the last 16,000 years, Quatern Int, 235, 26–39, https://doi.org/10.1016/j.quaint.2010.09.005, 2011.

Moffitt, S. E., Hill, T. M., Ohkushi, K., Kennett, J. P., and Behl, R. J.: Vertical oxygen minimum zone oscillations since 20 ka in Santa Barbara Basin: A benthic foraminiferal community perspective, Paleoceanography, 29, 44–57, https://doi.org/10.1002/2013pa002483, 2014.

Moffitt, S. E., Hill, T. M., Roopnarine, P. D., and Kennett, J. P.: Response of seafloor ecosystems to abrupt global climate change, P Natl Acad Sci USA, 112, 4684–4689, https://doi.org/10.1073/pnas.1417130112, 2015.

Murgese, D. S. and De Deckker, P.: The distribution of deep-sea benthic foraminifera in core tops from the eastern Indian Ocean, Marine Micropaleontology, 56, 25–49, https://doi.org/10.1016/j.marmicro.2005.03.005, 2005.

Myhre, S. E., Kroeker, K. J., Hill, T. M., Roopnarine, P., and Kennett, J. P.: Community benthic paleoecology from high-resolution climate records: Mollusca and foraminifera in post-glacial environments of the California margin, Quaternary Sci Rev, 155, 179–197, https://doi.org/10.1016/j.quascirev.2016.11.009, 2017.

Ohkushi, K., Kennett, J. P., Zeleski, C. M., Moffitt, S. E., Hill, T. M., Robert, C., Beaufort, L., and Behl, R. J.: Quantified intermediate water oxygenation history of the NE Pacific: A new benthic foraminiferal record from Santa Barbara basin, Paleoceanography, 28, 453–467, https://doi.org/10.1002/palo.20043, 2013.

Oksanen, J., Blanchet, F. G., Kindt, R., Legendre, P., Minchin, P. R., O'hara, R. B., Simpson, G. L., Solymos, P., Stevens, M. H. H., and Wagner, H.: Package 'vegan,' 2, 2013.

Oschlies, A., Brandt, P., Stramma, L., and Schmidtko, S.: Drivers and mechanisms of ocean deoxygenation, 11, 467–473, https://doi.org/10.1038/s41561-018-0152-2, 2018.

Palmer, H. M., Hill, T. M., Roopnarine, P. D., Myhre, S. E., Reyes, K. R., and Donnenfield, J. T.: Southern California margin benthic foraminiferal assemblages record recent centennial-scale changes in oxygen minimum zone, 17, 2923–2937, https://doi.org/10.5194/bg-17-2923-2020, 2020.

Praetorius, S. K., Mix, A. C., Walczak, M. H., Wolhowe, M. D., Addison, J. A., and Prahl, F. G.: North Pacific deglacial hypoxic events linked to abrupt ocean warming, Nature, 527, 362-+, https://doi.org/10.1038/nature15753, 2015.

Rathburn, A. E., Willingham, J., Ziebis, W., Burkett, A. M., and Corliss, B. H.: A New biological proxy for deep-sea paleo-oxygen: Pores of epifaunal benthic foraminifera, Sci Rep, 8, 9456, https://doi.org/10.1038/s41598-018-27793-4, 2018.

Roark, E. B., Ingram, B. L., Southon, J., and Kennett, J. P.: Holocene foraminiferal radiocarbon record of paleocirculation in the Santa Barbara Basin, Geology, 31, 379–382, https://doi.org/Doi 10.1130/0091-7613(2003)031<0379:Hfrrop>2.0.Co;2, 2003.

Schimmelmann, A., Hendy, I. L., Dunn, L., Pak, D. K., and Lange, C. B.: Revised similar to 2000-year chronostratigraphy of partially varved marine sediment in Santa Barbara Basin, California, Gff, 135, 258–264, https://doi.org/10.1080/11035897.2013.773066, 2013.

Schmidtko, S., Stramma, L., and Visbeck, M.: Decline in global oceanic oxygen content during the past five decades, Nature, 542, 335-+, https://doi.org/10.1038/nature21399, 2017.

Sharon, Belanger, C., Du, J., and Mix, A.: Reconstructing Paleo-oxygenation for the Last 54,000 Years in the Gulf of Alaska Using Cross-validated Benthic Foraminiferal and Geochemical Records, 36, e2020PA003986, https://doi.org/10.1029/2020PA003986, 2021.

Stott, L. D., Neumann, M., and Hammond, D.: Intermediate water ventilation on the northeastern Pacific margin during the late Pleistocene inferred from benthic foraminiferal delta C-13, Paleoceanography, 15, 161–169, https://doi.org/Doi 10.1029/1999pa000375, 2000.

Stramma, L., Johnson, G. C., Firing, E., and Schmidtko, S.: Eastern Pacific oxygen minimum zones: Supply paths and multidecadal changes, 115, 2010a.

Stramma, L., Schmidtko, S., Levin, L. A., and Johnson, G. C.: Ocean oxygen minima expansions and their biological impacts, Deep-Sea Res Pt I, 57, 587–595, https://doi.org/10.1016/j.dsr.2010.01.005, 2010b.

Stuiver, M. and Polach, H. A.: Discussion reporting of 14 C data, 19, 355–363, 1977.

Talley, L. D.: Distribution and Formation of North Pacific Intermediate Water, 23, 517–537, https://doi.org/10.1175/1520-0485(1993)023<0517:DAFONP>2.0.CO;2, 1993.

Taylor, M. A., Hendy, I. L., and Pak, D. K.: The California Current System as a transmitter of millennial scale climate change on the northeastern Pacific margin from 10 to 50 ka, Paleoceanography, 30, 1168–1182, https://doi.org/10.1002/2014pa002738, 2015.

Tetard, M., Licari, L., Tachikawa, K., Ovsepyan, E., and Beaufort, L.: Toward a global calibration for quantifying past oxygenation in oxygen minimum zones using benthic Foraminifera, 1–17, https://doi.org/10.5194/bg-2020-482, 2021.

Venturelli, R. A., Rathburn, A., Burkett, A., and Ziebis, W.: Epifaunal Foraminifera in an Infaunal World: Insights Into the Influence of Heterogeneity on the Benthic Ecology of Oxygen-Poor, Deep-Sea Habitats, 5, 344, 2018.

Wang, Y., Hendy, I. L., and Zhu, J.: Expansion of the Southern California oxygen minimum zone during the early-to mid-Holocene due to reduced ventilation of the Northeast Pacific, Quaternary Science Reviews, 238, 106326, https://doi.org/10.1016/j.quascirev.2020.106326, 2020.

Chapter 3

A systematic review of Holocene climate and oceanography of the coastal Western United States and Northeast Pacific

Abstract

To understand and contextualize modern climate change, we must improve our understanding of climatic and oceanographic changes in the Holocene (11.75 ka-present). Climate records of the Holocene can be utilized as a "baseline" from which to compare modern climate and can also provide insights into how environments and ecosystems (that are climatically and tectonically similar to present) experience and recover from environmental change. However, individual studies on Holocene climate in the literature tend to focus on a distinct geographic location, a specific proxy record, or a certain aspect of climate (e.g., upwelling or precipitation), resulting in localized, record-specific trends rather than a comprehensive view of climate variability through the Holocene. Here we synthesize the major oceanographic and terrestrial changes that have occurred in the coastal Western United States (bounded by 30°N to 52°N and 115°W to 130°W) through the most recent 11.75 ka and explore the impacts of these changes on marine and terrestrial ecosystems and human populations. This three-tiered systematic review combines interpretations from over 100 published studies, codes and geospatially analyzes temperature, hydroclimate, and fire history from over 50 published studies, and interprets nine representative time series through the Holocene. We find that the early Holocene is characterized by warming relative to pre-Holocene conditions, including warm sea surface conditions, a warm and dry Pacific Northwest, a warm and wet Southwest, and overall spatial and temporal stability. In the mid Holocene, these patterns reverse; this interval is characterized by cool sea surface temperatures, a cool and wet Pacific Northwest and warm and dry Southwest. The late Holocene is the most variable interval, both spatially and temporally, and a new spatial trend appears in terrestrial climate with warmer coastal areas and cooler inland areas relative to coastal. Human communities interacted with the environment throughout the entire Holocene, as

evidenced in archaeological and paleoenvironmental records, yet the recent era of colonization (1850-present) represents an unprecedented environmental interval in many records. Overall, our analysis shows linkages between terrestrial and oceanographic conditions, distinct environmental phases through time, and emphasizes the importance of local factors in controlling climate through the dynamic Holocene.

1 Introduction

1.1 Overview of Holocene Climate

In contrast to past intervals of glacial/interglacial variability, the Holocene has largely been regarded as a climatically stable interval. However, local and global changes in Holocene climate merit further investigation. Meta-analysis of global temperatures and patterns through the Holocene show a globally warm period from 11 to 5 ka, termed the Holocene Climatic Optimum, largely driven by a concurrent peak in solar insolation in the Northern Hemisphere (Mayewski et al., 2004; Wanner et al., 2008; Renssen et al., 2012; Marcott et al., 2013; Bader et al., 2020). Following this period of global warmth, competing lines of evidence show divergent global temperature regimes in the last 5ka, some records show global warming and others global cooling, this phenomenon is termed the Holocene Conundrum (Wanner et al., 2008; Marcott et al., 2013; Liu et al., 2014; Marsicek et al., 2018; Bader et al., 2020). Yet, these global reconstructions typically under-sample records from the North Pacific and Western North America, motivating the need for further analysis of Holocene change over time in this region (Marcott et al., 2013; Kaufman et al., 2020; Praetorius et al., 2020; Walczak et al., 2020).

General trends in global temperature are interrupted by multiple shifts of rapid climate change intervals between climate modes (marked changes in aridity and temperature) (Mayewski et al., 2004; Wanner et al., 2008). Holocene climate variability on various timescales has been attributed to multiple climate forcing mechanisms, including: changes in solar insolation, volcanic activity, land-use change, variations in atmospheric greenhouse gas concentrations, and resultant ocean-climate feedbacks (Crowley, 2000; Bradley, 2003; Atwood et al., 2016). Specifically, Northern Hemisphere solar insolation peaked at 9 ka

and decreased towards the present with important implications for global and regional climate (Renssen et al., 2012; Marcott et al., 2013; Marsicek et al., 2018; Bader et al., 2020). Peak summer insolation in the early Holocene contributed to a warmer Arctic and continued melting of northern hemisphere ice sheets at this time (Renssen et al., 2012; Bader et al., 2020). Globally, episodes of high fire activity were relatively common in the early Holocene with a globally observed increase in fire activity between 3-2 ka, likely due to a change in climate (Marlon et al., 2013).

In North America broadly, mean summer temperatures increased from the last glacial maximum (26-19 ka) (Clark et al., 2009; Waelbroeck et al., 2009) until between 6 and 3 ka by ~4^{O}C and subsequently decreased; variations are documented at 1100 year frequency (Viau et al., 2006). Across the continent, millennial-scale climate variability on the order of 0.2^{O}C occurs across the entire Holocene (Viau et al., 2006). In the early Holocene, solar insolation and ice-sheet dynamics are dominant drivers of North American climate; following the collapse of the Laurentide Ice Sheet, the impact of ice sheet feedbacks on climate is reduced (Viau et al., 2006). Analysis of global and continental trends show a high degree of temporal and spatial climate variability highlighting the need to assess region-specific changes through time. Understanding regional Holocene variability is particularly relevant in order to contextualize biotic and environmental responses to anthropogenic climate change.

1.2 Modern climate and oceanography of Western North America

Western North America currently experiences impacts of drought, fire, fisheries and agricultural changes, heatwaves, and ecological shifts due to climate change (Ainsworth et al., 2011; Westerling et al., 2011; Mann and Gleick, 2015; Wise, 2016). Quantifying climatic and environmental changes over time in this region is of particular importance as it hosts a large modern human population, a multitude of natural resources, and highly biodiverse and productive ecosystems. By investigating climate and environmental change through the Holocene, we can better understand how environments and ecosystems that are climatically and tectonically similar to present experience and recover from environmental change

(Finnegan et al., 2015; Barnosky et al., 2017). We consider integrated physical processes, ecological responses, and human connections in this review and outline modern climate conditions below.

We divide the region into the Pacific Northwest (abbreviated as PNW; including the US states Washington, Oregon, and northern California) and Southwest (abbreviated as SW; including the US states Nevada, Arizona and central/southern California). The interaction between the Aleutian Low-pressure system, North Pacific High-pressure system, and Continental Thermal Low-pressure system drive temperature and hydrographic gradients (Fig. 1). Modern terrestrial climate of the Western United States varies latitudinally with cooler temperatures and wintertime precipitation in the PNW and warmer temperatures, general aridity, and summer precipitation driven by the North American Monsoon (NAM) in the SW(Fig. 1) (Adams and Comrie, 1997; Barlow et al., 1998; Sheppard et al., 2002). Additionally, hydroclimate varies across topographic gradients from West to East with precipitation along the coast and increased aridity in the interior of coastal mountain ranges. Drought is a recurrent and salient feature of climate in the West, particularly in the context of anthropogenic climate change (Fig. 1) (Cook, 2004; Wise, 2016).

Wildfire is a dominant feature of the landscape of the Western United States with climate, vegetation, and human activity all contributing to fire activity (Westerling et al., 2003, 2011; Marlon et al., 2012; Higuera et al., 2021). In areas with sufficient vegetation productivity, high temperatures and drought are consistently linked with greater area burned (Westerling et al., 2003; Marlon et al., 2012; Dennison et al., 2014). In grasslands and shrublands, fire is linked to both antecedent precipitation that drives fuel development and duration of high temperatures. As high temperatures extend into spring and fall, the fire seasons coeval lengthen (Westerling et al., 2003; Marlon et al., 2012; Dennison et al., 2014). As such, the investigation of changes in the fire regime within the paleorecord is useful in identifying the relative importance of temperature, precipitation, vegetation, and human activity on wildfire.

Marine and terrestrial climates are linked in this region; Westerly winds influenced by North Pacific ocean-atmosphere dynamics result in high correlation between North Pacific sea surface temperatures (SST) and coastal air temperatures and hydrography (LaDochy et al., 2007; Barron and Anderson, 2011). The westerly winds generated by the Aleutian Low pressure system and North Pacific High pressure system fuel the California Current System (CCS), which flows southward from ~50° N to ~15°N (Fig. 1) (Hickey, 1979; Checkley and Barth, 2009). The CCS is characterized by strong seasonal wind-driven upwelling that drives high surface productivity along Western North America (Hickey, 1979; Checkley and Barth, 2009; Siedlecki et al., 2015). Respiration, remineralization, and decomposition lead to high organic carbon export and oxygen-depleted (CO_2-rich) bottom waters (Chelton et al., 1982; Checkley and Barth, 2009; Siedlecki et al., 2015). Point Conception is a major oceanographic and biogeographic boundary, with differing conditions and relative impacts of the CCS to the north and south of this point. The interaction of the equatorward California Current, the poleward Davidson Current, and the sub-surface, poleward California Undercurrent drive oceanographic conditions south of Point Conception (Bray et al., 1999). Seasonal, annual, and decadal events, including the Pacific Decadal Oscillation (PDO), North Pacific Gyre Oscillation, and El Niño Southern Oscillation (ENSO) play a significant role in driving Eastern North Pacific SST and productivity across multiple timescales (Lluch-Cota et al., 2001; Batchelder and Powell, 2002; Mantua et al., 2002; Chavez et al., 2003; Di Lorenzo et al., 2008).

Changes to climate and oceanographic conditions have important implications for ecological systems. The Northeast Pacific is a highly productive eastern boundary, upwelling system supporting diverse and productive coastal ecosystems. Changes in marine currents, upwelling regime, and temperature impact primary production, with cascading implications for the entire marine food web (Barron et al., 2003b; Yati et al., 2020). In terrestrial systems, variability in precipitation, air temperature, and fire regime exert strong control over plant and animal communities (Marlon et al., 2006; Beaty and Taylor, 2009; Clark et al., 2012; Kirby et al., 2015; Shuman et al., 2018).

Climate and environmental change through time impact human communities that have been present in Western North America throughout the Holocene. Evidence from over 40 archaeological sites in North America shows humans were likely present before, during, and after the Last Glacial Maximum (26.5-19 ka) (Becerra-Valdivia and Higham, 2020). Additional evidence for human presence and societal expansion within the geographic (Washington through Baja California) and temporal (Holocene) range of this review includes archaeological evidence from shell middens as well as Indigenous oral histories (Erlandson et al., 2007, 2009; Kennett et al., 2007; Rick, 2011; Braje et al., 2012; McKechnie, 2015; Becerra-Valdivia and Higham, 2020). Previous work has investigated linkages between climate and human communities on a local scale through the Holocene (Erlandson et al., 2007; Kennett et al., 2007; Rick, 2011; Braje et al., 2012; Glassow et al., 2012; McKechnie, 2015); these relationships will be further explored in this review.

Here, we summarize and synthesize over 100 published records of both marine and terrestrial systems from the Western US and Northeast Pacific (See Appendix) resulting in the most comprehensive multi-proxy Holocene climate reconstruction for this region to date. This systematic review addresses the following linked research questions:

- What are the major patterns and climatic phases during the Holocene for the Western United States?
- How do marine and terrestrial environments interact in this region during the Holocene?
- How do climate and oceanographic changes impact ecological and human communities in the Holocene?

2 Methodology

For the purposes of this paper we follow the standard convention formally recognized by the International Commission on Stratigraphy (Walker et al., 2018); early Holocene (Greenlandian, 11.75-8.2 ka), mid Holocene (Northgrippian, 8.2-4.2 ka), and late Holocene (Meghalayan, 4.2-0 ka). We do include

interpretations that span across these sub-epoch time intervals. We constrain our study to the geographic region bounded by 30°N to 52°N and 115°W to 130°W as this region has an abundance and variety of long-term records and well-documented human-environment interactions through the Holocene.

A multi-step systematic review was conducted to select previous studies for inclusion in this review. In the first step, we identified studies that met the following criteria: records from Western North America and the Northeast Pacific and that represented Holocene aged reconstructions. Records were initially found using the following topics as search terms: marine temperature, ocean circulation, marine productivity, terrestrial hydroclimate, drought, floods, terrestrial temperature, fire, archaeology, marine ecology, and terrestrial ecology. Each paper was then evaluated with a second set of criteria for inclusion in the paper. Records with a published age model and scope of the study within the defined geographic region (30°N to 52°N and 115°W to 130°W) were selected for inclusion.

A total of 101 papers matched these criteria and were categorized as providing constraints on: marine temperature, circulation, and productivity; terrestrial hydroclimate; terrestrial temperature and fire; archaeology, marine ecology, and terrestrial ecology. A wide range of archive types are represented here: archaeology (8 papers), dendrochronology (2), speleothem (3), lacustrine sediments (36), marine sediments (31), and other records including geomorphology, animal midden, and lichen archives (7). This paper makes no attempt to evaluate the effectiveness of each proxy or to re-examine the primary data; rather, interpretations of data from original work are maintained. Interpretations in original papers are based on a variety of well-established proxies: alkenones (2 papers), carbon and nitrogen isotopes of bulk sediments (3), charcoal (14), diatom and silicoflagellate assemblage (7), foraminiferal assemblage (9), geomorphology (3), hydrogen isotopes from leaf wax (4), oxygen and carbon isotopes of nearshore marine organisms (7), oxygen and carbon isotopes of biogenic and non-biogenic calcite (marine and terrestrial, 10), macrofossil abundance (6), pollen assemblage (25), radiocarbon dating (as a proxy, not

only for age model development 3), sedimentology, including grain size analysis, lithology, organic content, carbon content analysis (29), and tree ring/tree stump analysis (4).

In the second step of the systematic review process, we identified papers that met a second set of criteria, coded results through time, and conducted a spatial and temporal analysis of the synthesis. We selected all studies that span an interval of the Holocene, exceeding 3000 years, and in which the authors identified a clear climatic pattern for an entire Holocene interval. Results from each paper were binned into time intervals: early, mid, and late Holocene, and coded using the following categories: hydroclimate (wet or dry), temperature (warm or cold), and fire activity (high or low). Results were coded using keywords from the original authors' description of climate conditions at each point in time: temperature keywords: warm, cold, cool; hydroclimate keywords: wet, dry, moisture, arid(ity), pluvial, fluvial, precipitation; fire keywords: high, low, activity, frequency, return interval, intensity. We generated a database that contains paper (author, date), latitude, longitude (of all sites within each paper), region (PNW or SW), archive type, and coded results for each category (hydroclimate, temperature, fire activity) in each interval (early, mid, late). Primary data were not reevaluated; rather, interpretations of data from original work are maintained (Appendices 4-6). For example, changes in SST may be inferred from alkenones, foraminiferal assemblages, or foraminiferal isotope records in previously published studies, but all are represented as temperature in the coded database. We utilize the term "fire activity" to be inclusive of multiple paleofire proxy types including fire return intervals, CHAR, charcoal accumulation, and others. Some papers contributed multiple data points to this step, for example, some records included interpretations of multiple processes (e.g., temperature and hydroclimate) and some include interpretations across multiple time intervals (early, mid, late). Yet, papers that only included one interpretation in one interval are also included. For the papers analyzed here, the SW (30° - 40° N, 32 papers) is more data rich than the PNW (40°- 47°N, 17 papers) and data are fairly well distributed across all three time periods (Figs. 2,3). Results of coded analysis were plotted in space through the three time intervals (early, mid, late Holocene) (Figs. 2,3). Base maps with elevation were generated using the R

package marmap (Pante and Simon-Bouhet, 2013) accessing bathymetric and elevation data from the NOAA ETOPO1 global relief model (Amante and Eakins, 2009).

Following the spatial and temporal analysis, we highlight a subset of regionally representative time series records from the PNW (Fig. 4) and SW (Fig. 5). We prioritized records with high temporal resolution, continuous records, and records that span at least two intervals of the Holocene (Kaufman et al., 2020). Further, we selected records that represent temperature, hydroclimate, and fire activity for each region (PNW and SW). For these purposes, data was accessed through original papers, supplemental information, or through the NOAA Paleoclimate Database.

3 Results and discussion

3.1 Early Holocene (11.75-8.2 ka)

Thirty-seven papers encompassing 60 sites fit the criteria for inclusion in the spatial analysis. Archives included lake sediments (17 papers), marine sediments (15 papers), and three others (archaeological, geomorphology, speleothem) (Appendix 5).

3.1.1 Regional synthesis

Spatial analysis of coded hydroclimate, temperature, and fire history indicate that the early Holocene was generally characterized by a dry and warm PNW and a wet and warm SW (Fig. 2). These trends are also observed in time series data from both regions (Figs. 4, 5). In the PNW, sea surface temperatures were warm, winters were dry, and fire activity was high (Fig. 4). In the SW, sea surface temperatures were warm, terrestrial temperatures were cold, fire activity was low, and hydroclimate was generally wet (Fig. 5).

Generalized warming in the early Holocene relative to pre-Holocene conditions follows two abrupt Northern hemisphere climate transitions, characterized by rapid warming during the Bølling–Allerød

(14.7-12.9 ka) and rapid cooling associated with the Younger Dryas (12.9-11.7 ka) (Barron et al., 2003b; McGann, 2015). Sea surface temperatures were warm across the entire coastal Northeast Pacific during the early Holocene (Fig. 2), likely driven by high summer insolation (insolation maximum at 9 ka) and warming following deglaciation. Despite warm SST across the region, terrestrial hydroclimate and temperatures varied latitudinally, indicating regional differences in marine-terrestrial climate linkages and impacts of the insolation maximum (Fig. 3). In the PNW, warm SSTs co-occured with warm and dry terrestrial conditions (Heusser, 1998; Barron et al., 2003b; Steinman et al., 2016), while in the SW, wet conditions were driven by the evolution of the North American Monsoon (NAM) and the resultant increase in summertime precipitation in the early Holocene relative to pre-Holocene (Fig. 2) (Bird and Kirby, 2006; Kirby et al., 2015; Metcalfe, 2015).

3.1.2 Terrestrial climate

In the PNW, multiple records show warm and dry conditions in the early Holocene (Mohr et al., 2000; Hallett et al., 2003; Briles et al., 2005; Malamud-Roam et al., 2006; Marlon et al., 2006; Gavin et al., 2007; Long et al., 2011; Steinman et al., 2019). Drier than modern conditions existed in locations dominated by winter precipitation (largely PNW) (McGann, 2011; Hermann et al., 2018). An East-West precipitation gradient was established with warm and drier conditions in the East and wet conditions in the West (Brown and Hebda, 2002), fire activity was high at multiple locations (Hallett et al., 2003; Marlon et al., 2006; Gavin et al., 2007; Steinman et al., 2019), and the amount of biomass burning and the extent of tree cover increased during this time (Figs. 2, 3) (Marlon et al., 2006; Gavin et al., 2007). The early Holocene increase in fire activity in the PNW relative to pre-Holocene conditions may have been caused by warmer/drier conditions resulting from amplified seasonality due to increased insolation relative to pre-Holocene (Walsh et al., 2017; Steinman et al., 2019). In some locations (i.e., Scanlon and Castor Lake), fire frequency increased relative to glacial, but remained lower relative to the mid or late Holocene (Walsh et al., 2017). Few records show wet conditions in the PNW during the early Holocene (McQuoid and Hobson, 2001).

In California's Central Valley and Sierra Nevada, the early Holocene was wet with low or variable fire frequency (Figs. 2, 3) (Benson et al., 2002; Bacon et al., 2006; Negrini et al., 2006; Hallett and Anderson, 2010). Fuel abundance exerted a stronger control on fire than regional climate (Hallett and Anderson, 2010). In the Eastern Sierra Nevada (i.e., Lower Gaylor Lake and Barrett Lake near Mono Lake), low biomass (sparse pine dominated forests and chaparral shrubs) reinforced by low snowpack persistence due to the insolation maximum, led to low fire frequency (Hallett and Anderson, 2010). In the Lake Tahoe Basin, precipitation was high in the early Holocene and fire frequency was low in the very early Holocene (11-9 ka) and transitioned to higher fire frequency than modern from 9 ka through mid Holocene (Lindstrom, 1990; Benson et al., 2002; Beaty and Taylor, 2009).

In comparison to the arid PNW, early Holocene conditions in the SW were largely wetter than modern (Fig. 2). Lacustrine records from across the SW show heavy precipitation in the early Holocene (Bird and Kirby, 2006; Kirby et al., 2007, 2010, 2012, 2014, 2015; Bird et al., 2010; Du et al., 2018). Wet conditions at this time were driven by the development of the NAM (Bird and Kirby, 2006; Kirby et al., 2007; Marcott et al., 2013; Hermann et al., 2018). The enhancement of the NAM is attributed to warm SSTs in the Gulf of California and to the early Holocene winter insolation minimum and summer insolation maximum leading to an increased frequency of both winter storms and of tropical cyclones making landfall in southern California (Bird and Kirby, 2006; Kirby et al., 2007; Marcott et al., 2013; Hermann et al., 2018). A pluvial episode was synchronous across multiple sites in southern California from 9.1 to 8.25 ka and may have been driven by atmospheric river-like winter storms (Kirby et al., 2012). High moisture/precipitation is shown in both inland (desert) and coastal sites, including increased runoff into the Santa Barbara Basin from 9 to 8.5 ka (Kirby et al., 2007, 2010, 2012, 2014; Du et al., 2018). In contrast, lake sediment records from southern California that resolve summer evaporation show high evaporation and multiple intervals of drought in the early Holocene; high winter precipitation and

high summer evaporation may explain the differences between multiple records in this region (Kirby et al., 2019).

3.1.3 Marine conditions

Offshore of southern Oregon through Central California, the early Holocene was characterized by warm SSTs resulting from subtropical waters transported by currents comparable to the modern-day Davidson Current (Figs. 1, 2) (Mix et al., 1999; Barron et al., 2003b; Barron and Bukry, 2007a). In this area, the oceanographic regime was characterized by overall warm conditions, moderate to high export productivity, ventilation of deeper waters, and the development of the oxygen minimum zone (Barron et al., 2003b; McGann, 2011; Addison et al., 2017). During this time, the California Current was weaker than present allowing a strong northward Davidson-like current (Barron and Bukry, 2007a). Though upwelling was weaker than modern in the early Holocene, records from offshore Oregon show moderate marine productivity and multiple records indicate an increase in coastal upwelling beginning at 9 ka (Gardner et al., 1988; Barron et al., 2003b; Addison et al., 2017; Barron et al., 2017).

Offshore southern California (in Santa Barbara Basin), high productivity and overall warm SSTs occurred during the early Holocene (Kennett et al., 2007; Fisler and Hendy, 2008). Records extending from northern California south to the Baja California (Sur) peninsula indicate that in many locations, the onset of poorly oxygenated conditions in subsurface and intermediate waters occurred in the early Holocene, indicating changes in surface water productivity, intermediate water ventilation, or both relative to pre-Holocene conditions (Kennett and Ingram, 1995; Mix et al., 1999; Roark et al., 2003; van Geen et al., 2006; Moffitt et al., 2014). Changes in the strength or source of North Pacific Intermediate Water and the incursion of lower oxygen intermediate waters in Santa Barbara Basin (SBB) are also indicated (Roark et al., 2003; Moffitt et al., 2014).

3.1.4 8.2 ka Event

The end of the early Holocene is marked by a large-scale Northern Hemisphere cooling event initiated by an abrupt drainage of Lake Agassiz into the North Atlantic that weakened Atlantic Meridional Overturning Circulation, and is well documented in many records (Thomas et al., 2007; Matero et al., 2017; Estrella-Martínez et al., 2019; Voarintsoa et al., 2019). Although this is a globally well described event, relatively few records (fewer than 10 records reviewed in this paper) from the Northeastern Pacific and Western United States record impacts of this event. In central California (White Moon Cave), speleothem records show increased effective moisture at 8.2 ka which is attributed to intensification of the Pacific storm track that is synchronous on Eastern and Western sides of the Pacific (Oster et al., 2017). A lake record from Dry Lake in the SW (San Bernardino Mountains) shows a cooler, dryer and enhanced erosional period during the 8.2 ka event (Bird and Kirby, 2006). Marine records from off the coast of northern California (near the California-Oregon border) show a cold event at 8.2 ka, but this is not noted in other nearby marine records (Barron et al., 2003b). We hypothesize that the 8.2 ka event has a limited impact in this region, apart from the teleconnected impact of changes to the Pacific storm track impacting local hydroclimate.

3.1.5 Ecological responses to change

In the early Holocene, terrestrial plant communities generally indicate warm conditions, but show a process of succession out of glacial-associated ecosystems (Heusser, 1998). In the PNW, expansion of alder (*Alnus*) and ferns (*Pteridium*) began at the start of the Holocene, and Douglas fir (*Pseudotsuga menziessii*), western hemlock, grasses (*Poaceae*), and bracken fern (*Pteridium*) forests emerged by the end of the interval (Heusser, 1983; Pellatt et al., 2001). Southern Oregon cave records demonstrate taxonomic stability in plant communities through the early Holocene with communities dominated by pine (*Pinus*) and sagebrushes (*Amaranthaceae*, A*rtemisia*) (Beck et al., 2018). In the Klamath mountains, pine and oak (*Quercus*) dominated the pollen record during the warm dry early Holocene; similarly, pine, oak, and juniper dominated the record in the Siskiyou Mountains (Mohr et al., 2000; Briles et al., 2005).

In northern California, pollen assemblages indicate warm winters, including an expansion of coastal redwoods, and declining alder (*Alnus*) forests (Barron et al., 2003b; Lyle et al., 2012). The increasing upwelling during the Holocene led to enhanced coastal fog and as a result, increasing dominance of coastal redwood (*Sequoia sempervirens*) (Gardner et al., 1988; Barron et al., 2003b; McGann, 2015; Addison et al., 2017). In Central California, increases in redwoods, oaks, *Nepenthes densiflora*, and *Asteraceae* indicate warmer and wetter conditions relative to glacial (McGann, 2015). In southern California, the early Holocene maintained a forest ecosystem distinct from the modern with more pines and conifers than in the late Holocene and modern (Heusser, 1978).

In marine systems off the coast of northern California (Farallon Escarpment and offshore of the Russian River) transitions in planktic and benthic fauna occurred during the early Holocene as environmental conditions transition out of the glacial (Gardner et al., 1988; McGann, 2011). From 11.75 to 10 ka marine sediment records show low abundance of the upwelling-associated diatoms *Thalassionema nitzschioides* and *Thalassionema longissimi,* and the dominance of a cool, subpolar foraminiferal assemblage (Gardner et al., 1988). By 10.5-9 ka, carbonate productivity and total carbon peaked and warm water morphotypes of foraminifera were dominant across two northern California marine sediment records during this spike in productivity (Gardner et al., 1988; McGann, 2011). In coastal systems, kelp forests were present along the entire coastline from the SW to the PNW and increased in both size and range during the early Holocene (Erlandson et al., 2007; Graham et al., 2010). In deeper waters, the gradual development of the oxygen minimum zone in the early Holocene led to a transformation of seafloor ecosystems to a low oxygen-adapted assemblage (Cannariato and Kennett, 1999; Moffitt et al., 2014). Off the coast of Point Conception, seafloor fauna (e.g., benthic foraminifera) were variable in the early Holocene, with the establishment of the modern fauna by 9ka (McGann, 2015). In Northern (Farallon Escarpment) and southern California (SBB), low oxygen conditions developed during the early Holocene and caused a shift in benthic fauna during this interval (Cannariato and Kennett, 1999; McGann, 2015).

3.1.6 Human-environment interactions

Evidence for human presence and settlement along the North American Pacific coast throughout the Holocene is well documented in Indigenous ethno-history and archaeological records, yet these records are geographically disparate (Erlandson et al., 2007; McKechnie, 2015; Edinborough et al., 2017). In the PNW, archaeological evidence for human presence is documented prior to the start of the Holocene (Kaufman et al., 2016; Beck et al., 2018; Becerra-Valdivia and Higham, 2020). One hypothesis for human migration across this region suggests that the southward migration of people just prior to the Holocene was correlated with the availability of marine resources (Erlandson et al., 2007). Abundant early Holocene archaeological records from the Channel Islands show evidence of a diversified maritime economy, consumption of shellfish, marine mammals, and fin fish, yet a relatively small population size relative to later in the Holocene (Erlandson et al., 2007, 2009; Braje et al., 2012). Additional localized studies of human responses to environmental and ecological variability on the Channel Islands capture snapshots of human-environment interaction in the early Holocene, but do not capture the full time interval and thus are not included here.

3.2 Mid-Holocene (8.2-4.2 ka)

Thirty-five papers encompassing 60 sites met the criteria for spatial analysis and were coded and plotted in Figs. 2 and 3. Archives included lake sediments (n=19), marine sediments (n=14), and two others (terrestrial midden, tree stump) (Appendix 5).

3.2.1 Regional synthesis

Spatial analysis of coded hydroclimate, temperature, and fire history indicates that the mid Holocene was characterized by a wet and cool PNW and a dry and warm SW relative to modern conditions (Fig. 2). Fire activity was high in the Sierra Nevada mountains and variable and transitional in the PNW (Fig. 3). Time series analyses supports these findings: offshore of the PNW, sea surface temperatures were cool, upwelling activity was moderate and terrestrial PNW winters were wet, fire activity was low and variable,

and the overall hydroclimate was wet relative to the early Holocene (Fig. 4). In the SW, sea surface temperatures were warm, fire activity was high, hydroclimate was generally dry, and human-environment interactions increased as populations in this region increased relative to the early Holocene (Fig. 5).

Hydroclimate and temperature trends functionally reversed in the mid Holocene relative to the early Holocene, and the mid Holocene was a time of transition and variability in many records (Figs. 4, 5). In the PNW, SST transitions from warm to cool temperatures coeval with a shift from warm and dry to cool and wet terrestrial conditions. These coincident transitions suggest that the mechanisms for marine-terrestrial climate linkages persisted through the early and mid Holocene, namely a negative correlation between marine temperatures and terrestrial moisture/precipitation (Fig. 2). Yet nuanced changes occurring on shorter timescales may play an important role in determining hydroclimate of the region. A previously published review of hydroclimate records in Western North America (PNW, northern Rockies and most of California) at 6 ka shows aridity in areas that are dominated by winter precipitation, including multi-decadal to centuries-long 'mega droughts' due to reduced winter water vapor transport (Hermann et al., 2018). However, our findings reveal that when evaluated at a broader timescale (8.2-4.2 ka), the mid Holocene PNW is cool and wet (Fig. 2). We posit two hypotheses to reconcile these differences. First, we propose that the coastal PNW was wet and cool whereas interior areas may have been dry (Hermann et al., 2018). Alternatively, in the PNW, this time period may have been characterized by seasonal hydroclimate extremes, multiple records identify high winter precipitation and warm summers with high evaporation (Marlon et al., 2006; Whitlock et al., 2008; Steinman et al., 2016), thus exhibiting both wet and dry phases on short timescales. As such, seasonally resolved proxies are particularly advantageous to fully capture climate in the past.

The shift in SW terrestrial hydroclimate from wet in the early Holocene to dry in the mid Holocene (Fig. 2) may be due to several processes. A southward shift in NAM occurred between 9 and 6 ka, resulting in Mexico, rather than California, receiving a higher amount of precipitation (Metcalfe, 2015). Further,

pluvial episodes driven by atmospheric river-type storms are rare in the mid Holocene, with the exception of one pluvial episode from 7.0-6.4 ka that is synchronous across several southern California records (Kirby et al., 2012). Both phenomena (atmospheric rivers and NAM) are linked to changes in eastern tropical Pacific SSTs, rather than adjacent marine conditions in the Northeast Pacific (Fisler and Hendy, 2008; Kirby et al., 2012; Metcalfe, 2015). Thus, the lack of precipitation, driven by a local reduction in the NAM, a southward shift in the NAM, or absence of atmospheric river-like storms or the combination of all three led to overall aridity in the Southwest in the mid Holocene, and may not have been driven by local changes in SST of adjacent marine systems (Fig. 2).

3.2.2 Terrestrial climate

Between 8.2 to 4.2 ka, terrestrial conditions were generally cool and wet in the PNW and warm and dry in the SW, while marine systems were generally cool (Fig. 2), yet the mid Holocene was a time of transition and variability in terrestrial climate. A transition to cooler, wetter conditions during the mid Holocene occurred across several sites in the PNW (Nederbragt and Thurow, 2001; Marlon et al., 2006; Long et al., 2011; Walsh et al., 2017). For example, lake sediment records from north-central Washington (Scanlon and Castor Lake) demonstrate the variability in mid Holocene hydroclimate including low lake stand at 7 ka and high lake stand at 5 ka (Steinman et al., 2019).

Fire records from the PNW indicate a transition in hydroclimate and vegetation (Fig. 3). Fire activity increased on Vancouver Island, in the Oregon coast range, and in the Klamath and Siskiyou mountains through this interval (Brown and Hebda, 2002; Briles et al., 2005; Whitlock et al., 2008; Long et al., 2011). In Oregon and the northern Rocky Mountains, the combination of cooler, wetter conditions increased fuels and hot, dry summers led to more severe and larger fires relative to the early Holocene (Marlon et al., 2006; Whitlock et al., 2008). In coastal areas, increases in fire activity were linked to increased summer drought over time (Briles et al., 2005; Whitlock et al., 2008). Yet, in other nearby regions, fire activity was variable: on Mount Rainier, fire activity increased from 8 to 6.6 ka and

decreased from 6.6 to 4 ka (Walsh et al., 2017), in northern Washington, fire frequency decreased at the start of the mid Holocene with the development of cooler, wetter summers, yet increased again at 4.5 ka (Gavin et al., 2007).

In the mid Holocene, the Sierra Nevada was dry relative to the early and late Holocene (Lindstrom, 1990; Benson et al., 2002; Hallett and Anderson, 2010; MacDonald et al., 2016). A northerly shift in the Intertropical Convergence Zone (ITCZ) in the mid Holocene led to reduced winter precipitation (including snowpack), which led to drier summers and increased fire frequency relative to early Holocene (Hallett and Anderson, 2010). Previous work investigating paired marine-terrestrial records from the Sierra Nevada (Kirman Lake) and eastern tropical Pacific highlight the connection between SST cooling (in the eastern tropical Pacific) and increased aridity (MacDonald et al., 2016). The marine-terrestrial link driving precipitation patterns was strongest throughout the mid Holocene, particularly from ~ 8 to 3 ka (MacDonald et al., 2016). The combination of aridity and increased biomass, led to control of fire by climate in the Sierra Nevada Mountains (Fig. 3) (Hallett and Anderson, 2010). Increased fire activity was synchronous with warming in the Eastern Sierra beginning at 5 ka (Hallett and Anderson, 2010). Additionally, high fire frequency in Lake Tahoe Basin in the mid Holocene (peak at 6.5 ka) was synchronous with high fire frequency in N. California and Oregon and is attributed to warm dry climate in the Lake Tahoe Basin at this time (Beaty and Taylor, 2009).

In the SW, the mid Holocene is characterized by generalized arid conditions. Lake records from the Mojave Desert (Silver Lake, California) indicate a distinct dry period from ~4.2-7.8ka (Kirby et al., 2015). Vegetation traces (macrofossils and pollen) from packrat middens in the Mojave Desert indicate increased aridity compared to modern with a particularly arid period from 6.8 to 5.0 ka (Spaulding, 1991). Pollen records from marine sediments offshore Central California identify a “mid Holocene dry period” from 8-6.4 ka (McGann, 2015). On the Channel Islands, hydroclimate conditions shifted from dry to wet at ~6.9 ka, coincident with an increase in fire activity (Anderson et al., 2010). Despite aridity in the desert

SW, marine sediment records from SBB show extreme precipitation events with increased flooding occurring between 7.3-6.6 ka and 5.5-3.0 ka (Du et al., 2018). Finally, lake sediment records from Lake Elsinore show multiple pluvial episodes and lower relative evaporation in the mid Holocene (Kirby et al., 2019).

3.2.3 Marine conditions

In the mid Holocene, records indicate that off the coast of Oregon and California, sea surface temperatures were cool, while the Santa Barbara Basin was warm (Fig. 2) (Mix et al., 1999; Fisler and Hendy, 2008; Barron and Anderson, 2011; Barron et al., 2019). Generally, the North Pacific was experiencing negative PDO or La Niña-like conditions, with a weak/west-shifted winter Aleutian Low and strong/northward summer North Pacific High (Barron and Anderson, 2011). A dominant feature of mid Holocene Eastern North Pacific oceanography was an increase in coastal upwelling. Marine sediment records from offshore of northern California (40.9°N, 124.6°W) suggests a two-fold increase in upwelling and coastal fog beginning at 5.4 ka and a decrease in SST at 5 ka (Barron et al., 2003b; Addison et al., 2017). Coastal upwelling off California was enhanced during the summer and fall but suppressed during the spring as a result of a strong North Pacific High driven by orbital forcing (Diffenbaugh et al., 2003; Diffenbaugh and Ashfaq, 2007; Barron and Anderson, 2011). The increase in upwelling is due to a strengthening of the California Current and is documented as far south as Point Conception but is not documented in Santa Barbara Basin (Barron and Bukry, 2007a). Despite a cooling trend seen in multiple records from off the coast of Oregon and northern California, records from offshore Central California (Farallon Escarpment) show a slight warming trend through time, but at a decreased rate relative to the early Holocene, a decrease in carbonate productivity and total carbon export, relative to the early Holocene and continued low oxygen at depth (McGann, 2011). Warming conditions through the mid Holocene observed offshore Central California conflict with studies from further north showing a cooling trend, but compare favorably with records of warming from farther south (McGann, 2011).

Sea surface temperatures during the mid Holocene were generally warm in SBB and periodically punctuated by short cool periods at 8.2, 7.6, 5, 4.2 ka (Fisler and Hendy, 2008) and an interval of cold, high productivity from 5.8-6.3 ka (Kennett et al., 2007). Additional evidence from SBB shows that the mid Holocene was warmer and more variable than the early Holocene which may have been due to increased decadal scale variability (Friddell et al., 2003; Fisler and Hendy, 2008). SSTs in SBB initially rose by 3-4^{O}C followed by an abrupt increase of > 2^{O}C in less than 40 years at 7.5 ka (Friddell et al., 2003). Nearshore conditions on the Channel Islands were variable with an interval of cooler than modern SST during 6.3-5.3 ka preceded and followed by intervals of warmer than modern SSTs (Glassow et al., 2012). Circulation and ventilation of relatively young North Pacific Intermediate Water into SBB was stable through the mid Holocene (Roark et al., 2003). When compared to global records, SST trends from the North Pacific (generalized warming in the North Pacific from 7 ka to present) are inversely correlated with the SST in the North Atlantic (Kim et al., 2004).

3.2.4 Ecological responses to climate change

In the PNW, ecosystems responded to increases in moisture in the mid Holocene. The establishment of rainforest taxa in northern Cascades forest occurred during wet conditions and a variable fire regime in the mid Holocene (Hallett et al., 2003). Lake sediment records from near Mount Rainier show a shift to cooler, wetter conditions and a transition to mesic forests, indicating an increase in effective moisture (Walsh et al., 2017). In British Columbia, mild winters led to an increase in oaks, hemlock, and grasses during this interval (Pellatt et al., 2001). In northern Washington, lodgepole pine-dominated forest transitioned to a forest with abundant western white pines and Douglas-fir trees (Gavin et al., 2003, 2007). Near the end of the mid Holocene (~4.5 ka), fire frequency once again increased, despite the development of the modern western hemlock and redcedar forest that typically indicate cooler, wetter climate and mild summers (Gavin et al., 2003, 2007). In contrast, one record from the Saanich Inlet (British Columbia) shows that oak and Douglas fir increased during this time (Heusser, 1983, p.19). In

northern California, terrestrial systems shifted from dominance by pine to an increased presence of *Sequoia* coastal redwoods, indicating an increase in fog (Barron et al., 2017)

Farther south, pollen records from Santa Barbara Basin show numerous changes in terrestrial ecosystems during this interval, including a decrease in *Pinus* and conifers; a general decrease in all trees leads to a temporary peak in herbaceous plants (*Asteraceae*) (at 5 ka) followed by a transition to a chaparral, coastal sage scrub dominated ecosystem and an increase in oaks (Heusser, 1978, 1998). A brief period of dry conditions from 8-6.4 ka led to an increase in herbs (*Asteraceae*) and pines with a coincident decrease in oaks and tanoak (*N. densiflora*) in Central California (McGann, 2015). In southern California, salt marsh fauna peaks at 6 ka and riparian community plants generally decrease through the Holocene; changes that are linked to drying trends in the SW in the mid Holocene (Heusser, 1978).

In marine systems offshore northern California, the increase in upwelling through the mid Holocene impacted both planktic and benthic ecosystems. For example, *T. nitzschioides* dominate the diatom/silicoflagellate assemblage, which indicates a shallow thermocline, high productivity within the California Current, and increased upwelling (Gardner et al., 1988; Barron et al., 2017). In SBB, an increase in warm water planktics and a *Neogloboquadrina incompta* dominated assemblage indicates a stable, warm, and stratified water column (Fisler and Hendy, 2008). The establishment of the modern low oxygen zone continues in this interval, with important implications for seafloor ecosystems including the development of a novel community between 7-5 ka, associated with sulfide-rich, anoxic chemosynthetic seafloor ecosystems in SBB (Moffitt et al., 2015).

3.2.5 Human-environment interactions

Similar to the early Holocene, much of the evidence of human activity and interaction with the environment during the mid Holocene is centered at the Channel Islands due to exceptional preservation of shell middens. In the mid Holocene, human population on the Channel Islands increased resulting in

enhanced marine harvesting pressure after 6 ka, as indicated by an increase in shell midden diversity (Fig. 5) (Braje et al., 2012). Increased reliance on marine resources for food may have also been due to severe arid conditions (6.3 – 5.0 ka) that reduced terrestrial resources and availability of drinking water. This environmental shift facilitated an increase in fisheries as well as coastal shellfish harvesting (Kennett and Kennett, 2000; Kennett et al., 2007). Further, evidence of exchange between people on the Channel Islands with people in the Great Basin increased during this time and by the mid Holocene, semi-permanent villages were established on the Channel Islands (Kennett and Kennett, 2000; Kennett et al., 2007). As in the early Holocene, records of human community occupation and interactions with the environment are widespread in the mid Holocene, yet most represent snapshots in time and thus, are not included in the review.

3.3 Late Holocene (4.2 ka-present)

Twenty-eight papers encompassing 66 sites met the criteria for spatial analysis and were coded and plotted in Figs. 2 and 3. Archives included lake sediments (n=16) and marine sediments (n=12) (Appendix 5).

3.3.1 Regional synthesis

Analysis of coded hydroclimate, temperature, and fire history shows that the late Holocene was characterized by a wet PNW and wet and variable SW relative to the early and mid Holocene (Fig. 2). Marine temperatures were warm while terrestrial temperatures were cool and variable across both regions (Fig. 2). Fire activity was high and varied across both regions (Fig. 3). In the PNW, SSTs were warm, upwelling activity was high, coastal fog and moisture increased, fire activity was high, and the overall hydroclimate was variable (Fig. 4). In the SW, SSTs were variable, fire activity was high and variable, hydroclimate was generally wet, and human-environment interactions increased as populations in this region grew (Fig. 5). Due to the accessibility of more recent records, late Holocene records are abundant, yet despite this, fewer late Holocene studies were included in the coded spatial analysis relative to the mid

or early Holocene as relatively few presented a coherent finding for the entire interval and intra-record variability was high in the late Holocene. Although for some records, temporal resolution increases towards the present, increased variability relative to the early and mid Holocene is persistent across multiple proxy types and temporal scale of record.

In comparison to the early and mid Holocene, the late Holocene shows greater variability in hydroclimate, temperature, and fire history both within and among records. Marine-terrestrial linkages in the late Holocene also show high variability and an increase in dominance of decadal to annual phenomena (Fig. 2). Coastal upwelling and precipitation are linked; intervals of stronger upwelling are linked to wetter conditions, and reduced upwelling is tied to aridity. In the late Holocene, upwelling and precipitation increased in magnitude and variability through this interval (Ingram, 1998; Addison et al., 2017). Changes in PDO exerted control on terrestrial hydroclimate. A period of negative PDO at 1.1-0.7 ka, with cooler North Pacific SST and higher upwelling, is coeval with prolonged drought in western North America (MacDonald and Case, 2005). Southwestern droughts in late Holocene co-occur with cooler than average SST in SBB. Similarly, nearshore records from Central California show high SST variability coincided with drought during the interval from 0.7-0.5 ka (Fig. 2) (Jones and Kennett, 1999; Barron et al., 2010). Late Holocene changes to PDO and ENSO progressed northward, with enhanced ENSO/PDO effects beginning at 4 ka in southern California and 3.4 ka in northern California (Barron and Anderson, 2011). Further, the late Holocene exhibited alternating wet and dry cycles that may be linked oscillation of precipitation sources between tropical and North Pacific-sourced water (Feakins et al., 2014; Kirby et al., 2014). High variability within and between records (Figs. 2, 3) is a dominant trend across both the PNW and SW in the late Holocene.

3.3.2 Terrestrial climate

Hydroclimate varies spatially and temporally through the late Holocene with the highest and most variable fire activity relative to the early or mid Holocene (Figs. 2, 3). In the PNW, multiple records

show a cool and wet climate, with pronounced wet periods (Mohr et al., 2000; Nederbragt and Thurow, 2001; Reyes and Clague, 2004; Briles et al., 2005; Malamud-Roam et al., 2006). However, trends of increasing aridity towards the present and intervals of drought are also documented (Steinman et al., 2016, 2019; Walsh et al., 2017; Shuman et al., 2018). In the San Francisco Bay region, hydroclimate was also variable, with intervals of aridity documented at 3.0-2.5 ka and 1.7-0.73 ka (Byrne et al., 2001; McGann, 2008).

In the PNW, fire activity was high and variable in the late Holocene, despite intra-regional differences in hydroclimate and vegetation. Fire activity on Mount Rainier was highest in the past 4 ka relative to the rest of the Holocene, and conditions became increasingly dry throughout the late Holocene (Steinman et al., 2016, 2019; Walsh et al., 2017). Vegetation records show a surprising dominance of flora associated with cooler, wetter conditions despite the highest number of fire episodes and shortest fire return intervals during this period (Walsh et al., 2017). In North Cascades National Park in northern Washington, high variability in fire frequency and lower synchrony among forest fire events occurred even within the same forest. A decrease in fire frequency from 3.5-2.4 ka corresponded with a cool, humid climate, while high fire frequency from 2.4-1.3 ka suggests more frequent prolonged summer drought (Hallett et al., 2003; Gavin et al., 2007). In this region, the present-day fire regime was established by 1.3 ka (Hallett et al., 2003; Gavin et al., 2007). In the Oregon coast range, changes in vegetation led to a decrease in fire activity beginning at 2.75 ka. The increase in fire frequency and variability in the PNW may have been due to changes in forest composition, changes in temperature and precipitation, increased ENSO frequency leading to increased summer drought, or due to increases in human population and thus, human-induced fire (Walsh et al., 2017). Despite an increase in precipitation and a decrease in temperature, charcoal accumulation rates from the Oregon Coast Range and northern California (Klamath-Siskiyou Mountains) suggest that fires became larger and more severe in this region, with high variability during the latter part of the Holocene, likely due to increases in woody vegetation to fuel forest fires (Marlon et al., 2006, 2013; Whitlock et al., 2008).

Spatial and temporal variability in climate and fire history occurred across the Sierra Nevada mountains (Figs. 2, 3). In the eastern Sierras, hydroclimate varied throughout the late Holocene; Mono Lake water level fluctuated through this time (3.77 ka- highest in last 7 ka, 1.8 ka low stand, multiple rapid fluctuations in last 1.2 ka), Owens Lake exhibited three intervals of wetter and cooler climate at 3.6 ka, 0.8 ka, and 0.35 ka (Bacon et al., 2018), and increased precipitation through the late Holocene at Pyramid Lake led to rising lake levels (Benson et al., 2002). Strong fire synchrony occurred in the Sierra Nevada since 2.5 ka which is linked to periods of drought (Hallett and Anderson, 2010). In the Lake Tahoe Basin, changes in vegetation from open forest to mesic forest drive a decline in fire frequency from the Mid-Holocene to modern, with a particularly low fire interval from 4.0 to 3.5 ka (Beaty and Taylor, 2009). Records from the Sierra Nevada show glacial advancement linked to cooling beginning 3.9 ka (Konrad and Clark, 1998)

In Central and southern California, multiple wet and dry phases occurred through the late Holocene (Fig. 2) (Feakins et al., 2014; Kirby et al., 2014). In coastal Central California, marine records show that winter precipitation increased in the late Holocene (McGann, 2011). Several lake records from southern California (Lower Bear Lake, Lake Elsinore, Tulare Lake, and Owens Lake) all indicate a return to wetter conditions beginning between 4.0-3.35 ka (Kirby et al., 2010, 2014). Records from coastal lagoons on Santa Rosa Island and in southern California show multi-centennial fluctuations between wet and dry conditions (Davis, 1992; Anderson and Byrd, 1998; Cole and Wahl, 2000; Anderson et al., 2010). Similarly, records from Zaca Lake and Lake Elsinore indicate multiple wet and dry intervals, including multi-centennial drought from 2.0-2.7 ka (Dingemans et al., 2014; Kirby et al., 2014, 2019). This alternation of wet and dry cycles may be linked to alternation of precipitation source water between more tropical and more North Pacific source water (Feakins et al., 2014; Kirby et al., 2014). In some records, a late Holocene Dry Period (1 – 0.2 ka) is identified (Platzman and Lund, 2019), and persistent droughts and elevated aridity are dominant across the Western US from 1.1 to 0.7 ka (Cook, 2004). In the Mojave

Desert (Silver Lake, California) conditions returned to ephemeral, wet lake conditions beginning at 3.8 ka after a mid Holocene period of aridity (Fig. 5) (Kirby et al., 2015). Yet other records show increased aridity in the Mojave Desert compared to the mid Holocene (Spaulding, 1991).

Across the study region, extreme events (rainfall, drought, flooding) become a dominant feature across multiple records over the past 2 ka (Cook, 2004; Malamud-Roam et al., 2006; Rasmussen et al., 2006; Kirby et al., 2015). A pronounced megadrought occurred in Western North America from 1.1 - 0.7 ka, that was previously linked to cool SST over the Eastern Tropical North Pacific (Cook, 2004). More variable conditions have been attributed to changes in insolation as well as shorter term processes including ENSO and PDO (Cook, 2004; Kirby et al., 2007, 2010; Barron and Anderson, 2011). Gradual decreases in summer insolation and increases in winter insolation contribute to maximum drying in the late Holocene relative to the early Holocene (Kirby et al., 2007). Enhanced PDO and ENSO variability in the last 4 ka contribute to increased terrestrial hydroclimate and temperature variability (Kirby et al., 2010; Barron and Anderson, 2011).

3.3.3 Marine Conditions

In the late Holocene, SST increased and spring upwelling increased off the coast of Oregon and California and SST decreased in the Santa Barbara Basin relative to the mid Holocene (Figs. 2, 4, 5) (Barron et al., 2003a; Kennett et al., 2007; Barron and Anderson, 2011). Late Holocene marine conditions show increased variability in SST, intensification of the California Current System, and increased upwelling relative to the mid Holocene (Fig. 3) (Barron and Bukry, 2007a; Barron and Anderson, 2011). While global records suggest a shift in climate characteristics at 4.2 ka, several California and Oregon records experience a delayed mid to late Holocene shift (Barron and Bukry, 2007a; Addison et al., 2017; Barron et al., 2017). Modern seasonality within the California Current (strong spring-summer upwelling with cool SSTs, and relaxation with warmer SSTs during fall) was established between 3.5 and 3.2 ka (Barron and Bukry, 2007a). Diatom-based productivity increased at 2.9 ka offshore of northern California

and changes in relative abundance of diatom and pollen species suggest significantly increased upwelling and productivity at this time (Addison et al., 2017). Additional evidence from offshore of northern California shows cooler SSTs occurred from ~3.6 and 2.8 ka, accompanied by increased precipitation, an abrupt warming of winter SSTs at 2.8ka, and an intensification of spring upwelling beginning 2.6 ka (Barron et al., 2017). Since 2.6 ka, PDO-like warm-cool oscillations have dominated the SST regime (Barron et al., 2017).

Further south, off the coast of Santa Cruz, California, upwelling and productivity increased steadily through the late Holocene (Barron et al., 2019). Additional records from offshore Central California indicate the late Holocene marked the onset of warm modern offshore conditions with high productivity (total and organic carbon export) relative to the mid and early Holocene (McGann, 2011; Barron et al., 2019). Marine oxygenation off the coast of Central California declined through the late Holocene (McGann, 2011). Nearshore records from Central California show that SST was $1^{O}C$ cooler than modern from 2-0.7 ka (Jones and Kennett, 1999).

In southern California, late Holocene SST cooling with high SST variability (in Santa Barbara Basin) began at ~4 ka (Fig. 5) (Kennett et al., 2007; Fisler and Hendy, 2008). High amplitude changes in salinity due to variability of input of freshwater into the basin are documented within SBB (Kennett et al., 2007). Brief cold events occurred in SBB at ~4.2-3.8, 1.5-1.2, and 0.8-0.3 ka and correspond to glacial advances in the Sierras (Fisler and Hendy, 2008). Variable oceanographic conditions in the late Holocene may be due to increasing ENSO variability in the tropical Pacific (Barron and Bukry, 2007b). Intensification of the California Current and increased East-West seasonal gradients (driving increased winds that enhance upwelling) are documented offshore northern California (Barron et al., 2003b; Barron and Bukry, 2007b, b) and across the southern California Borderlands. Nearshore records from Santa Cruz Island show persistently cold SSTs and persistent upwelling on the west coast of Santa Cruz Island in late Holocene compared to a wider range of nearshore conditions on the south side of the island (Flores, 2017). In

deeper waters, a drastic change in the age of North Pacific Intermediate Water in SBB (shift to older water and lower bioturbation) at 2 ka with a subsequent stable age of water entering from 2 ka to present suggests changes in the North Pacific Intermediate Water circulation pattern (Roark et al., 2003). This shift is concurrent with a decrease in Greenland temperature and increase in ice accumulation rate suggesting trends in SBB relate to larger atmospheric circulation patterns (Roark et al., 2003). Further, the oxygen minimum zone persists in intermediate waters off the coast of southern California, but is reduced in intensity relative to the mid Holocene (Balestra et al., 2018; Wang et al., 2020).

3.3.4 Ecological responses to change

Forested ecosystems in the PNW and northern California transitioned to modern temperate, cool, wet, highly fire-adapted systems with increased fir and pine (Heusser, 1983; Mohr et al., 2000; Pellatt et al., 2001; Barron et al., 2003b, 2019; Briles et al., 2005; Anderson et al., 2013) while SW systems became increasingly dominated by chaparral and sage scrub ecosystems (particularly since ~2.5 ka) (Heusser, 1978; Anderson and Byrd, 1998; Cole and Wahl, 2000; Anderson et al., 2010; Dingemans et al., 2014). In the Siskiyou mountains, a shift in hydroclimate to wet, cool conditions at 2.1 ka led to the development of the modern forest dominated by firs (*Abies*) and cypress (*Pseudotsuga*) and moderated by a modern fire regime (Briles et al., 2005). In parallel with increases in hydroclimate and temperature variability, in northern California the amplitude and frequency of changes between pine and alder intensified in the late Holocene and coastal scrub expanded (Fig. 4) (Barron et al., 2003b; Anderson et al., 2013). In Central California, changes to forest assemblages occurred gradually through time, trending towards decreased dominance of pine in the modern (Fig. 5) (McGann, 2015; Barron et al., 2019). Finally, in southern California, ecological change varied locally, with transitions in pollen regimes occurring around 2 ka in multiple records (Anderson and Byrd, 1998; Cole and Wahl, 2000; Dingemans et al., 2014).

Marine ecosystems reflect the establishment of modern levels of coastal upwelling and productivity in the late Holocene (Addison et al., 2017; Barron et al., 2017). Offshore northern California, the gyre-

associated diatom species *Pseudoeunntia doliolus* increased threefold indicating the onset of modern oceanographic conditions in this region (Barron et al., 2003b). Offshore Central California, upwelling evolved gradually over time and the upwelling-indicator diatom species *T. nitzschioides* gradually increased through this interval (Barron et al., 2019). In SBB, late Holocene cooling led to an increase in the abundance of cold-associated (*N. incompta*) and upwelling-associated (*Globigerina quinqueloba)* planktic foraminifera (Fisler and Hendy, 2008). Oxygen deficient zones were well established by the late Holocene and persisted throughout the interval, structuring seafloor and pelagic ecosystems (Ohkushi et al., 2013; Moffitt et al., 2014, 2015).

3.3.5 Human-environment interactions

Human-environment interactions are well documented in the late Holocene relative to previous time intervals due to the increase in human population, the preservation bias in archaeological records, and the recency bias in oral histories. In multiple locations, a late Holocene drought was a destabilizing factor for societies. In the SW, a 26-year-long drought that occurred 0.8 ka is linked to social destabilization and abandonment of well-established Ancestral Puebloan villages (deMenocal, 2001). In northern California, the abandonment of shell mounds following four millennia of occupation (5 to ~1.2 ka) co-occurs with drought in this region revealing potential societal impacts of drought (Ingram, 1998). Human control of the fire regime led to land use and ecosystem changes across the Western US during this interval. In Washington, an increase in human artifacts in the subalpine zone beginning at 3.6 ka, combined with a change in climate and thus ranges of game species, provide some evidence for increased presence of people in subalpine terrain and potentially an increase in human-caused fire (Walsh et al., 2017). Across California, late Holocene increases in chaparral, grassland, and sage scrub ecosystems were reinforced by intentional burning and prescribed burning played an important role in structuring ecosystems (Heusser, 1978; Anderson et al., 2010, 2013; Cowart and Byrne, 2013; Lightfoot and Cuthrell, 2015; Klimaszewski-Patterson et al., 2021).

Human interactions with the marine environment were critical factors in structuring societies, and conversely, changes in ocean conditions impacted users of coastal resources. In Central California, marine resources including shellfish and fish, were harvested throughout the late Holocene (Jones and Kennett, 1999). Occurrence of drought from 0.5-0.3 ka led to an increase in fish bone presence in middens, indicating enhanced use of fisheries as a resource during a time of drought, despite a documented decrease in marine productivity and high-amplitude marine seasonality coeval with the interval of drought (Jones and Kennett, 1999). Indigenous coastal populations were highly reliant on marine resources (largely *Mytilus californianus*) and even inland occupants of Central California traveled to the coast seasonally to harvest mussels (Jones et al., 2008). On the Channel Islands, human population and sociopolitical complexity increased in the late Holocene (Rick, 2011; Braje et al., 2012). As populations increased, diet breadth expanded and human harvesting pressure on marine ecosystems increased, including an expansion of consumption of finfish and pinnipeds and a diversification of taxa in middens (Erlandson et al., 2009; Rick, 2011; Braje et al., 2012). Expansion of sociological complexity, and competitive (including violent conflict) and cooperative strategies on the northern Channel Islands from 1.3-0.7 ka is attributed to high climatic instability, cool marine conditions with relatively high productivity, low terrestrial productivity, and aridity (Kennett and Kennett, 2000). This climate instability led to conflicts over resources, but eventually resulted in more complex sociopolitical societies due to the need to cooperate, regulate, and manage resources (Kennett and Kennett, 2000). Human-environment interactions and Indigenous land stewardship were important environmental and ecological drivers throughout the late Holocene. The onset of colonization, genocide of Indigenous people, land-use change, urbanization, industrialization, and anthropogenic climate change in the last few hundred years dramatically impacted climate, ecosystems, and records used to interpret past change (see Sect. 3.5 on Era of Colonization below).

3.4 Medieval Climate Anomaly and Little Ice Age

Specific investigation of the Medieval Climate Anomaly (MCA) and the Little Ice Age (LIA) are included in some of the papers reviewed here. Generally, the MCA was an anomalously warm event that is linked to pronounced drought conditions throughout the Western United States. Alternatively, the LIA was a brief period of cooling predominantly identified in Northern Hemisphere records (Cook, 2004). Evidence of dry conditions during the MCA is indicated in a breadth of records: from Mono Lake and Owens Lake in the Eastern Sierra Nevada (Stine, 1990; Bacon et al., 2018), freshwater input into San Francisco Bay, Abbot Lake and Zaca Lake in coastal Central California (Dingemans et al., 2014; Hiner et al., 2016; Platzman and Lund, 2019), Central California pollen history (McGann, 2015), flood events in SBB (Schimmelmann et al., 2013; Du et al., 2018), tree stump dating in the Sierra Nevada (Stine, 1994), and a synthesis of tree-ring records (Cook, 2004). Dry conditions were likely caused by anomalously warm terrestrial temperatures and are linked to cool SSTs over the Eastern Tropical Pacific (Cook, 2004) and in the adjacent Santa Barbara Basin (Kennett and Kennett, 2000; Fisler and Hendy, 2008; Barron et al., 2010; Asmerom et al., 2013). Fire activity increased in the MCA in the Eastern Sierra and Lake Tahoe Basin, which may be due to warm summer enhanced growth and decreased snowpack, but in Western North America more broadly, fire activity was reduced during the MCA and LIA relative to the past 3 ka (Beaty and Taylor, 2009; Hallett and Anderson, 2010). The LIA was characterized by warm SSTs in southern California, wetter conditions in the Sierra Nevada and southern California, and minimum fire frequency in Western North America (Reyes and Clague, 2004; Whitlock et al., 2008; Barron et al., 2010; Feakins et al., 2014; Kirby et al., 2019). Further investigation of the MCA and LIA are merited but are not within the scope of this paper.

3.5 Era of Colonization

Humans have been interacting with the environment in Western North America throughout the entirety of the Holocene. As described above, Indigenous peoples exerted control of fire and interacted with, managed, and cultivated marine and terrestrial plants and animals throughout the Holocene (Minnis,

2004; Braje et al., 2012; Taylor et al., 2016; Platzman and Lund, 2019; Ellis et al., 2021; Klimaszewski-Patterson et al., 2021). Yet, the impacts of settler colonization, genocide of indigenous people, and conversion to Western, Euro-centric land and marine management practices are evident in many records examined here and represent an unprecedented environmental regime in multiple records (Ellis et al., 2021).

Impacts of land-use change and human control of fire at the time of colonization precede changes due to urbanization and anthropogenic climate change (Waters et al., 2016). Changes in the view and management of fire shaped the landscape and climate in the last several hundred years, beginning with a measurable increase in fire (relative to Indigenous prescribed burning) following settler colonization and a subsequent measurable decrease in fire in the last 100 years due to fire suppression (Gavin et al., 2007; Anderson et al., 2010, 2013; Dingemans et al., 2014; Taylor et al., 2016; Walsh et al., 2017; Platzman and Lund, 2019). Prior to 1860, fire activity in the Sierra Nevada was positively correlated with temperature, but in the last 150 years (after 1860 CE) fires are linked to human activity and socio-ecological change, rather than temperature or moisture (Anderson et al., 2013; Taylor et al., 2016). In the Sierra Nevada the highest fire activity in the last 400 years occurred following Spanish colonialism and the lowest fire activity occurred with the onset of fire suppression beginning in 1904 CE (Taylor et al., 2016). In coastal Central California recent increases in fire beginning in the mid nineteenth century are attributed to burning of logging slash (Cowart and Byrne, 2013).

Increases in extractive processes and land-use conversions for ranching and agriculture have also contributed to changing fire regimes over the last several hundred years and led to changes in hydrology and landscape geomorphology (Heusser, 1983; Byrne et al., 2001; Cowart and Byrne, 2013; Platzman and Lund, 2019). Pollen records in British Columbia show the impacts of colonization, logging, farming, and urbanization on local terrestrial ecosystems (Heusser, 1983). Influx of freshwater to the San Francisco Bay decreased dramatically relative to the late Holocene at 1930 CE due to diversion of upstream water

flow (Byrne et al., 2001). The extractive processes of the Gold Rush Era (beginning at 1850) in northern California led to increased sedimentation and heavy metal pollution in the San Francisco Bay Delta; post-colonization lead (Pb) levels are unprecedented throughout the rest of the Holocene and concentrations of Sr, Ti, Cu, Ni, and Zn also increased following colonization (Fard et al., 2021). The onset of logging and ranching caused land use change including transition of redwood forest to grasses and oak landscapes in coastal Central California (Cowart and Byrne, 2013). Further, the introduction of non-native species is well documented across the region (Anderson and Byrd, 1998; Cole and Wahl, 2000; Anderson et al., 2010, 2013; Dingemans et al., 2014). The impact of both a changing fire regime and land use change resulted in shifts in terrestrial ecosystems (Cowart and Byrne, 2013; Dingemans et al., 2014; Platzman and Lund, 2019).

Human impacts on nearshore marine ecosystems are documented throughout the Holocene (as discussed above). Yet widespread and detectable impacts of land use change and anthropogenic climate change on marine systems do not appear until the last several hundred years, following colonization and the Industrial Revolution, respectively. Land use change and the conversion of land to rangeland and cultivated agricultural land beginning around 1800 CE led to the collapse of benthic marine ecosystems and may have contributed to a decrease in oxygenation across the southern California Bight (Christensen et al., 1994; Tomasovych and Kidwell, 2017; Wang et al., 2017; Palmer et al., 2020). Impacts of anthropogenic climate change on marine systems in this region include species range shifts caused by rising SSTs and geochemical and structural changes to organisms due to ocean acidification; these changes represent a divergence from scales of past variability (Field et al., 2006; Pak et al., 2016; Osborne et al., 2020). Human activity, including intentional use and alteration of marine and terrestrial systems, has been a feature of Western North America throughout the Holocene that is detectable in multiple archives (lake sediments, marine sediments, archaeological records), yet colonization, urbanization, and industrialization led to a novel environmental interval.

4 Conclusions

Understanding Holocene climate and oceanographic patterns in the Western United States and Northeast Pacific is critical for contextualizing and predicting modern changes. Relative to pre-Holocene conditions, the early Holocene was dry and warm in the PNW and wet and warm in the SW; sea surface temperature was warm along the coast (Fig. 2). The mid Holocene was characterized by a wet, cool PNW and dry, warm SW with generalized cool SST, except for Santa Barbara Basin (Fig. 2). The late Holocene is the most variable interval with a general pattern of warm marine conditions and cool terrestrial conditions (Fig. 2). Control of fire regime shifts throughout the Holocene; in the early Holocene, fire activity is linked to changes in vegetation following the deglacial, but in multiple locations shifts to control by climate in the mid Holocene and in most records is highest and most variable in the late Holocene (Fig. 3). Human-environment interactions persist throughout the Holocene and impact the climate, landscape, and ecosystems of Western North America. Prior to settler colonization, marine harvesting, fishing pressure and prescribed burning shaped past ecosystems and landscapes, while intervals of drought and variability in marine productivity impacted sociological complexity and migration of Indigenous people. Impacts of settler colonization, urbanization, and industrialization in recent centuries are documented broadly and, in some cases, represent divergences from scales of expected variability as recorded throughout the rest of the Holocene.

Multiple factors combine and interact to drive climate changes through the Holocene across timescales including orbital forcing, ice sheet dynamics, solar forcing, annual to decadal phenomena, and marine-terrestrial interactions. Orbital forcing, including the northern hemisphere solar insolation peak in the early Holocene, drives climate change on millennial timescales. Annual to decadal phenomena such as ENSO and PDO become dominant drivers of climate in the late Holocene and lead to increased temporal variability. The relationship between marine and terrestrial systems evolves through time; notably, continental conditions in the Pacific Northwest and Southwest respond differently to changes in marine conditions. In the PNW broadly, marine temperatures are inversely correlated with precipitation. In the

early Holocene, warm SSTs occur synchronously with warm, dry inland conditions. In the mid Holocene, the trend reverses. Yet, the increase in upwelling as a dominant oceanographic feature throughout the Holocene complicates this relationship, as upwelling in the PNW is positively correlated with precipitation yet characterized by cool SSTs. Thus, in the late Holocene, the interaction between an enhanced upwelling regime yet generalized warm SST patterns may both play a role in influencing terrestrial hydroclimate. In contrast, in the SW, marine temperatures are generally positively correlated with precipitation: warm intervals (such as the early Holocene) coeval with wet intervals and periods of drought coeval with cool SSTs offshore southern California. In addition to marine-terrestrial interactions on regional scales, changes in source and strength of precipitation sources impact hydroclimate of the region; for example, changes in the intensity or geographic extent of the North American Monsoon and occurrence of atmospheric-river storms are both linked to processes in the Eastern Tropical North Pacific and have implications for hydroclimate across the region studied here.

Although general trends can be identified across broad regions (PNW and SW), local factors play a key role in determining the exact conditions for a particular location. Complete synchrony between records across an entire geologic sub-epoch for marine conditions, for terrestrial climate, or for fire activity is functionally absent; multiple anomalous or contradictory records exist (Figs. 2, 3). For example, fire activity in adjacent lake basins show different trends and nearshore vs. offshore records of marine conditions present apparently competing evidence (Fig. 3). Marine sediment records from Santa Barbara Basin are often utilized as records of the entire North Pacific, but here we find that trends in Santa Barbara Basin are not always synchronous with other records in this region (Fig. 2). We posit that these instances do not present competing evidence, but rather that local factors are critical in determining local climate. This is of critical importance for interpreting present and future climate change. This synthesis of climate and oceanographic processes and resultant impacts on ecosystems and human communities provides a window into understanding modern patterns of climate and climate change in the Western United States and Northeast Pacific and amplifies the need for future research investigating marine-

terrestrial interactions, local and regional scale processes, and integrated physical-ecological-human systems.

5 Acknowledgements

We acknowledge that this paper includes histories and discussion of Indigenous peoples of Western North America (Turtle Island) who have stewarded the land and sea for millennia. We aim to document the broad histories of interactions between people and environment, but we acknowledge that this record is incomplete due to the erasure of Indigenous histories and oral traditions, genocide of knowledge keepers, and destruction of cultural artifacts. We acknowledge the keepers of intergenerational Indigenous knowledge who maintain stories and data of the human, ecosystem, and climate impacts of settler colonization described here. We do not attempt to name all tribes whose ancestral and present homelands make up this study area, but we acknowledge that the majority of the geographic area covered here represents unceded land of Indigenous tribes and that data used here from previously published studies may have been acquired without consent from Indigenous peoples. We direct readers to the open-source resource: nativelands.ca to identify the homelands of the diverse Indigenous people of this region and encourage readers to use this resource as a starting place to learn about the land and marine stewardship of Indigenous peoples past and present.

6 Figures

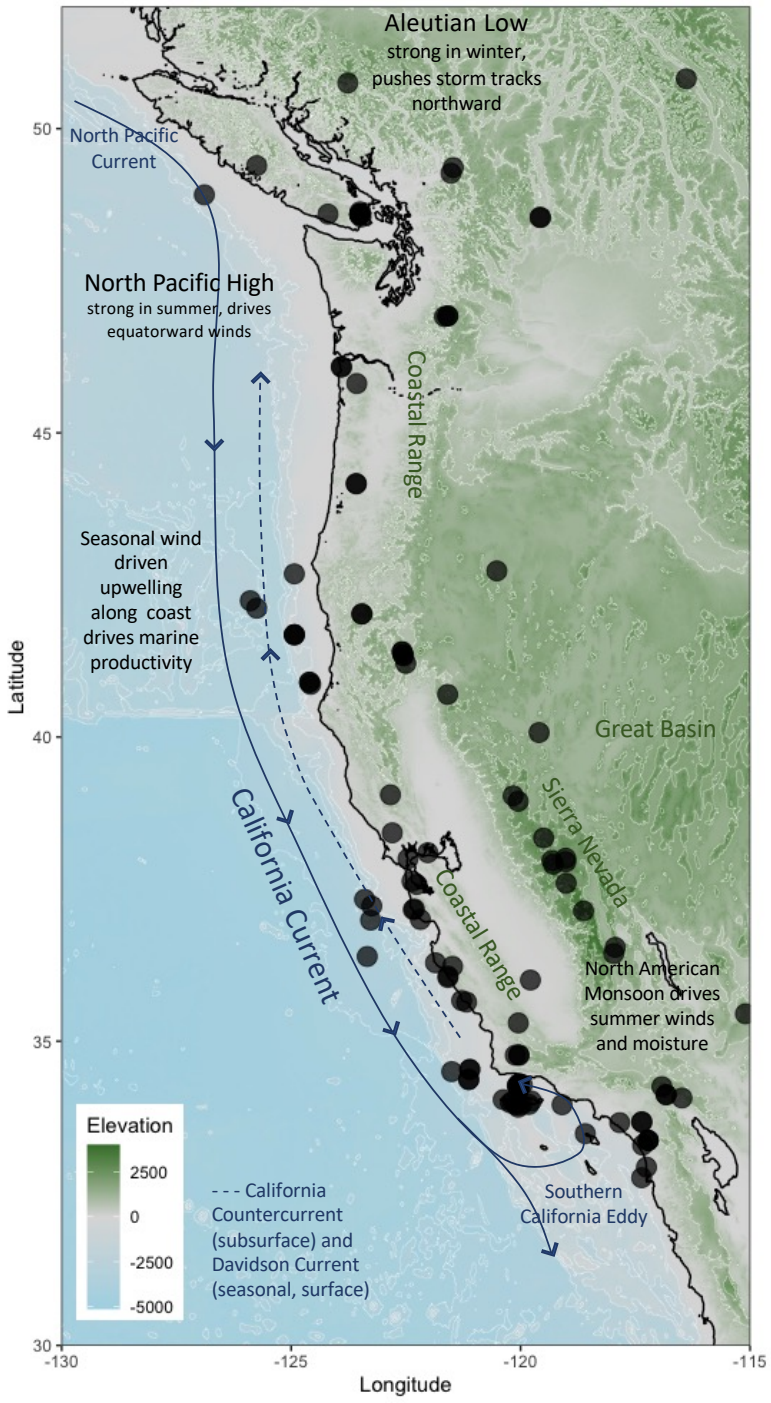

Figure 1: Map of locations of all studies reviewed in the paper with simplified schematic of modern oceanographic and hydrographic conditions.

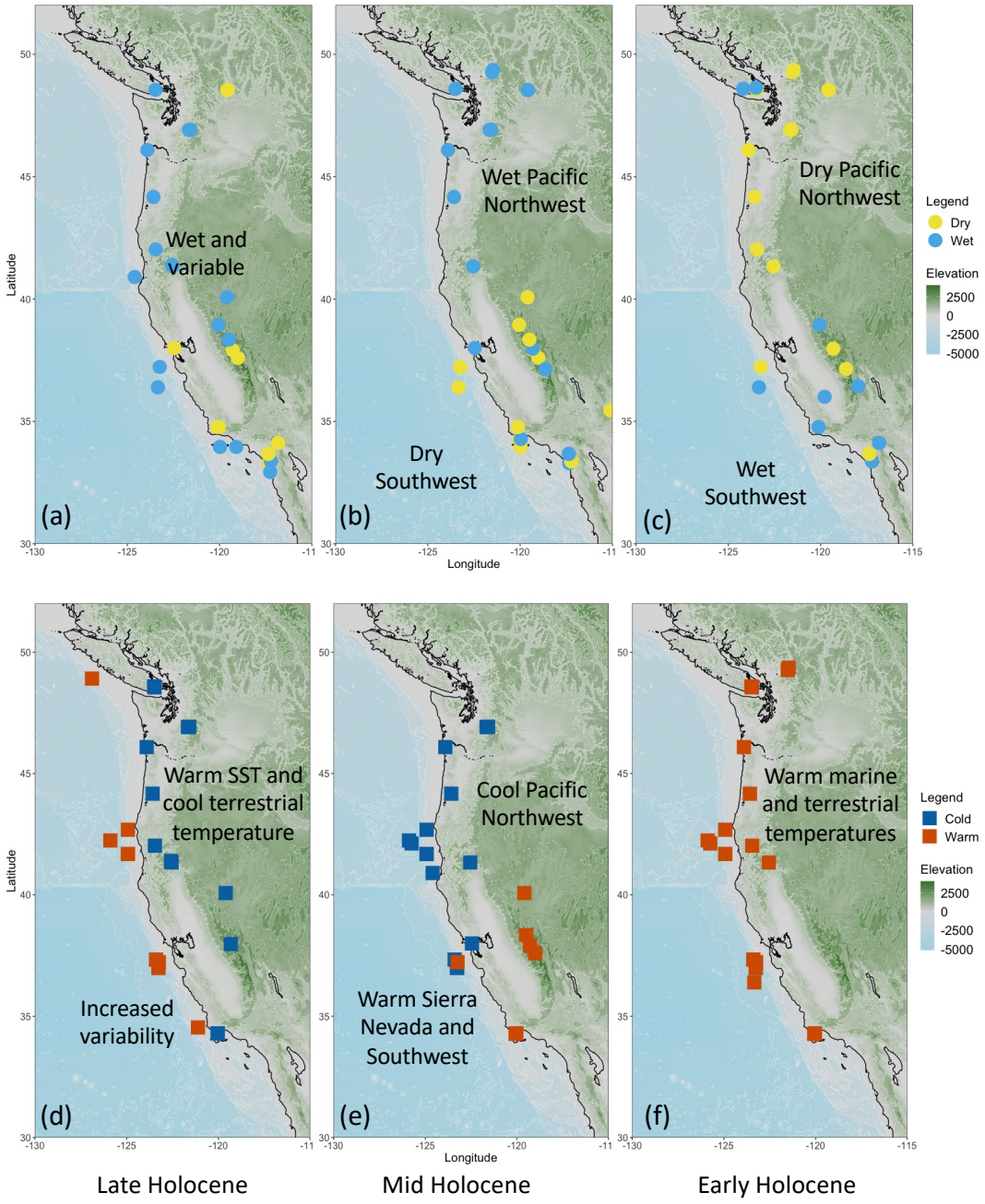

Figure 2: Top panel shows hydroclimate records in early (11.7 - 8.2 ka, (c)), mid (8.2 - 4.2 ka, (b)), and late (4.2 - 0 ka, (a)) Holocene: yellow dots represent dry and light blue represents wet. Bottom panel shows temperature records from early (f), mid (e), and late (d) Holocene: dark blue squares represent cold temperatures and orange represents warm temperatures.

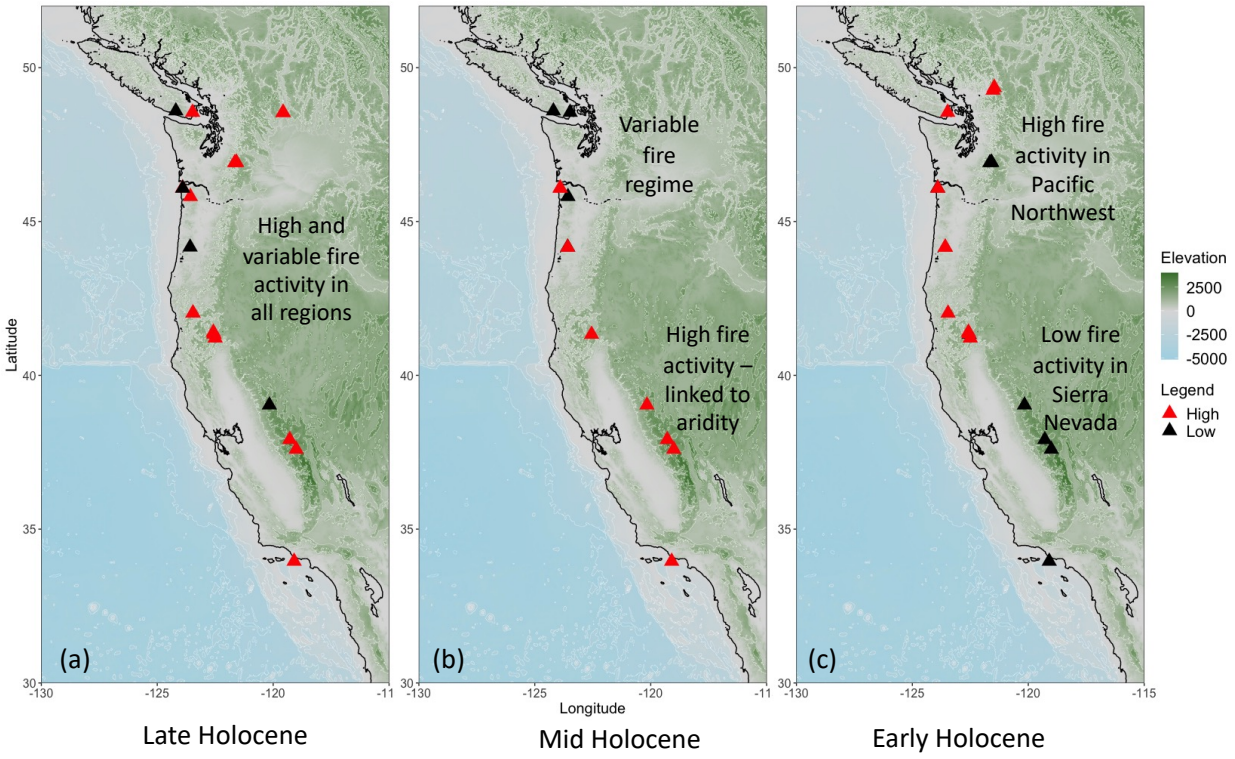

Figure 3: Fire activity as reconstructed by charcoal records through the early (11.7 - 8.2 ka, (c)), mid (8.2 - 4.2 ka, (b)), and late (4.2 - 0 ka, (a)) Holocene; red indicates high fire activity, black indicates low fire activity. Multiple metrics for fire activity are used; interpretations of original authors are preserved.

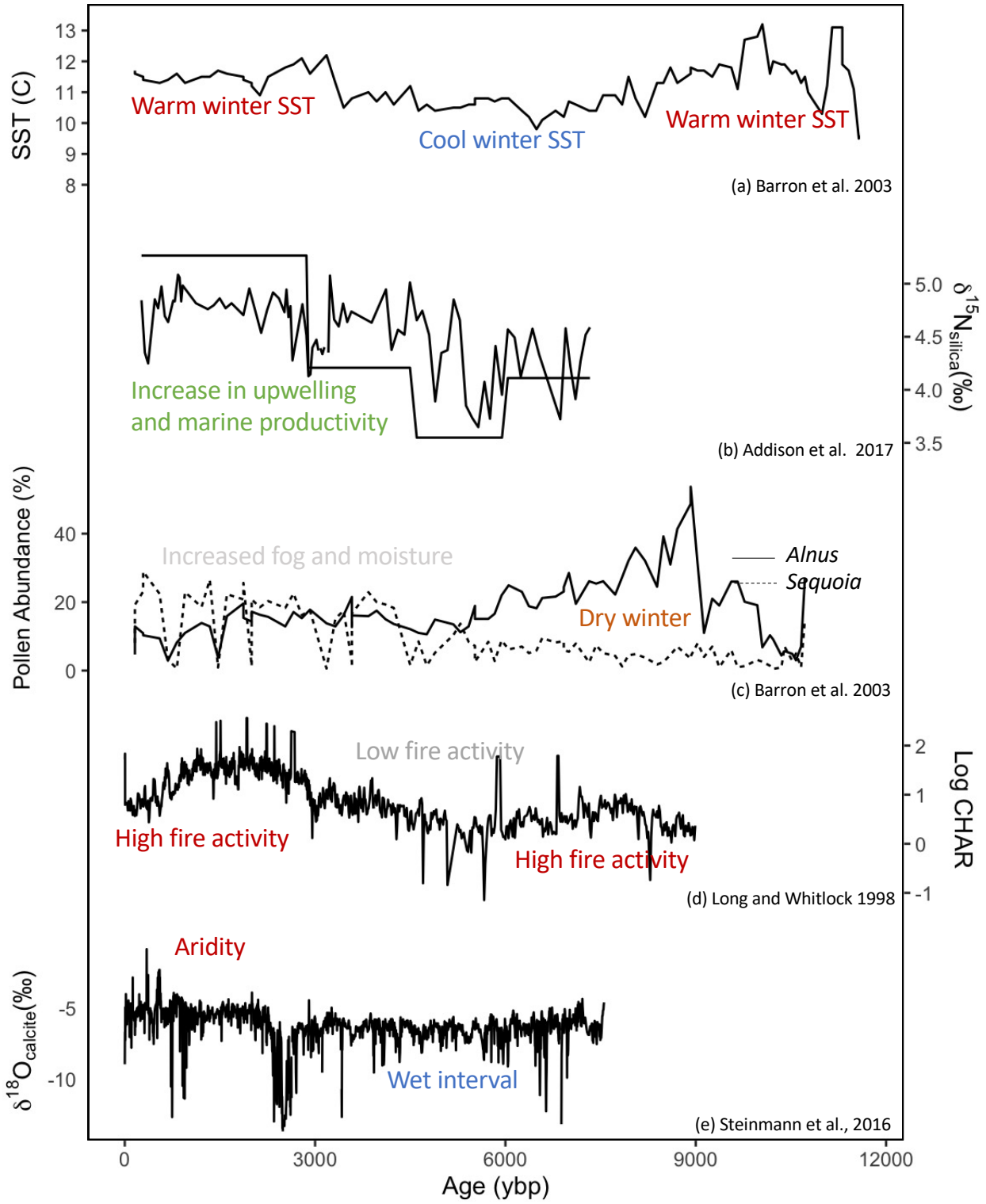
SST (C)
13
12
11
10
9
8
Warm winter SST
Cool winter SST
Warm winter SST
(a) Barron et al. 2003
Increase in upwelling
and marine productivity
(b) Addison et al. 2017
5.0
4.5
4.0
3.5
δ15Nsilica(‰)
Pollen Abundance (%)
40
20
0
Increased fog and moisture
Alnus
Sequoia
Dry winter
(c) Barron et al. 2003
Low fire activity
High fire activity
High fire activity
(d) Long and Whitlock 1998
2
1
0
-1
Log CHAR
Aridity
δ18Ocalcite(‰)
-5
-10
Wet interval
(e) Steinmann et al., 2016
0
3000
6000
9000
12000
Age (ybp)

Figure 4: Representative datasets from the Pacific Northwest. Panels from top to bottom Alkenone sea surface temperature from core ODP1019 ((a), Barron et al. 2003). Bulk sediment δ15N and opal regime index from core TN062-O550 ((b), Addison et al. 2017). Relative abundance of pollen: solid line is *Alnus* (alder) and dashed line is *Sequoia* (coastal redwood) from core ODP1019 ((c), Barron et al 2003). Log charcoal accumulation rate at Little Lake ((d), Long and Whitlock 1998). Lake sediment bulk calcite δ18O from Cleland Lake, Washington ((e), Steinman et al. 2016).

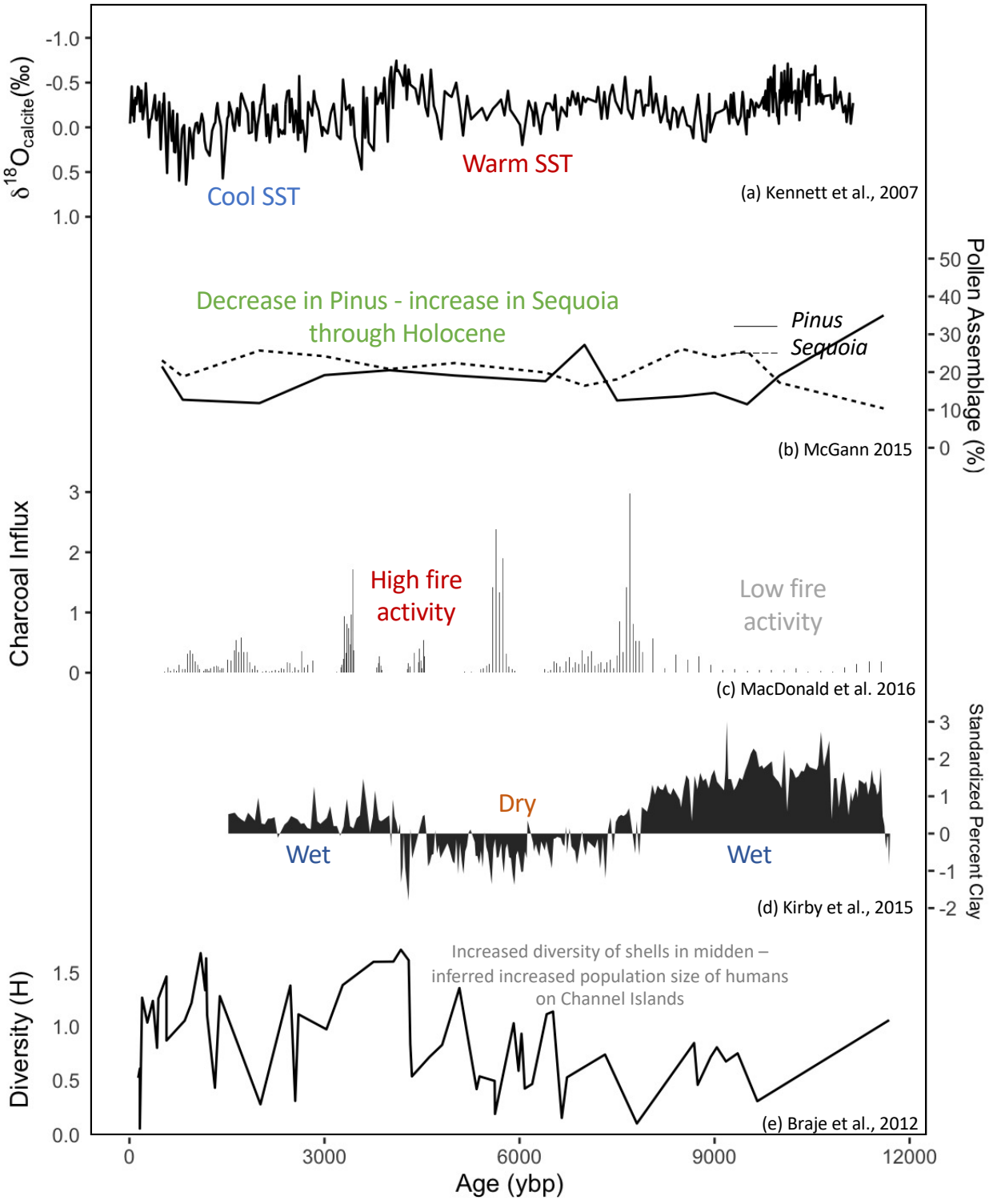
δ18Ocalcite (‰)
-1.0
-0.5
0.0
0.5
1.0
Cool SST
Warm SST
(a) Kennett et al., 2007
Decrease in Pinus - increase in Sequoia through Holocene
Pinus
Sequoia
Pollen Assemblage (%)
50
40
30
20
10
0
(b) McGann 2015
Charcoal Influx
3
2
1
0
High fire activity
Low fire activity
(c) MacDonald et al. 2016
Dry
Wet
Wet
Standardized Percent Clay
3
2
1
0
-1
-2
(d) Kirby et al., 2015
Diversity (H)
1.5
1.0
0.5
0.0
Increased diversity of shells in midden – inferred increased population size of humans on Channel Islands
(e) Braje et al., 2012
0
3000
6000
9000
12000
Age (ybp)

Figure 5: Representative datasets from the Southwest. Oxygen isotope record from planktonic foraminifera G. bulloides from Santa Barbara Basin core ODP 893 ((a), Kennett et al. 2007). Pollen assemblage (%) of Pinus and Sequoia from Central California marine sediment core ((b), McGann 2015). Charcoal influx to Kirman Lake in the Sierra Nevada mountains ((c), Macdonald et al., 2016). Standardized percent clay as a proxy for relative lake status for Silver Lake ((d), Kirby et al., 2015). Diversity of shells from shell midden sites on Channel Islands ((e), Braje et al. 2012).

7 References

Adams, D. K. and Comrie, A. C.: The North American Monsoon, 78, 2197–2214, https://doi.org/10.1175/1520-0477(1997)078<2197:TNAM>2.0.CO;2, 1997.

Addison, J. A., Barron, J., Finney, B., Kusler, J., Bukry, D., Heusser, L. E., and Alexander, C. R.: A Holocene record of ocean productivity and upwelling from the northern California continental slope, Quatern Int, 2017.

Ainsworth, C. H., Samhouri, J. F., Busch, D. S., Cheung, W. W. L., Dunne, J., and Okey, T. A.: Potential impacts of climate change on Northeast Pacific marine foodwebs and fisheries, ICES Journal of Marine Science, 68, 1217–1229, https://doi.org/10.1093/icesjms/fsr043, 2011.

Amante, C. and Eakins, B. E.: ETOPO1 1 ARC-MINUTE GLOBAL RELIEF MODEL: PROCEDURES, DATA SOURCES AND ANALYSIS, 25, 2009.

Anderson, R. S. and Byrd, B. F.: LATE-HOLOCENE VEGETATION CHANGES FROM THE LAS FLORES CREEK COASTAL LOWLANDS, SAN DIEGO COUNTY, CALIFORNIA, 45, 171–182, 1998.

Anderson, R. S., Starratt, S., Jass, R. M. B., and Pinter, N.: Fire and vegetation history on Santa Rosa Island, Channel Islands, and long-term environmental change in southern California, 25, 782–797, https://doi.org/10.1002/jqs.1358, 2010.

Anderson, R. S., Ejarque, A., Brown, P. M., and Hallett, D. J.: Holocene and historical vegetation change and fire history on the north-central coast of California, USA, The Holocene, 23, 1797–1810, https://doi.org/10.1177/0959683613505344, 2013.

Asmerom, Y., Polyak, V. J., Rasmussen, J. B. T., Burns, S. J., and Lachniet, M.: Multidecadal to multicentury scale collapses of Northern Hemisphere monsoons over the past millennium, Proceedings of the National Academy of Sciences, 110, 9651–9656, https://doi.org/10.1073/pnas.1214870110, 2013.

Atwood, A. R., Wu, E., Frierson, D. M. W., Battisti, D. S., and Sachs, J. P.: Quantifying Climate Forcings and Feedbacks over the Last Millennium in the CMIP5–PMIP3 Models*, 29, 1161–1178, https://doi.org/10.1175/JCLI-D-15-0063.1, 2016.

Bacon, S. N., Burke, R. M., Pezzopane, S. K., and Jayko, A. S.: Last glacial maximum and Holocene lake levels of Owens Lake, eastern California, USA, Quaternary Science Reviews, 25, 1264–1282, https://doi.org/10.1016/j.quascirev.2005.10.014, 2006.

Bacon, S. N., Lancaster, N., Stine, S., Rhodes, E. J., and McCarley Holder, G. A.: A continuous 4000-year lake-level record of Owens Lake, south-central Sierra Nevada, California, USA, Quat. res., 90, 276–302, https://doi.org/10.1017/qua.2018.50, 2018.

Bader, J., Jungclaus, J., Krivova, N., Lorenz, S., Maycock, A., Raddatz, T., Schmidt, H., Toohey, M., Wu, C.-J., and Claussen, M.: Global temperature modes shed light on the Holocene temperature conundrum, 11, 4726, https://doi.org/10.1038/s41467-020-18478-6, 2020.

Balestra, B., Krupinski, N. B. Q., Erohina, T., Fessenden-Rahn, J., Rahn, T., and Paytan, A.: Bottom-water oxygenation and environmental change in Santa Monica Basin, Southern California during the last 23 kyr, 490, 17–37, 2018.

Barlow, M., Nigam, S., and Berbery, E. H.: Evolution of the North American Monsoon System, 11, 2238–2257, https://doi.org/10.1175/1520-0442(1998)011<2238:EOTNAM>2.0.CO;2, 1998.

Barnosky, A. D., Hadly, E. A., Gonzalez, P., Head, J., Polly, P. D., Lawing, A. M., Eronen, J. T., Ackerly, D. D., Alex, K., Biber, E., Blois, J., Brashares, J., Ceballos, G., Davis, E., Dietl, G. P., Dirzo, R., Doremus, H., Fortelius, M., Greene, H. W., Hellmann, J., Hickler, T., Jackson, S. T., Kemp, M., Koch, P. L., Kremen, C., Lindsey, E. L., Looy, C., Marshall, C. R., Mendenhall, C., Mulch, A., Mychajliw, A. M., Nowak, C., Ramakrishnan, U., Schnitzler, J., Das Shrestha, K., Solari, K., Stegner, L., Stegner, M. A., Stenseth, N. C., Wake, M. H., and Zhang, Z. B.: Merging paleobiology with conservation biology to guide the future of terrestrial ecosystems, 355, 594-+, https://doi.org/10.1126/science.aah4787, 2017.

Barron, J. A. and Anderson, L.: Enhanced Late Holocene ENSO/PDO expression along the margins of the eastern North Pacific, Quaternary International, 235, 3–12, https://doi.org/10.1016/j.quaint.2010.02.026, 2011.

Barron, J. A. and Bukry, D.: Development of the California Current during the past 12,000 yr based on diatoms and silicoflagellates, Palaeogeography, Palaeoclimatology, Palaeoecology, 248, 313–338, https://doi.org/10.1016/j.palaeo.2006.12.009, 2007a.

Barron, J. A. and Bukry, D.: Solar forcing of Gulf of California climate during the past 2000 yr suggested by diatoms and silicoflagellates, Marine Micropaleontology, 62, 115–139, https://doi.org/10.1016/j.marmicro.2006.08.003, 2007b.

Barron, J. A., Heusser, L., Herbert, T., and Lyle, M.: High-resolution climatic evolution of coastal northern California during the past 16,000 years, Paleoceanography, 18, 2003a.

Barron, J. A., Heusser, L., Herbert, T., and Lyle, M.: High-resolution climatic evolution of coastal northern California during the past 16,000 years: CLIMATIC EVOLUTION OF COASTAL CALIFORNIA, Paleoceanography, 18, n/a-n/a, https://doi.org/10.1029/2002PA000768, 2003b.

Barron, J. A., Bukry, D., and Field, D.: Santa Barbara Basin diatom and silicoflagellate response to global climate anomalies during the past 2200 years, Quaternary International, 215, 34–44, https://doi.org/10.1016/j.quaint.2008.08.007, 2010.

Barron, J. A., Bukry, D., Heusser, L. E., Addison, J. A., and Alexander, C. R.: High-resolution climate of the past~ 7300 years of coastal northernmost California: Results from diatoms, silicoflagellates, and pollen, Quatern Int, 2017.

Barron, J. A., Addison, J. A., Heusser, L. E., Bukry, D., Schwartz, V., and Wagner, A.: An 11,300 yr record of paleoclimatology and paleoceanography of the central California coast in a gravity core from Pioneer Seamount, Quaternary International, https://doi.org/10.1016/j.quaint.2019.12.019, 2019.

Batchelder, H. P. and Powell, T. M.: Physical and biological conditions and processes in the northeast Pacific Ocean, Progress in Oceanography, 53, 105–114, https://doi.org/10.1016/S0079-6611(02)00026-5, 2002.

Beaty, R. M. and Taylor, A. H.: A 14 000 year sedimentary charcoal record of fire from the northern Sierra Nevada, Lake Tahoe Basin, California, USA, The Holocene, 19, 347–358, https://doi.org/10.1177/0959683608101386, 2009.

Becerra-Valdivia, L. and Higham, T.: The timing and effect of the earliest human arrivals in North America, 584, 93–97, https://doi.org/10.1038/s41586-020-2491-6, 2020.

Beck, C. W., Bryant, V. M., and Jenkins, D. L.: Analysis of Younger Dryas–Early Holocene pollen in sediments of Paisley Cave 2, south-central Oregon, Palynology, 42, 168–179, https://doi.org/10.1080/01916122.2017.1319883, 2018.

Benson, L., Kashgarian, M., Rye, R., Lund, S., Paillet, F., Smoot, J., Kester, C., Mensing, S., Meko, D., and Lindström, S.: Holocene multidecadal and multicentennial droughts affecting Northern California and Nevada, Quaternary Science Reviews, 21, 659–682, https://doi.org/10.1016/S0277-3791(01)00048-8, 2002.

Bird, B. W. and Kirby, M. E.: An Alpine Lacustrine Record of Early Holocene North American Monsoon Dynamics from Dry Lake, Southern California (USA), J Paleolimnol, 35, 179–192, https://doi.org/10.1007/s10933-005-8514-3, 2006.

Bird, B. W., Kirby, M. E., Howat, I. M., and Tulaczyk, S.: Geophysical evidence for Holocene lake-level change in southern California (Dry Lake), 39, 131–144, https://doi.org/10.1111/j.1502-3885.2009.00114.x, 2010.

Bradley, R. S.: Climate Forcing During the Holocene, PAGES news, 11, 18–19, https://doi.org/10.22498/pages.11.2-3.18, 2003.

Braje, T. J., Rick, T. C., and Erlandson, J. M.: A trans-Holocene historical ecological record of shellfish harvesting on California's Northern Channel Islands, 264, 109–120, 2012.

Bray, N. A., Keyes, A., and Morawitz, W. M. L.: The California Current system in the Southern California Bight and the Santa Barbara Channel, 104, 7695–7714, https://doi.org/10.1029/1998JC900038, 1999.

Briles, C. E., Whitlock, C., and Bartlein, P. J.: Postglacial vegetation, fire, and climate history of the Siskiyou Mountains, Oregon, USA, Quat. res., 64, 44–56, https://doi.org/10.1016/j.yqres.2005.03.001, 2005.

Brown, K. J. and Hebda, R. J.: Origin, development, and dynamics of coastal temperate conifer rainforests of southern Vancouver Island, Canada, Can. J. For. Res., 32, 353–372, https://doi.org/10.1139/x01-197, 2002.

Byrne, R., Ingram, B. L., Starratt, S., Malamud-Roam, F., Collins, J. N., and Conrad, M. E.: Carbon-Isotope, Diatom, and Pollen Evidence for Late Holocene Salinity Change in a Brackish Marsh in the San Francisco Estuary, Quaternary Research, 55, 66–76, https://doi.org/10.1006/qres.2000.2199, 2001.

Cannariato, K. G. and Kennett, J. P.: Climatically related millennial-scale fluctuations in strength of California margin oxygen-minimum zone during the past 60 k.y., Geology, 27, 975–978, https://doi.org/Doi 10.1130/0091-7613(1999)027<0975:Crmsfi>2.3.Co;2, 1999.

Chavez, F., Ryan, J., Lluch-Cota, S., and Niquen, M.: From Anchovies to Sardines and Back: multidecadal CHANGE in the Pacific Ocean, Science (New York, N.Y.), 299, 217–21, https://doi.org/10.1126/science.1075880, 2003.

Checkley, D. M. and Barth, J. A.: Patterns and processes in the California Current System, Prog Oceanogr, 83, 49–64, https://doi.org/10.1016/j.pocean.2009.07.028, 2009.

Chelton, D., Bernal, P., and Mcgowan, J.: Large-scale interannual physical and biological interaction in the California Current (El Nino)., Journal of Marine Research, 40, 1982.

Christensen, C. J., Gorsline, D. S., Hammond, D. E., and Lund, S. P.: Non-annual laminations and expansion of anoxic basin-floor conditions in Santa Monica Basin, California Borderland, over the past four centuries, Mar Geol, 116, 399–418, 1994.

Clark, P. U., Dyke, A. S., Shakun, J. D., Carlson, A. E., Clark, J., Wohlfarth, B., Mitrovica, J. X., Hostetler, S. W., and McCabe, A. M.: The Last Glacial Maximum, Science, 325, 710–714, https://doi.org/10.1126/science.1172873, 2009.

Clark, P. U., Shakun, J. D., Baker, P. A., Bartlein, P. J., Brewer, S., Brook, E., Carlson, A. E., Cheng, H., Kaufman, D. S., Liu, Z., Marchitto, T. M., Mix, A. C., Morrill, C., Otto-Bliesner, B. L., Pahnke, K., Russell, J. M., Whitlock, C., Adkins, J. F., Blois, J. L., Clark, J., Colman, S. M., Curry, W. B., Flower, B. P., He, F., Johnson, T. C., Lynch-Stieglitz, J., Markgraf, V., McManus, J., Mitrovica, J. X., Moreno, P. I., and Williams, J. W.: Global climate evolution during the last deglaciation, Proceedings of the National Academy of Sciences, 109, E1134–E1142, https://doi.org/10.1073/pnas.1116619109, 2012.

Cole, K. L. and Wahl, E.: A Late Holocene Paleoecological Record from Torrey Pines State Reserve, California, Quaternary Research, 53, 341–351, https://doi.org/10.1006/qres.1999.2121, 2000.

Cook, E. R.: Long-Term Aridity Changes in the Western United States, Science, 306, 1015–1018, https://doi.org/10.1126/science.1102586, 2004.

Cowart, A. and Byrne, R.: A Paleolimnological Record of Late Holocene Vegetation Change from the Central California Coast, California Archaeology, 5, 337–352, https://doi.org/10.1179/1947461X13Z.00000000018, 2013.

Crowley, T. J.: Causes of Climate Change Over the Past 1000 Years, 289, 270–277, https://doi.org/10.1126/science.289.5477.270, 2000.

Davis, O. K.: Rapid Climatic Change in Coastal Southern California Inferred from Pollen Analysis of San Joaquin Marsh, Quat. res., 37, 89–100, https://doi.org/10.1016/0033-5894(92)90008-7, 1992.

deMenocal, P. B.: Cultural Responses to Climate Change During the Late Holocene, 292, 667–673, https://doi.org/10.1126/science.1059827, 2001.

Dennison, P. E., Brewer, S. C., Arnold, J. D., and Moritz, M. A.: Large wildfire trends in the western United States, 1984–2011, 41, 2928–2933, https://doi.org/10.1002/2014GL059576, 2014.

Di Lorenzo, E., Schneider, N., Cobb, K. M., Franks, P. J. S., Chhak, K., Miller, A. J., McWilliams, J. C., Bograd, S. J., Arango, H., Curchitser, E., Powell, T. M., and Rivière, P.: North Pacific Gyre

Oscillation links ocean climate and ecosystem change, Geophys. Res. Lett., 35, L08607, https://doi.org/10.1029/2007GL032838, 2008.

Diffenbaugh, N. S. and Ashfaq, M.: Response of California Current forcing to mid-Holocene insolation and sea surface temperatures: WIND FORCING OF THE CALIFORNIA CURRENT, Paleoceanography, 22, n/a-n/a, https://doi.org/10.1029/2006PA001382, 2007.

Diffenbaugh, N. S., Sloan, L. C., and Snyder, M. A.: Orbital suppression of wind-driven upwelling in the California Current at 6 ka, Paleoceanography, 18, https://doi.org/Artn 1051 10.1029/2002pa000865, 2003.

Dingemans, T., Mensing, S. A., Feakins, S. J., Kirby, M. E., and Zimmerman, S. R. H.: 3000 years of environmental change at Zaca Lake, California, USA, Front. Ecol. Evol., 2, https://doi.org/10.3389/fevo.2014.00034, 2014.

Du, X., Hendy, I., and Schimmelmann, A.: A 9000-year flood history for Southern California: A revised stratigraphy of varved sediments in Santa Barbara Basin, Marine Geology, 397, 29–42, https://doi.org/10.1016/j.margeo.2017.11.014, 2018.

Edinborough, K., Porčić, M., Martindale, A., Brown, T. J., Supernant, K., and Ames, K. M.: Radiocarbon test for demographic events in written and oral history, PNAS, 114, 12436–12441, 2017.

Ellis, E. C., Gauthier, N., Goldewijk, K. K., Bird, R. B., Boivin, N., Díaz, S., Fuller, D. Q., Gill, J. L., Kaplan, J. O., Kingston, N., Locke, H., McMichael, C. N. H., Ranco, D., Rick, T. C., Shaw, M. R., Stephens, L., Svenning, J.-C., and Watson, J. E. M.: People have shaped most of terrestrial nature for at least 12,000 years, PNAS, 118, https://doi.org/10.1073/pnas.2023483118, 2021.

Erlandson, J. M., Graham, M. H., Bourque, B. J., Corbett, D., Estes, J. A., and Steneck, R. S.: The Kelp Highway Hypothesis: Marine Ecology, the Coastal Migration Theory, and the Peopling of the Americas, The Journal of Island and Coastal Archaeology, 2, 161–174, https://doi.org/10.1080/15564890701628612, 2007.

Erlandson, J. M., Rick, T. C., and Braje, T. J.: Fishing up the Food Web?: 12,000 Years of Maritime Subsistence and Adaptive Adjustments on California's Channel Islands, Pacific Science, 63, 711–724, https://doi.org/10.2984/049.063.0411, 2009.

Estrella-Martínez, J., Ascough, P. L., Schöne, B. R., Scourse, J. D., and Butler, P. G.: 8.2 ka event North Sea hydrography determined by bivalve shell stable isotope geochemistry, 9, 6753, https://doi.org/10.1038/s41598-019-43219-1, 2019.

Fard, E., Brown, L. N., Lydon, S., Smol, J. P., and MacDonald, G. M.: High-resolution sedimentological and geochemical records of three marshes in San Francisco Bay, California, Quaternary International, https://doi.org/10.1016/j.quaint.2021.05.002, 2021.

Feakins, S. J., Kirby, M. E., Cheetham, M. I., Ibarra, Y., and Zimmerman, S. R. H.: Fluctuation in leaf wax D/H ratio from a southern California lake records significant variability in isotopes in precipitation during the late Holocene, Organic Geochemistry, 66, 48–59, https://doi.org/10.1016/j.orggeochem.2013.10.015, 2014.

Field, D. B., Baumgartner, T. R., Charles, C. D., Ferreira-Bartrina, V., and Ohman, M. D.: Planktonic foraminifera of the California Current reflect 20th-century warming, 311, 63–66, https://doi.org/10.1126/science.1116220, 2006.

Finnegan, S., Anderson, S. C., Harnik, P. G., Simpson, C., Tittensor, D. P., Byrnes, J. E., Finkel, Z. V., Lindberg, D. R., Liow, L. H., Lockwood, R., Lotze, H. K., McClain, C. R., McGuire, J. L., O'Dea, A., and Pandolfi, J. M.: Paleontological baselines for evaluating extinction risk in the modern oceans, 348, 567–570, https://doi.org/10.1126/science.aaa6635, 2015.

Fisler, J. and Hendy, I. L.: California Current System response to late Holocene climate cooling in southern California, 35, https://doi.org/Artn L09702 10.1029/2008gl033902, 2008.

Flores, C.: Importance of small-scale paleo-oceanographic conditions to interpret changes in size of California mussel (Mytilus californianus). Late Holocene, Santa Cruz island, California, Quaternary International, 427, 137–150, https://doi.org/10.1016/j.quaint.2016.01.036, 2017.

Friddell, J. E., Thunell, R. C., Guilderson, T. P., and Kashgarian, M.: Increased northeast Pacific climatic variability during the warm middle Holocene, 30, 2003.

Gardner, J. V., Heusser, L. E., Quinterno, P. J., Stone, S. M., Barron, J. A., and Poore, R. Z.: Clear Lake record vs. the adjacent marine record; A correlation of their past 20,000 years of paleoclimatic and paleoceanographic responses, in: Geological Society of America Special Papers, vol. 214, Geological Society of America, 171–182, https://doi.org/10.1130/SPE214-p171, 1988.

Gavin, D. G., Brubaker, L. B., and Lertzman, K. P.: HOLOCENE FIRE HISTORY OF A COASTAL TEMPERATE RAIN FOREST BASED ON SOIL CHARCOAL RADIOCARBON DATES, Ecology, 84, 186–201, https://doi.org/10.1890/0012-9658(2003)084[0186:HFHOAC]2.0.CO;2, 2003.

Gavin, D. G., Hallett, D. J., Hu, F. S., Lertzman, K. P., Prichard, S. J., Brown, K. J., Lynch, J. A., Bartlein, P., and Peterson, D. L.: Forest fire and climate change in western North America: insights from sediment charcoal records, Frontiers in Ecology and the Environment, 5, 499–506, https://doi.org/10.1890/060161, 2007.

van Geen, A., Smethie, W. M., Horneman, A., and Lee, H.: Sensitivity of the North Pacific oxygen minimum zone to changes in ocean circulation: A simple model calibrated by chlorofluorocarbons, J. Geophys. Res., 111, C10004, https://doi.org/10.1029/2005JC003192, 2006.

Glassow, M. A., Thakar, H. B., and Kennett, D. J.: Red abalone collecting and marine water temperature during the Middle Holocene occupation of Santa Cruz Island, California, Journal of Archaeological Science, 39, 2574–2582, https://doi.org/10.1016/j.jas.2012.03.017, 2012.

Graham, M. H., Kinlan, B. P., and Grosberg, R. K.: Post-glacial redistribution and shifts in productivity of giant kelp forests, https://doi.org/10.1098/rspb.2009.1664, 2010.

Hallett, D. J. and Anderson, R. S.: Paleofire reconstruction for high-elevation forests in the Sierra Nevada, California, with implications for wildfire synchrony and climate variability in the late Holocene, Quat. res., 73, 180–190, https://doi.org/10.1016/j.yqres.2009.11.008, 2010.

Hallett, D. J., Lepofsky, D. S., Mathewes, R. W., and Lertzman, K. P.: 11 000 years of fire history and climate in the mountain hemlock rain forests of southwestern British Columbia based on sedimentary charcoal, Can. J. For. Res., 33, 292–312, https://doi.org/10.1139/x02-177, 2003.

Hermann, N. W., Oster, J. L., and Ibarra, D. E.: Spatial patterns and driving mechanisms of mid-Holocene hydroclimate in western North America: MID-HOLOCENE HYDROCLIMATE IN WESTERN NORTH AMERICA, J. Quaternary Sci., 33, 421–434, https://doi.org/10.1002/jqs.3023, 2018.

Heusser, L.: Direct correlation of millennial-scale changes in western North American vegetation and climate with changes in the California Current System over the past ~60 kyr, Paleoceanography, 13, 252–262, https://doi.org/10.1029/98PA00670, 1998.

Heusser, L. E.: Pollen in Santa Barbara Basin, California: A 12,000 year record, 89, 673–678, 1978.

Heusser, L. E.: Palynology and paleoecology of postglacial sediments in an anoxic basin, Saanich Inlet, British Columbia, 13, 1983.

Hickey, B. M.: The California current system—hypotheses and facts, Progress in Oceanography, 8, 191–279, https://doi.org/10.1016/0079-6611(79)90002-8, 1979.

Higuera, P. E., Shuman, B. N., and Wolf, K. D.: Rocky Mountain subalpine forests now burning more than any time in recent millennia, PNAS, 118, https://doi.org/10.1073/pnas.2103135118, 2021.

Hiner, C. A., Kirby, M. E., Bonuso, N., Patterson, W. P., Palermo, J., and Silveira, E.: Late Holocene hydroclimatic variability linked to Pacific forcing: evidence from Abbott Lake, coastal central California, J Paleolimnol, 56, 299–313, https://doi.org/10.1007/s10933-016-9912-4, 2016.

Ingram, B. L.: Differences in Radiocarbon Age between Shell and Charcoal from a Holocene Shellmound in Northern California, Quat. res., 49, 102–110, https://doi.org/10.1006/qres.1997.1944, 1998.

Jones, T. L. and Kennett, D. J.: Late Holocene Sea Temperatures along the Central California Coast, Quat. res., 51, 74–82, https://doi.org/10.1006/qres.1998.2000, 1999.

Jones, T. L., Kennett, D. J., Kennett, J. P., and Codding, B. F.: Seasonal stability in Late Holocene shellfish harvesting on the central California coast, Journal of Archaeological Science, 35, 2286–2294, https://doi.org/10.1016/j.jas.2008.03.002, 2008.

Kaufman, D., McKay, N., Routson, C., Erb, M., Davis, B., Heiri, O., Jaccard, S., Tierney, J., Dätwyler, C., Axford, Y., Brussel, T., Cartapanis, O., Chase, B., Dawson, A., de Vernal, A., Engels, S., Jonkers, L., Marsicek, J., Moffa-Sánchez, P., Morrill, C., Orsi, A., Rehfeld, K., Saunders, K., Sommer, P. S., Thomas, E., Tonello, M., Tóth, M., Vachula, R., Andreev, A., Bertrand, S., Biskaborn, B., Bringué, M., Brooks, S., Caniupán, M., Chevalier, M., Cwynar, L., Emile-Geay, J., Fegyveresi, J., Feurdean, A., Finsinger, W., Fortin, M.-C., Foster, L., Fox, M., Gajewski, K., Grosjean, M., Hausmann, S., Heinrichs, M., Holmes, N., Ilyashuk, B., Ilyashuk, E., Juggins, S., Khider, D., Koinig, K., Langdon, P., Larocque-Tobler, I., Li, J., Lotter, A., Luoto, T., Mackay, A., Magyari, E., Malevich, S., Mark, B., Massaferro, J., Montade, V., Nazarova, L., Novenko, E., Pařil, P., Pearson, E., Peros, M., Pienitz, R., Płóciennik, M., Porinchu, D., Potito, A., Rees, A., Reinemann, S., Roberts, S., Rolland, N., Salonen, S., Self, A., Seppä, H., Shala, S., St-Jacques, J.-M., Stenni, B., Syrykh, L., Tarrats, P., Taylor, K., van den Bos, V., Velle, G., Wahl, E., Walker, I., Wilmshurst, J., Zhang, E., and Zhilich, S.: A global database of Holocene paleotemperature records, Sci Data, 7, 115, https://doi.org/10.1038/s41597-020-0445-3, 2020.

Kaufman, D. S., Axford, Y. L., Henderson, A. C. G., McKay, N. P., Oswald, W. W., Saenger, C., Anderson, R. S., Bailey, H. L., Clegg, B., Gajewski, K., Hu, F. S., Jones, M. C., Massa, C., Routson, C. C., Werner, A., Wooller, M. J., and Yu, Z.: Holocene climate changes in eastern Beringia (NW North America) – A systematic review of multi-proxy evidence, Quaternary Science Reviews, 147, 312–339, https://doi.org/10.1016/j.quascirev.2015.10.021, 2016.

Kennett, D. J. and Kennett, J. P.: Competitive and cooperative responses to climatic instability in coastal southern California, Am Antiquity, 65, 379–395, https://doi.org/Doi 10.2307/2694065, 2000.

Kennett, D. J., Kennettb, J. P., Erlandson, J. M., and Cannariato, K. G.: Human responses to Middle Holocene climate change on California's Channel Islands, Quaternary Sci Rev, 26, 351–367, https://doi.org/10.1016/j.quascirev.2006.07.019, 2007.

Kennett, J. P. and Ingram, B. L.: A 20,000 Year Record of Ocean Circulation and Climate-Change from the Santa-Barbara Basin, Nature, 377, 510–514, https://doi.org/DOI 10.1038/377510a0, 1995.

Kim, J.-H., Rimbu, N., Lorenz, S. J., Lohmann, G., Nam, S.-I., Schouten, S., Rühlemann, C., and Schneider, R. R.: North Pacific and North Atlantic sea-surface temperature variability during the Holocene, Quaternary Science Reviews, 23, 2141–2154, https://doi.org/10.1016/j.quascirev.2004.08.010, 2004.

Kirby, M. E., Lund, S. P., Anderson, M. A., and Bird, B. W.: Insolation forcing of Holocene climate change in Southern California: a sediment study from Lake Elsinore, J Paleolimnol, 38, 395–417, https://doi.org/10.1007/s10933-006-9085-7, 2007.

Kirby, M. E., Lund, S. P., Patterson, W. P., Anderson, M. A., Bird, B. W., Ivanovici, L., Monarrez, P., and Nielsen, S.: A Holocene record of Pacific Decadal Oscillation (PDO)-related hydrologic variability in Southern California (Lake Elsinore, CA), J Paleolimnol, 44, 819–839, https://doi.org/10.1007/s10933-010-9454-0, 2010.

Kirby, M. E., Zimmerman, S. R. H., Patterson, W. P., and Rivera, J. J.: A 9170-year record of decadal-to-multi-centennial scale pluvial episodes from the coastal Southwest United States: a role for atmospheric rivers?, Quaternary Science Reviews, 46, 57–65, https://doi.org/10.1016/j.quascirev.2012.05.008, 2012.

Kirby, M. E., Feakins, S. J., Hiner, C. A., Fantozzi, J., Zimmerman, S. R. H., Dingemans, T., and Mensing, S. A.: Tropical Pacific forcing of Late-Holocene hydrologic variability in the coastal southwest United States, Quaternary Science Reviews, 102, 27–38, https://doi.org/10.1016/j.quascirev.2014.08.005, 2014.

Kirby, M. E., Knell, E. J., Anderson, W. T., Lachniet, M. S., Palermo, J., Eeg, H., Lucero, R., Murrieta, R., Arevalo, A., Silveira, E., and Hiner, C. A.: Evidence for insolation and Pacific forcing of late glacial through Holocene climate in the Central Mojave Desert (Silver Lake, CA), Quat. res., 84, 174–186, https://doi.org/10.1016/j.yqres.2015.07.003, 2015.

Kirby, M. E. C., Patterson, W. P., Lachniet, M., Noblet, J. A., Anderson, M. A., Nichols, K., and Avila, J.: Pacific Southwest United States Holocene Droughts and Pluvials Inferred From Sediment δ18O(calcite) and Grain Size Data (Lake Elsinore, California), Front. Earth Sci., 7, https://doi.org/10.3389/feart.2019.00074, 2019.

Klimaszewski-Patterson, A., Morgan, C. T., and Mensing, S.: Identifying a Pre-Columbian Anthropocene in California, Annals of the American Association of Geographers, 111, 784–794, https://doi.org/10.1080/24694452.2020.1846488, 2021.

Konrad, S. K. and Clark, D. H.: Evidence for an Early Neoglacial Glacier Advance from Rock Glaciers and Lake Sediments in the Sierra Nevada, California, U.S.A., 30, 272–284, https://doi.org/10.1080/00040851.1998.12002901, 1998.

LaDochy, S., Medina, R., and Patzert, W.: Recent California climate variability: spatial and temporal patterns in temperature trends, Clim. Res., 33, 159–169, https://doi.org/10.3354/cr033159, 2007.

Lightfoot, K. G. and Cuthrell, R. Q.: Anthropogenic burning and the Anthropocene in late-Holocene California, The Holocene, 25, 1581–1587, https://doi.org/10.1177/0959683615588376, 2015.

Lindstrom, S.: Submerged Tree Stumps as Indicators of Mid-Holocene Aridity in the Lake Tahoe Basin, 13, 1990.

Liu, Z., Zhu, J., Rosenthal, Y., Zhang, X., Otto-Bliesner, B. L., Timmermann, A., Smith, R. S., Lohmann, G., Zheng, W., and Timm, O. E.: The Holocene temperature conundrum, PNAS, 111, E3501–E3505, https://doi.org/10.1073/pnas.1407229111, 2014.

Lluch-Cota, D. B., Wooster, W. S., and Hare, S. R.: Sea surface temperature variability in coastal areas of the northeastern Pacific related to the El Niño-Southern Oscillation and the Pacific Decadal Oscillation, Geophys. Res. Lett., 28, 2029–2032, https://doi.org/10.1029/2000GL012429, 2001.

Long, C. J., Whitlock, C., Bartlein, P. J., and Millspaugh, S. H.: A 9000-year fire history from the Oregon Coast Range, based on a high-resolution charcoal study, https://doi.org/10.1139/x98-051, 2011.

Lyle, M., Heusser, L., Ravelo, C., Yamamoto, M., Barron, J., Diffenbaugh, N. S., Herbert, T., and Andreasen, D.: Out of the Tropics: The Pacific, Great Basin Lakes, and Late Pleistocene Water Cycle in the Western United States, Science, 337, 1629–1633, https://doi.org/10.1126/science.1218390, 2012.

MacDonald, G. M. and Case, R. A.: Variations in the Pacific Decadal Oscillation over the past millennium, 32, https://doi.org/Artn L08703 10.1029/2005gl022478, 2005.

MacDonald, G. M., Moser, K. A., Bloom, A. M., Potito, A. P., Porinchu, D. F., Holmquist, J. R., Hughes, J., and Kremenetski, K. V.: Prolonged California aridity linked to climate warming and Pacific sea surface temperature, Sci Rep, 6, 33325, https://doi.org/10.1038/srep33325, 2016.

Malamud-Roam, F. P., Lynn Ingram, B., Hughes, M., and Florsheim, J. L.: Holocene paleoclimate records from a large California estuarine system and its watershed region: linking watershed climate and bay conditions, Quaternary Science Reviews, 25, 1570–1598, https://doi.org/10.1016/j.quascirev.2005.11.012, 2006.

Mann, M. E. and Gleick, P. H.: Climate change and California drought in the 21st century, PNAS, 112, 3858–3859, https://doi.org/10.1073/pnas.1503667112, 2015.

Mantua, N. J., Munn, T., Wiley, J., and Mantua, N. J.: Pacific–Decadal Oscillation, 2002.

Marcott, S. A., Shakun, J. D., Clark, P. U., and Mix, A. C.: A Reconstruction of Regional and Global Temperature for the Past 11,300 Years, 339, 1198–1201, https://doi.org/10.1126/science.1228026, 2013.

Marlon, J., Bartlein, P. J., and Whitlock, C.: Fire-fuel-climate linkages in the northwestern USA during the Holocene, The Holocene, 16, 1059–1071, https://doi.org/10.1177/0959683606069396, 2006.

Marlon, J. R., Bartlein, P. J., Gavin, D. G., Long, C. J., Anderson, R. S., Briles, C. E., Brown, K. J., Colombaroli, D., Hallett, D. J., Power, M. J., Scharf, E. A., and Walsh, M. K.: Long-term perspective on wildfires in the western USA, PNAS, 109, E535–E543, https://doi.org/10.1073/pnas.1112839109, 2012.

Marlon, J. R., Bartlein, P. J., Daniau, A.-L., Harrison, S. P., Maezumi, S. Y., Power, M. J., Tinner, W., and Vanniére, B.: Global biomass burning: a synthesis and review of Holocene paleofire records and their controls, Quaternary Science Reviews, 65, 5–25, https://doi.org/10.1016/j.quascirev.2012.11.029, 2013.

Marsicek, J., Shuman, B. N., Bartlein, P. J., Shafer, S. L., and Brewer, S.: Reconciling divergent trends and millennial variations in Holocene temperatures, 554, 92–96, https://doi.org/10.1038/nature25464, 2018.

Matero, I. S. O., Gregoire, L. J., Ivanovic, R. F., Tindall, J. C., and Haywood, A. M.: The 8.2 ka cooling event caused by Laurentide ice saddle collapse, Earth and Planetary Science Letters, 473, 205–214, https://doi.org/10.1016/j.epsl.2017.06.011, 2017.

Mayewski, P. A., Rohling, E. E., Curt Stager, J., Karlén, W., Maasch, K. A., Meeker, L. D., Meyerson, E. A., Gasse, F., van Kreveld, S., Holmgren, K., Lee-Thorp, J., Rosqvist, G., Rack, F., Staubwasser, M., Schneider, R. R., and Steig, E. J.: Holocene climate variability, Quat. res., 62, 243–255, https://doi.org/10.1016/j.yqres.2004.07.001, 2004.

McGann, M.: High-Resolution Foraminiferal, Isotopic, and Trace Element Records from Holocene Estuarine Deposits of San Francisco Bay, California, Journal of Coastal Research, 245, 1092–1109, https://doi.org/10.2112/08A-0003.1, 2008.

McGann, M.: Paleoceanographic changes on the Farallon Escarpment off central California during the last 16,000 years, Quatern Int, 235, 26–39, https://doi.org/10.1016/j.quaint.2010.09.005, 2011.

McGann, M.: Correlation of marine and coastal terrestrial records of central California: Response to paleoceanographic and paleoclimatic change during the past 19,000 years, Quatern Int, 387, 58–71, https://doi.org/10.1016/j.quaint.2015.01.037, 2015.

McKechnie, I.: Indigenous Oral History and Settlement Archaeology in Barkley Sound, Western Vancouver Island, 36, 2015.

McQuoid, M. R. and Hobson, L. A.: A Holocene record of diatom and silico¯agellate microfossils in sediments of Saanich Inlet, ODP Leg 169S, 13, 2001.

Metcalfe, S. E.: The Holocene history of the North American Monsoon: `known knowns' and `known unknowns' in understanding its spatial and temporal complexity, 27, 2015.

Minnis, P. E.: People and plants in ancient western North America, University of Arizona Press, 492 pp., 2004.

Mix, A. C., Lund, D. C., Pisias, N. G., Bodén, P., Bornmalm, L., Lyle, M., and Pike, J.: Rapid climate oscillations in the Northeast Pacific during the last deglaciation reflect Northern and Southern Hemisphere sources, in: Geophysical Monograph Series, vol. 112, edited by: Clark, U., Webb, S., and Keigwin, D., American Geophysical Union, Washington, D. C., 127–148, https://doi.org/10.1029/GM112p0127, 1999.

Moffitt, S. E., Hill, T. M., Ohkushi, K., Kennett, J. P., and Behl, R. J.: Vertical oxygen minimum zone oscillations since 20 ka in Santa Barbara Basin: A benthic foraminiferal community perspective, Paleoceanography, 29, 44–57, https://doi.org/10.1002/2013pa002483, 2014.

Moffitt, S. E., Hill, T. M., Roopnarine, P. D., and Kennett, J. P.: Response of seafloor ecosystems to abrupt global climate change, P Natl Acad Sci USA, 112, 4684–4689, https://doi.org/10.1073/pnas.1417130112, 2015.

Mohr, J. A., Whitlock, C., and Skinner, C. N.: Postglacial vegetation and fire history, eastern Klamath Mountains, California, USA, The Holocene, 10, 587–601, https://doi.org/10.1191/095968300675837671, 2000.

Nederbragt, A. J. and Thurow, J. W.: A 6000 yr varve record of Holocene climate in Saanich Inlet, British Columbia, from digital sediment colour analysis of ODP Leg 169S cores, Marine Geology, 174, 95–110, https://doi.org/10.1016/S0025-3227(00)00144-4, 2001.

Negrini, R. M., Wigand, P. E., Draucker, S., Gobalet, K., Gardner, J. K., Sutton, M. Q., and Yohe, R. M.: The Rambla highstand shoreline and the Holocene lake-level history of Tulare Lake, California, USA, Quaternary Science Reviews, 25, 1599–1618, https://doi.org/10.1016/j.quascirev.2005.11.014, 2006.

Ohkushi, K., Kennett, J. P., Zeleski, C. M., Moffitt, S. E., Hill, T. M., Robert, C., Beaufort, L., and Behl, R. J.: Quantified intermediate water oxygenation history of the NE Pacific: A new benthic foraminiferal record from Santa Barbara basin, Paleoceanography, 28, 453–467, https://doi.org/10.1002/palo.20043, 2013.

Osborne, E. B., Thunell, R. C., Gruber, N., Feely, R. A., and Benitez-Nelson, C. R.: Decadal variability in twentieth-century ocean acidification in the California Current Ecosystem, Nat. Geosci., 13, 43–49, https://doi.org/10.1038/s41561-019-0499-z, 2020.

Oster, J. L., Sharp, W. D., Covey, A. K., Gibson, J., Rogers, B., and Mix, H.: Climate response to the 8.2 ka event in coastal California, Sci Rep, 7, 3886, https://doi.org/10.1038/s41598-017-04215-5, 2017.

Pak, D. K., Hendy, I. L., Weaver, J. C., Schimmelmann, A., and Clayman, L.: Foraminiferal proxy response to ocean temperature variability and acidification over the last 150 years in the Santa Barbara Basin (California), Quatern Int, https://doi.org/10.1016/j.quaint.2016.07.049, 2016.

Palmer, H. M., Hill, T. M., Roopnarine, P. D., Myhre, S. E., Reyes, K. R., and Donnenfield, J. T.: Southern California margin benthic foraminiferal assemblages record recent centennial-scale changes in oxygen minimum zone, 17, 2923–2937, https://doi.org/10.5194/bg-17-2923-2020, 2020.

Pante, E. and Simon-Bouhet, B.: marmap: A Package for Importing, Plotting and Analyzing Bathymetric and Topographic Data in R, PLOS ONE, 8, e73051, https://doi.org/10.1371/journal.pone.0073051, 2013.

Pellatt, M. G., Hebda, R. J., and Mathewes, R. W.: High-resolution Holocene vegetation history and climate from Hole 1034B, ODP leg 169S, Saanich Inlet, Canada, Marine Geology, 174, 211–226, https://doi.org/10.1016/S0025-3227(00)00151-1, 2001.

Platzman, E. and Lund, S.: High-resolution environmental magnetic study of a Holocene sedimentary record from Zaca Lake, California, The Holocene, 29, 17–25, https://doi.org/10.1177/0959683618804636, 2019.

Praetorius, S. K., Condron, A., Mix, A. C., Walczak, M. H., McKay, J. L., and Du, J.: The role of Northeast Pacific meltwater events in deglacial climate change, 6, eaay2915, https://doi.org/10.1126/sciadv.aay2915, 2020.

Rasmussen, J. B. T., Polyak, V. J., and Asmerom, Y.: Evidence for Pacific-modulated precipitation variability during the late Holocene from the southwestern USA, Geophys. Res. Lett., 33, L08701, https://doi.org/10.1029/2006GL025714, 2006.

Renssen, H., Seppä, H., Crosta, X., Goosse, H., and Roche, D. M.: Global characterization of the Holocene Thermal Maximum, Quaternary Science Reviews, 48, 7–19, https://doi.org/10.1016/j.quascirev.2012.05.022, 2012.

Reyes, A. V. and Clague, J. J.: Stratigraphic evidence for multiple Holocene advances of Lillooet Glacier, southern Coast Mountains, British Columbia, Canadian Journal of Earth Sciences, 41, 903–918, https://doi.org/10.1139/e04-039, 2004.

Rick, T. C.: Weathering the storm: Coastal subsistence and ecological resilience on Late Holocene Santa Rosa Island, California, Quaternary International, 239, 135–146, https://doi.org/10.1016/j.quaint.2010.06.008, 2011.

Roark, E. B., Ingram, B. L., Southon, J., and Kennett, J. P.: Holocene foraminiferal radiocarbon record of paleocirculation in the Santa Barbara Basin, Geology, 31, 379–382, https://doi.org/Doi 10.1130/0091-7613(2003)031<0379:Hfrrop>2.0.Co;2, 2003.

Schimmelmann, A., Hendy, I. L., Dunn, L., Pak, D. K., and Lange, C. B.: Revised similar to 2000-year chronostratigraphy of partially varved marine sediment in Santa Barbara Basin, California, Gff, 135, 258–264, https://doi.org/10.1080/11035897.2013.773066, 2013.

Sheppard, P. R., Comrie, A. C., Packin, G. D., Angersbach, K., and Hughes, M. K.: The climate of the US Southwest, 21, 219–238, https://doi.org/10.3354/cr021219, 2002.

Shuman, B. N., Routson, C., McKay, N., Fritz, S., Kaufman, D., Kirby, M. E., Nolan, C., Pederson, G. T., and St-Jacques, J.-M.: Placing the Common Era in a Holocene context: millennial to centennial patterns and trends in the hydroclimate of North America over the past 2000 years, Clim. Past, 14, 665–686, https://doi.org/10.5194/cp-14-665-2018, 2018.

Siedlecki, S. A., Banas, N. S., Davis, K. A., Giddings, S., Hickey, B. M., MacCready, P., Connolly, T., and Geier, S.: Seasonal and interannual oxygen variability on the Washington and Oregon continental shelves, 120, 608–633, https://doi.org/10.1002/2014JC010254, 2015.

Spaulding, W. G.: A Middle Holocene Vegetation Record from the Mojave Desert of North America and its Paleoclimatic Significance, Quat. res., 35, 427–437, https://doi.org/10.1016/0033-5894(91)90055-A, 1991.

Steinman, B. A., Pompeani, D. P., Abbott, M. B., Ortiz, J. D., Stansell, N. D., Finkenbinder, M. S., Mihindukulasooriya, L. N., and Hillman, A. L.: Oxygen isotope records of Holocene climate variability in the Pacific Northwest, Quaternary Science Reviews, 142, 40–60, https://doi.org/10.1016/j.quascirev.2016.04.012, 2016.

Steinman, B. A., Nelson, D. B., Abbott, M. B., Stansell, N. D., Finkenbinder, M. S., and Finney, B. P.: Lake sediment records of Holocene hydroclimate and impacts of the Mount Mazama eruption, north-central Washington, USA, Quaternary Science Reviews, 204, 17–36, https://doi.org/10.1016/j.quascirev.2018.09.018, 2019.

Stine, S.: Late holocene fluctuations of Mono Lake, eastern California, Palaeogeography, Palaeoclimatology, Palaeoecology, 78, 333–381, https://doi.org/10.1016/0031-0182(90)90221-R, 1990.

Stine, S.: Extreme and persistent drought in California and Patagonia during mediaeval time, 369, 546–549, https://doi.org/10.1038/369546a0, 1994.

Taylor, A. H., Trouet, V., Skinner, C. N., and Stephens, S.: Socioecological transitions trigger fire regime shifts and modulate fire–climate interactions in the Sierra Nevada, USA, 1600–2015 CE, Proc Natl Acad Sci USA, 113, 13684–13689, https://doi.org/10.1073/pnas.1609775113, 2016.

Thomas, E. R., Wolff, E. W., Mulvaney, R., Steffensen, J. P., Johnsen, S. J., Arrowsmith, C., White, J. W. C., Vaughn, B., and Popp, T.: The 8.2ka event from Greenland ice cores, Quaternary Science Reviews, 26, 70–81, https://doi.org/10.1016/j.quascirev.2006.07.017, 2007.

Tomasovych, A. and Kidwell, S. M.: Nineteenth-century collapse of a benthic marine ecosystem on the open continental shelf, P Roy Soc B-Biol Sci, 284, https://doi.org/ARTN 20170328 10.1098/rspb.2017.0328, 2017.

Viau, A. E., Gajewski, K., Sawada, M. C., and Fines, P.: Millennial-scale temperature variations in North America during the Holocene, J. Geophys. Res., 111, D09102, https://doi.org/10.1029/2005JD006031, 2006.

Voarintsoa, N. R. G., Matero, I. S. O., Railsback, L. B., Gregoire, L. J., Tindall, J., Sime, L., Cheng, H., Edwards, R. L., Brook, G. A., Kathayat, G., Li, X., Michel Rakotondrazafy, A. F., and Madison Razanatseheno, M. O.: Investigating the 8.2 ka event in northwestern Madagascar: Insight from data–model comparisons, Quaternary Science Reviews, 204, 172–186, https://doi.org/10.1016/j.quascirev.2018.11.030, 2019.

Waelbroeck, C., Paul, A., Kucera, M., Rosell-Melé, A., Weinelt, M., Schneider, R., Mix, A. C., Abelmann, A., Armand, L., Bard, E., Barker, S., Barrows, T. T., Benway, H., Cacho, I., Chen, M.-T., Cortijo, E., Crosta, X., de Vernal, A., Dokken, T., Duprat, J., Elderfield, H., Eynaud, F., Gersonde, R., Hayes, A., Henry, M., Hillaire-Marcel, C., Huang, C.-C., Jansen, E., Juggins, S., Kallel, N., Kiefer, T., Kienast, M., Labeyrie, L., Leclaire, H., Londeix, L., Mangin, S., Matthiessen, J., Marret, F., Meland, M., Morey, A. E., Mulitza, S., Pflaumann, U., Pisias, N. G., Radi, T., Rochon, A., Rohling, E. J., Sbaffi, L., Schäfer-Neth, C., Solignac, S., Spero, H., Tachikawa, K., Turon, J.-L., and MARGO Project Members: Constraints on the magnitude and

patterns of ocean cooling at the Last Glacial Maximum, Nature Geosci, 2, 127–132, https://doi.org/10.1038/ngeo411, 2009.

Walczak, M. H., Mix, A. C., Cowan, E. A., Fallon, S., Fifield, L. K., Alder, J. R., Du, J., Haley, B., Hobern, T., Padman, J., Praetorius, S. K., Schmittner, A., Stoner, J. S., and Zellers, S. D.: Phasing of millennial-scale climate variability in the Pacific and Atlantic Oceans, https://doi.org/10.1126/science.aba7096, 2020.

Walker, M., Head, M. J., Berkelhammer, M., Björck, S., Cheng, H., Cwynar, L., Fisher, D., Gkinis, V., Long, A., Lowe, J., Newnham, R., Rasmussen, S. O., and Weiss, H.: Formal ratification of the subdivision of the Holocene Series/Epoch (Quaternary System/Period): two new Global Boundary Stratotype Sections and Points (GSSPs) and three new stages/subseries, Episodes, 41, 213–223, https://doi.org/10.18814/epiiugs/2018/018016, 2018.

Walsh, M. K., Lukens, M. L., McCutcheon, P. T., and Burtchard, G. C.: Fire-climate-human interactions during the postglacial period at Sunrise Ridge, Mount Rainier National Park, Washington (USA), Quaternary Science Reviews, 177, 246–264, https://doi.org/10.1016/j.quascirev.2017.10.032, 2017.

Wang, Y., Hendy, I., and Napier, T. J.: Climate and Anthropogenic Controls of Coastal Deoxygenation on Interannual to Centennial Timescales, 2017.

Wang, Y., Hendy, I. L., and Zhu, J.: Expansion of the Southern California oxygen minimum zone during the early-to mid-Holocene due to reduced ventilation of the Northeast Pacific, Quaternary Science Reviews, 238, 106326, https://doi.org/10.1016/j.quascirev.2020.106326, 2020.

Wanner, H., Beer, J., Bütikofer, J., Crowley, T. J., Cubasch, U., Flückiger, J., Goosse, H., Grosjean, M., Joos, F., Kaplan, J. O., Küttel, M., Müller, S. A., Prentice, I. C., Solomina, O., Stocker, T. F., Tarasov, P., Wagner, M., and Widmann, M.: Mid- to Late Holocene climate change: an overview, Quaternary Science Reviews, 27, 1791–1828, https://doi.org/10.1016/j.quascirev.2008.06.013, 2008.

Waters, C. N., Zalasiewicz, J., Summerhayes, C., Barnosky, A. D., Poirier, C., Galuszka, A., Cearreta, A., Edgeworth, M., Ellis, E. C., Ellis, M., Jeandel, C., Leinfelder, R., McNeill, J. R., Richter, D., Steffen, W., Syvitski, J., Vidas, D., Wagreich, M., Williams, M., Zhisheng, A., Grinevald, J., Odada, E., Oreskes, N., and Wolfe, A. P.: The Anthropocene is functionally and stratigraphically distinct from the Holocene, 351, aad2622, https://doi.org/10.1126/science.aad2622, 2016.

Westerling, A. L., Gershunov, A., Brown, T. J., Cayan, D. R., and Dettinger, M. D.: Climate and Wildfire in the Western United States, 84, 595–604, https://doi.org/10.1175/BAMS-84-5-595, 2003.

Westerling, A. L., Bryant, B. P., Preisler, H. K., Holmes, T. P., Hidalgo, H. G., Das, T., and Shrestha, S. R.: Climate change and growth scenarios for California wildfire, Climatic Change, 109, 445–463, https://doi.org/10.1007/s10584-011-0329-9, 2011.

Whitlock, C., Marlon, J., Briles, C., Brunelle, A., Long, C., and Bartlein, P.: Long-term relations among fire, fuel, and climate in the north-western US based on lake-sediment studies, Int. J. Wildland Fire, 17, 72, https://doi.org/10.1071/WF07025, 2008.

Wise, E. K.: Five centuries of U.S. West Coast drought: Occurrence, spatial distribution, and associated atmospheric circulation patterns, 43, 4539–4546, https://doi.org/10.1002/2016GL068487, 2016.

Yati, E., Minobe, S., Mantua, N., Ito, S., and Di Lorenzo, E.: Marine Ecosystem Variations Over the North Pacific and Their Linkage to Large-Scale Climate Variability and Change, Front. Mar. Sci., 7, https://doi.org/10.3389/fmars.2020.578165, 2020.

Appendices

Appendix 1: Appendix to Chapter 2. Benthic foraminiferal assemblage raw faunal counts.

Core	Basin	Age (ka)	Depth in core (top, cm)	Fraction Factor	Bolivina pseudoberyethes	Bolivina spissa	Cassisulina sp.	Cibicides mckanni	Epistominella pacifica	Episotominella exigua	Globobulimina ovata2	Globobulimina pacifica	Globocassidulina subglobosa	Hansensica soldanii
Tanner	EW9504_09	1.92	0	4	1	7	2	5	12	6	2	1	18	34
Tanner	EW9504_09	2.10	2	4	1	22	14	21	19	16	7	0	28	34
Tanner	EW9504_09	2.29	4	4	2	28	11	23	23	18	11	0	42	62
Tanner	EW9504_09	2.48	6	4	0	24	4	26	15	10	12	0	35	63
Tanner	EW9504_09	2.67	8	4	0	20	10	19	16	9	5	1	30	30
Tanner	EW9504_09	2.85	10	4	1	20	2	20	21	4	5	1	31	40
Tanner	EW9504_09	3.04	12	4	0	26	6	7	7	11	33	1	39	39
Tanner	EW9504_09	3.23	14	4	1	66	27	9	24	61	69	2	60	45
Tanner	EW9504_09	3.42	16	8	0	23	8	8	8	20	22	1	22	19
Tanner	EW9504_09	3.60	18	8	2	25	13	4	1	24	21	0	32	21
Tanner	EW9504_09	3.98	22	4	1	56	16	2	4	23	19	0	22	11
Tanner	EW9504_09	4.16	24	4	2	21	14	1	6	9	12	0	29	10
Tanner	EW9504_09	4.35	26	2	0	58	13	14	10	8	14	1	47	45
Tanner	EW9504_09	4.54	28	4	0	48	8	3	1	10	4	0	30	3
Tanner	EW9504_09	4.73	30	2	0	38	11	0	3	4	5	1	23	1
Tanner	EW9504_09	4.91	32	2	1	65	16	4	7	23	14	0	30	13
Tanner	EW9504_09	5.10	34	4	0	30	9	1	2	9	3	0	20	3
Tanner	EW9504_09	5.29	36	4	2	45	23	5	0	14	5	0	57	5
Tanner	EW9504_09	5.48	38	4	0	33	7	3	2	6	7	1	14	5
San Clemente	EW9504-05	7.07	30	1	0	0	1	27	7	15	5	0	1	1
San Clemente	EW9504-05	7.45	32	1	0	2	1	20	1	30	8	0	0	0
San Clemente	EW9504-05	7.83	34	1	0	1	0	27	3	19	10	2	1	7
San Clemente	EW9504-05	8.20	36	1	0	1	1	20	1	21	6	1	1	2
San Clemente	EW9504-05	8.58	38	1	0	1	0	18	0	19	9	4	1	0
San Clemente	EW9504-05	9.34	42	1	0	0	0	9	0	14	6	1	1	3
San Clemente	EW9504-05	9.72	44	1	0	0	0	18	3	14	3	0	1	0
San Clemente	EW9504-05	10.09	46	1	0	1	0	26	9	10	6	0	0	2
San Clemente	EW9504-05	10.47	48	1	0	0	0	36	12	17	7	0	4	3
San Clemente	EW9504-05	10.85	50	1	0	1	2	21	25	14	7	1	3	4

San Clemente	EW9504-05	11.23	52	1	0	0	1	21	21	7	12	0	0	7
San Nicolas	EW9504-08	2.86	0	1	1	30	13	11	12	69	1	0	21	0
San Nicolas	EW9504-08	3.08	2	4	2	22	7	13	14	46	0	3	14	0
San Nicolas	EW9504-08	3.31	4	2	0	12	11	13	4	21	1	0	2	0
San Nicolas	EW9504-08	3.53	6	2	1	26	10	19	20	35	1	1	18	0
San Nicolas	EW9504-08	3.76	8	2	2	13	9	12	5	22	2	1	15	1
San Nicolas	EW9504-08	3.98	10	2	1	26	16	33	17	28	0	1	22	1
San Nicolas	EW9504-08	4.21	12	2	2	25	4	105	15	18	0	0	24	0
San Nicolas	EW9504-08	4.43	14	2	1	22	4	130	20	9	1	1	12	8
San Nicolas	EW9504-08	4.66	16	2	1	20	15	104	24	26	3	3	17	0
San Nicolas	EW9504-08	5.33	22	2	2	29	15	21	10	42	2	1	17	2
San Nicolas	EW9504-08	6.01	28	2	1	20	5	17	15	50	2	1	25	7
San Nicolas	EW9504-08	6.68	34	2	4	23	6	41	37	49	1	0	31	5
San Nicolas	EW9504-08	7.35	40	4	6	23	3	10	11	26	3	2	3	1
San Nicolas	EW9504-08	8.03	46	1	9	0	2	3	10	14	1	2	0	0
San Nicolas	EW9504-08	8.70	52	4	2	9	10	9	17	19	5	2	11	0
San Nicolas	EW9504-08	9.38	58	4	0	17	4	2	6	9	3	0	7	0
San Nicolas	EW9504-08	10.05	64	4	0	37	13	0	21	20	2	3	0	0

Core	Basin	Age (ka)	Depth in core (top, cm)	Fraction Factor	Oridorsalis umbonatus	Pyrgo murrhina	Quinqueloculina sp.	Uvigerina sp.	Cibicides sp.	Uvgerina peregrina	Hansensica sp.	Globobulimina barbata	Elphidium sp.	Nonionella stella
Tanner	EW9504_09	1.92	0	4	5	7	11	2	1	1	3	0	0	0
Tanner	EW9504_09	2.10	2	4	5	25	22	4	2	3	18	1	1	2
Tanner	EW9504_09	2.29	4	4	6	25	32	5	2	5	19	5	1	2
Tanner	EW9504_09	2.48	6	4	3	18	26	6	0	4	16	0	0	0
Tanner	EW9504_09	2.67	8	4	5	25	33	5	1	4	12	2	1	1
Tanner	EW9504_09	2.85	10	4	2	15	28	4	0	4	10	1	2	3
Tanner	EW9504_09	3.04	12	4	6	15	13	1	0	3	10	2	0	0
Tanner	EW9504_09	3.23	14	4	16	25	20	13	0	10	12	8	3	2
Tanner	EW9504_09	3.42	16	8	4	12	14	2	0	8	4	1	0	0
Tanner	EW9504_09	3.60	18	8	6	17	13	6	0	4	10	1	0	2
Tanner	EW9504_09	3.98	22	4	3	13	20	7	0	12	0	3	1	1
Tanner	EW9504_09	4.16	24	4	9	18	7	10	0	9	0	4	2	2
Tanner	EW9504_09	4.35	26	2	10	23	28	10	0	22	0	4	2	1
Tanner	EW9504_09	4.54	28	4	4	14	11	5	0	8	0	6	0	1
Tanner	EW9504_09	4.73	30	2	3	15	21	9	0	14	0	1	0	2
Tanner	EW9504_09	4.91	32	2	5	20	27	24	2	23	3	4	2	2
Tanner	EW9504_09	5.10	34	4	9	16	10	14	3	9	2	1	0	2
Tanner	EW9504_09	5.29	36	4	7	11	4	24	0	50	2	3	1	3
Tanner	EW9504_09	5.48	38	4	7	7	11	14	0	11	2	2	0	1
San Clemente	EW9504-05	7.07	30	1	12	1	1	7	0	13	2	0	4	5
San Clemente	EW9504-05	7.45	32	1	1	2	5	8	0	29	14	0	1	6
San Clemente	EW9504-05	7.83	34	1	13	2	8	9	0	27	28	0	5	5
San Clemente	EW9504-05	8.20	36	1	9	0	6	8	0	20	10	0	3	4
San Clemente	EW9504-05	8.58	38	1	10	3	14	9	0	41	0	0	1	9
San Clemente	EW9504-05	9.34	42	1	1	2	6	4	0	28	0	0	0	10
San Clemente	EW9504-05	9.72	44	1	5	0	5	5	0	18	3	0	0	0
San Clemente	EW9504-05	10.09	46	1	5	3	11	5	0	32	0	0	0	0
San Clemente	EW9504-05	10.47	48	1	4	4	24	10	0	36	2	0	2	15
San Clemente	EW9504-05	10.85	50	1	5	4	27	19	0	58	1	0	1	12
San Clemente	EW9504-05	11.23	52	1	5	0	25	11	0	37	5	0	0	18
San Nicolas	EW9504-08	2.86	0	1	9	0	4	29	0	82	1	6	2	13

San Nicolas	EW9504-08	3.08	2	4	3	4	7	24	0	123	6	1	0	18
San Nicolas	EW9504-08	3.31	4	2	2	1	3	0	0	34	0	1	0	4
San Nicolas	EW9504-08	3.53	6	2	14	2	7	0	0	65	0	0	0	0
San Nicolas	EW9504-08	3.76	8	2	1	1	6	19	0	83	0	5	1	12
San Nicolas	EW9504-08	3.98	10	2	8	10	3	37	0	66	0	4	0	15
San Nicolas	EW9504-08	4.21	12	2	6	7	6	27	0	24	0	8	1	4
San Nicolas	EW9504-08	4.43	14	2	13	9	0	26	0	42	0	7	1	4
San Nicolas	EW9504-08	4.66	16	2	26	5	1	42	0	75	3	6	1	11
San Nicolas	EW9504-08	5.33	22	2	15	7	2	46	0	145	0	1	0	18
San Nicolas	EW9504-08	6.01	28	2	12	2	1	28	0	138	0	1	0	15
San Nicolas	EW9504-08	6.68	34	2	30	2	4	53	0	288	0	4	1	27
San Nicolas	EW9504-08	7.35	40	4	10	0	4	17	0	66	0	4	0	13
San Nicolas	EW9504-08	8.03	46	1	5	3	0	13	0	33	0	0	0	3
San Nicolas	EW9504-08	8.70	52	4	7	2	3	23	0	77	0	3	1	8
San Nicolas	EW9504-08	9.38	58	4	1	0	2	7	0	21	0	1	0	5
San Nicolas	EW9504-08	10.05	64	4	0	2	3	9	0	21	0	3	0	1

Core	Basin	Age (ka)	Depth in core (top, cm)	Fraction Factor	Uvigerina proboscoidea	Chilostomella ovoidea	Bulimina tenuata	Other	Bolivina argentea	Furkensonia sp.	Quinqueloculina sp2.	Globobulimina ovata1	Melonis affinis	Globocassidulina sp.
Tanner	EW9504_09	1.92	0	4	0	0	0	0	0	0	0	0	0	0
Tanner	EW9504_09	2.10	2	4	1	0	0	0	0	0	0	0	0	0
Tanner	EW9504_09	2.29	4	4	0	2	0	0	0	0	0	0	0	0
Tanner	EW9504_09	2.48	6	4	0	2	0	1	0	0	0	0	0	0
Tanner	EW9504_09	2.67	8	4	3	0	0	0	0	0	0	0	0	0
Tanner	EW9504_09	2.85	10	4	4	0	0	0	0	0	0	0	0	0
Tanner	EW9504_09	3.04	12	4	1	0	0	0	0	0	0	0	0	0
Tanner	EW9504_09	3.23	14	4	5	3	0	0	0	0	0	0	0	0
Tanner	EW9504_09	3.42	16	8	1	1	0	2	0	0	0	0	0	0
Tanner	EW9504_09	3.60	18	8	8	1	1	2	0	0	0	0	0	0
Tanner	EW9504_09	3.98	22	4	5	1	5	1	0	0	0	0	0	0
Tanner	EW9504_09	4.16	24	4	0	2	1	0	0	0	0	0	0	0
Tanner	EW9504_09	4.35	26	2	3	1	7	2	0	0	0	0	0	0
Tanner	EW9504_09	4.54	28	4	4	2	2	2	0	0	0	0	0	0
Tanner	EW9504_09	4.73	30	2	2	0	3	4	0	0	0	0	0	0
Tanner	EW9504_09	4.91	32	2	3	1	12	8	0	0	0	0	0	0
Tanner	EW9504_09	5.10	34	4	2	0	5	5	0	0	0	0	0	0
Tanner	EW9504_09	5.29	36	4	0	2	4	5	0	0	0	0	0	0
Tanner	EW9504_09	5.48	38	4	3	2	6	6	0	0	0	0	0	0
San Clemente	EW9504-05	7.07	30	1	2	0	0	2	1	0	0	0	0	0
San Clemente	EW9504-05	7.45	32	1	2	2	2	0	0	1	0	0	0	0
San Clemente	EW9504-05	7.83	34	1	3	0	0	0	0	1	2	0	0	0
San Clemente	EW9504-05	8.20	36	1	1	0	0	0	0	2	1	0	0	0
San Clemente	EW9504-05	8.58	38	1	5	0	0	2	0	4	4	0	0	0
San Clemente	EW9504-05	9.34	42	1	1	0	0	0	0	6	5	4	0	0
San Clemente	EW9504-05	9.72	44	1	5	0	0	0	0	8	1	1	0	0
San Clemente	EW9504-05	10.09	46	1	4	0	0	0	0	1	0	2	0	0
San Clemente	EW9504-05	10.47	48	1	2	0	0	0	0	3	3	4	0	0
San Clemente	EW9504-05	10.85	50	1	6	0	0	0	0	7	3	0	0	0
San Clemente	EW9504-05	11.23	52	1	2	0	0	0	4	8	5	3	0	0
San Nicolas	EW9504-08	2.86	0	1	0	1	0	2	0	5	0	0	8	4

San Nicolas	EW9504-08	3.08	2	4	1	0	0	0	6	0	0	0	0	9
San Nicolas	EW9504-08	3.31	4	2	1	7	0	4	0	0	0	0	1	3
San Nicolas	EW9504-08	3.53	6	2	0	0	0	12	0	5	0	0	0	8
San Nicolas	EW9504-08	3.76	8	2	2	0	0	6	0	7	0	0	0	10
San Nicolas	EW9504-08	3.98	10	2	1	0	0	4	0	4	0	0	5	11
San Nicolas	EW9504-08	4.21	12	2	1	0	0	3	0	5	0	0	0	1
San Nicolas	EW9504-08	4.43	14	2	1	0	0	2	0	1	0	0	0	2
San Nicolas	EW9504-08	4.66	16	2	1	0	0	2	0	9	0	0	2	3
San Nicolas	EW9504-08	5.33	22	2	1	0	0	2	0	9	0	0	5	20
San Nicolas	EW9504-08	6.01	28	2	0	0	0	0	0	8	0	0	11	15
San Nicolas	EW9504-08	6.68	34	2	0	0	0	2	0	8	0	0	13	36
San Nicolas	EW9504-08	7.35	40	4	1	0	0	1	0	7	0	0	0	5
San Nicolas	EW9504-08	8.03	46	1	0	1	0	0	0	0	0	0	2	1
San Nicolas	EW9504-08	8.70	52	4	0	2	0	0	0	1	0	0	6	5
San Nicolas	EW9504-08	9.38	58	4	0	0	0	0	0	7	0	0	0	1
San Nicolas	EW9504-08	10.05	64	4	0	3	0	3	0	2	0	0	0	1

Appendix 2: Appendix to Chapter 2. Benthic and planktic $\delta^{13}C$ and $\delta^{18}O$ from Tanner Basin.

Basin	Core	Water depth (m)	Age (ka)	Depth in core (top, cm)	G. bulloides $\delta^{13}C$	G. bulloides $\delta^{18}O$	C. mckannai $\delta^{13}C$	C. mckannai $\delta^{18}O$	Publication
Tanner	EW9504_09	1194	1.92	0.00		0.98	-0.04	2.62	this study
Tanner	EW9504_09	1194	2.10	2.00	-0.72	0.65			this study
Tanner	EW9504_09	1194	2.29	4.00	-0.43	1.08	-0.01	2.53	this study
Tanner	EW9504_09	1194	2.48	6.00		-0.04	-0.06	2.31	Stott et al., 2000
Tanner	EW9504_09	1194	2.67	8.00	-0.05	0.41	-0.01	2.48	this study
Tanner	EW9504_09	1194	2.85	10.00	-0.25	0.39	-0.01	2.48	this study
Tanner	EW9504_09	1194	3.04	12.00	-0.40	-0.09	0.00	2.47	this study
Tanner	EW9504_09	1194	3.23	14.00		-0.15	0.00	2.41	Stott et al., 2000
Tanner	EW9504_09	1194	3.42	16.00	-0.53	0.30	-0.02	2.58	this study
Tanner	EW9504_09	1194	3.60	18.00	-0.63	0.41	0.04	2.45	this study
Tanner	EW9504_09	1194	3.79	20.00		0.20			this study
Tanner	EW9504_09	1194	3.98	22.00					this study
Tanner	EW9504_09	1194	4.16	24.00	-0.76	0.32	0.06	2.44	this study
Tanner	EW9504_09	1194	4.35	26.00	-0.92	0.03	0.00	2.53	this study
Tanner	EW9504_09	1194	4.54	28.00	-0.51	-0.08	0.04	2.55	this study
Tanner	EW9504_09	1194	4.73	30.00	-0.83	0.24			this study
Tanner	EW9504_09	1194	4.91	32.00	-0.90	-0.06	-0.02	2.57	this study
Tanner	EW9504_09	1194	5.10	34.00	-0.64	0.07	0.03	2.53	this study
Tanner	EW9504_09	1194	5.29	36.00	-0.72	0.30	-0.07	2.36	this study
Tanner	EW9504_09	1194	5.48	38.00		0.04	-0.04	2.39	Stott et al., 2000
Tanner	EW9504_09	1194	5.67	40.00			-0.04	2.39	Stott et al., 2000
Tanner	EW9504_09	1194	7.04	54.00		-0.02	-0.03	2.44	Stott et al., 2000
Tanner	EW9504_09	1194	7.82	62.00		0.17			Stott et al., 2000
Tanner	EW9504_09	1194	8.60	70.00		0.07	0.01	2.49	Stott et al., 2000
Tanner	EW9504_09	1194	9.38	78.00		0.05	-0.19	3.03	Stott et al., 2000
Tanner	EW9504_09	1194	9.77	82.00			-0.19	2.47	Stott et al., 2000
Tanner	EW9504_09	1194	10.16	86.00		0.06	-0.19	2.65	Stott et al., 2000
Tanner	EW9504_09	1194	10.94	94.00		0.19	-0.09	2.91	Stott et al., 2000
Tanner	EW9504_09	1194	11.72	102.00		0.33	-0.10	3.05	Stott et al., 2000
Tanner	EW9504_09	1194	1.92	0			0.04	2.51	this study
Tanner	EW9504_09	1194	2.29	4			0.02	2.53	this study
Tanner	EW9504_09	1194	2.48	6			-0.06	2.31	this study
Tanner	EW9504_09	1194	2.67	8			-0.01	2.51	this study

Tanner	EW9504_09	1194	2.85	10			0.01	2.31	this study
Tanner	EW9504_09	1194	3.04	12			0.00	2.47	this study
Tanner	EW9504_09	1194	3.23	14			0.00	2.41	this study
Tanner	EW9504_09	1194	3.42	16			-0.02	2.58	this study
Tanner	EW9504_09	1194	3.60	18			0.05	2.33	this study
Tanner	EW9504_09	1194	4.16	24			0.06	2.44	this study
Tanner	EW9504_09	1194	4.35	26			0.02	2.52	this study
Tanner	EW9504_09	1194	4.54	28			0.03	2.64	this study
Tanner	EW9504_09	1194	4.73	30					this study
Tanner	EW9504_09	1194	4.91	32			0.08	2.65	this study
Tanner	EW9504_09	1194	5.10	34			0.04	2.55	this study
Tanner	EW9504_09	1194	5.29	36			-0.06	2.39	this study
Tanner	EW9504_09	1194	5.48	38			-0.04	2.39	this study
Tanner	EW9504_09	1194	1.92	0			-0.13	2.73	this study
Tanner	EW9504_09	1194	2.29	4			-0.04	2.53	this study
Tanner	EW9504_09	1194	2.67	8			-0.08	2.58	this study
Tanner	EW9504_09	1194	2.85	10			-0.04	2.65	this study
Tanner	EW9504_09	1194	3.60	18			0.02	2.57	this study
Tanner	EW9504_09	1194	4.35	26			0.03	2.54	this study
Tanner	EW9504_09	1194	4.54	28			0.05	2.47	this study
Tanner	EW9504_09	1194	4.91	32			-0.12	2.49	this study
Tanner	EW9504_09	1194	5.10	34			0.02	2.52	this study
Tanner	EW9504_09	1194	5.29	36			-0.07	2.33	this study
Tanner	EW9504_09	1194	1.92	0			-0.02	2.29	this study
Tanner	EW9504_09	1194	2.67	8			0.10	2.52	this study
Tanner	EW9504_09	1194	4.35	26			-0.04	2.56	this study
San Clemente	EW9504_05	1818	1.40	0.00			-0.45	2.51	Stott et al., 2000
San Clemente	EW9504_05	1818	2.54	6.00		0.46	-0.23	2.62	Stott et al., 2000
San Clemente	EW9504_05	1818	2.91	8.00			-0.10	2.50	Stott et al., 2000
San Clemente	EW9504_05	1818	4.05	14.00		0.96	-0.25	2.58	Stott et al., 2000
San Clemente	EW9504_05	1818	4.80	18.00			-0.17	2.83	Stott et al., 2000
San Clemente	EW9504_05	1818	6.32	26.00		0.37	-0.59	2.70	Stott et al., 2000
San Clemente	EW9504_05	1818	6.69	28.00			-0.40	2.43	Stott et al., 2000
San Clemente	EW9504_05	1818	7.07	30.00		0.18	-0.41	2.81	Stott et al., 2000
San Clemente	EW9504_05	1818	8.58	38.00		0.97			Stott et al., 2000
San Clemente	EW9504_05	1818	10.09	46.00		0.48	-0.59	3.04	Stott et al., 2000
San Clemente	EW9504_05	1818	10.47	48.00			-0.61	3.36	Stott et al., 2000

San Clemente	EW9504_05	1818	11.61	54.00		0.74	-0.55	2.97	Stott et al., 2000
San Nicolas	EW9504_05	1442	2.86	0.00		0.95	0.13	2.33	Stott et al., 2000
San Nicolas	EW9504_05	1442	3.53	6.00		1.40	-0.30	2.31	Stott et al., 2000
San Nicolas	EW9504_05	1442	4.21	12.00		0.88	0.04	2.34	Stott et al., 2000
San Nicolas	EW9504_05	1442	5.11	20.00		1.52	-0.17	3.33	Stott et al., 2000
San Nicolas	EW9504_05	1442	6.01	28.00		1.22	-0.19	3.61	Stott et al., 2000
San Nicolas	EW9504_05	1442	6.91	36.00		0.76	-0.12	3.50	Stott et al., 2000
San Nicolas	EW9504_05	1442	7.80	44.00		0.35			Stott et al., 2000
San Nicolas	EW9504_05	1442	8.70	52.00		0.57	-0.22	2.95	Stott et al., 2000
San Nicolas	EW9504_05	1442	9.15	56.00			-0.20	3.59	Stott et al., 2000
San Nicolas	EW9504_05	1442	9.60	60.00		0.19	-0.09	2.26	Stott et al., 2000
San Nicolas	EW9504_05	1442	9.83	68.00		0.31	-0.62	3.41	Stott et al., 2000

Appendix 3: Appendix to Chapter 2. Microfossil metazoan faunal counts.

Core	Basin	Age (ka)	Depth in core (upper cm)	Fraction Factor	Urchin Spines Count	Urchin Spines Presence/ Absence	Ostracod Count	Ostracod Presence/ Absence
San Clemente	EW9504-05	7.07	30	1	2	P	1	P
San Clemente	EW9504-05	7.45	32	1	5	P	0	A
San Clemente	EW9504-05	7.83	34	1	4	P	2	P
San Clemente	EW9504-05	8.20	36	1	1	P	7	P
San Clemente	EW9504-05	8.58	38	1	4	P	5	P
San Clemente	EW9504-05	9.34	42	1	4	P	5	P
San Clemente	EW9504-05	9.72	44	1	4	P	4	P
San Clemente	EW9504-05	10.09	46	1	4	P	2	P
San Clemente	EW9504-05	10.47	48	1	4	P	6	P
San Clemente	EW9504-05	10.85	50	1	6	P	12	P
San Clemente	EW9504-05	11.23	52	1	2	P	9	P
San Nicolas	EW9504-08	2.86	0	1	0	A	0	A
San Nicolas	EW9504-08	3.08	2	4	0	A	0	A
San Nicolas	EW9504-08	3.31	4	2	0	A	0	A
San Nicolas	EW9504-08	3.53	6	2	1	P	0	A
San Nicolas	EW9504-08	3.76	8	2	0	A	0	A
San Nicolas	EW9504-08	3.98	10	2	0	A	0	A
San Nicolas	EW9504-08	4.21	12	2	1	P	1	P
San Nicolas	EW9504-08	4.43	14	2	0	A	0	A
San Nicolas	EW9504-08	4.66	16	2	1	P	0	A
San Nicolas	EW9504-08	5.33	22	2	1	P	0	A
San Nicolas	EW9504-08	6.01	28	2	0	A	0	A
San Nicolas	EW9504-08	6.68	34	2	1	P	0	A
San Nicolas	EW9504-08	7.35	40	4	0	A	0	A
San Nicolas	EW9504-08	8.03	46	1	0	A	0	A
San Nicolas	EW9504-08	8.70	52	4	1	P	0	A
San Nicolas	EW9504-08	9.38	58	4	0	A	0	A
San Nicolas	EW9504-08	10.05	64	4	0	A	1	P
Tanner	EW9504_09	1.92	0	4	0	A	0	A
Tanner	EW9504_09	2.10	2	4	0	A	0	A
Tanner	EW9504_09	2.29	4	4	2	P	0	A
Tanner	EW9504_09	2.48	6	4	0	A	0	A
Tanner	EW9504_09	2.67	8	4	0	A	0	A
Tanner	EW9504_09	2.85	10	4	0	A	0	A
Tanner	EW9504_09	3.04	12	4	1	P	0	A

Tanner	EW9504_09	3.23	14	4	2	P	0	A
Tanner	EW9504_09	3.42	16	8	2	P	0	A
Tanner	EW9504_09	3.60	18	8	2	P	1	P
Tanner	EW9504_09	3.98	22	4	6	P	2	P
Tanner	EW9504_09	4.16	24	4	0	A	1	P
Tanner	EW9504_09	4.35	26	2	4	P	3	P
Tanner	EW9504_09	4.54	28	4	1	P	0	A
Tanner	EW9504_09	4.73	30	2	5	P	1	P
Tanner	EW9504_09	4.91	32	2	4	P	0	A
Tanner	EW9504_09	5.10	34	4	1	P	0	A
Tanner	EW9504_09	5.29	36	4	2	P	0	A
Tanner	EW9504_09	5.48	38	4	2	P	0	A

Appendix 4: Appendix to Chapter 3. Table of papers used in literature review (step 1 of systematic review).

Paper	Paper	Latitude	Longitude	Region	Archive
Addison et al., 2017	Addisson et al 2017	40.8656	-124.573	PNW	Marine sediment
Anderson and Byrd 1998	Anderson and Byrd 1998	33.291667	-117.341667	SW	Lake sediment
Anderson et al., 2010	Anderson et al., 2010	33.965278	-120.097222	SW	Lake sediment
	Anderson et al., 2010	33.955556	-119.095833	SW	Marine sediment
Asmerom et al., 2013	Asmerom et al 2013	32.163745	-104.517682	SW	Speleothem
Bacon et al 2018	Bacon et al 2018	36.542	-117.938	SW	Geomorphology
Bacon et al., 2006	Bacon et al., 2006	36.441174	-117.970433	SW	Lake sediment
Barron and Anderson 2011	Barron and Anderson 2011	review paper			
Barron and Burky 2007	Barron and Bukry, 2007	42.24	-125.89	PNW	Marine sediment
	Barron and Bukry, 2007	36.99	-123.268	SW	Marine sediment
	Barron and Bukry, 2007	41.68	-124.93	PNW	Marine sediment
Barron et al., 2003	Barron et al 2003	42.682	-124.93	PNW	Marine sediment
Barron et al., 2010	Barron et al., 2010	34.2875	-120.036667	SW	Marine sediment
	Barron et al., 2010	34.221667	-120.028333	SW	Marine sediment
Barron et al 2017	Barron et al., 2017	40.9	-124.6	PNW	Marine sediment
	Barron et al., 2017	40.9	-124.6	PNW	Marine sediment
Barron et al., 2019	Barron et al., 2019	37.3317	-123.3992	SW	Marine sediment
Beatty and Taylor 2009	Beatty and Taylor 2009	39.034637	-120.1624	SW	Lake sediment
Beck et al 2018	Beck et al 2018	42.730113	-120.517458	PNW	Lake sediment
Benson et al., 2002	Benson et al 2002	40.073646	-119.5969	PNW	Lake sediment
Bird and Kirby 2006	Bird & Kirby 2006	34.120426	-116.82766	SW	Lake sediment
Bird et al., 2010	Bird et al., 2010	34.121045	-116.828569	SW	Lake sediment
Braje et al., 2012	Braje et al 2012	34.038578	-120.37907	SW	Archeological record
	Braje et al 2012	34.016987	-119.765051	SW	Archeological record
	Braje et al 2012	33.955317	-120.1062	SW	Archeological record
Briles et al., 2005	Briles et al., 2005	42.025	-123.458333	PNW	Lake sediment
Brown and Hebda 2002	Brown and Hebda 2002	48.595278	-124.197325	PNW	Lake sediment
	Brown and Hebda 2002	48.547796	-123.475786	PNW	Lake sediment
Byrne et al., 2001	Byrne et al., 2001	38.098287	-122.02125	SW	Marine sediment
Cannariato and Kennett 1999	Cannariato and Kennett 1999	34.535	-121.107167	SW	Marine sediment
	Cannariato and Kennett 1999	34.5	-121.5	SW	Marine sediment
Cole and Liu 1994	Cole and Liu 1994	33.956389	-119.976667	SW	Lake sediment
Cole and Wahl 2000	Cole and Wahl 2000	32.929595	-117.256734	SW	Lake sediment
Cook et al., 2000	Cook et al., 2000	review/modeling paper			
Cowart and Byrne 2013	Cowart and Byrne 2013	37.173889	-122.314444	SW	Lake sediment
Davis 1992	Davis 1992	33.660482	-117.840775	SW	Marine sediment

Dingemans et al 2014	Dingemans et al 2014	34.76666667	-120.0333333	SW	Lake sediment
Du et al 2018	Du et al., 2018	34.281767	-119.963967	SW	Marine sediment
Erlandson et al., 2007	Erlandson et al., 2007				
Erlandson et al., 2009	Erlandson et al., 2009				
Feakins et al 2014	Feakins et al 2014	34.777634	-120.039859	SW	Lake sediment
Field et al 2006	Field et al., 2006	34.287133	-120.035583	SW	Marine sediment
Fisler and Hendy 2008	Fisler and Hendy 2008	34.2875	-120.036667	SW	Marine sediment
Flores et al., 2017	Flores et al., 2017	33.987079	-120.222156	SW	Archeological record
	Flores et al., 2017	33.914652	-120.053465	SW	Archeological record
Friddell et al 2003	Friddell et al 2003	34.271167	-120.072667	SW	Marine sediment
Gardener et al., 1988	Gardner et al., 1988	39.05	-122.835583	SW	Lake sediment
	Gardner et al., 1988	38.425167	-122.796167	SW	Marine sediment
Gavin et al. 2007	Gavin et al. 2007	review paper			
Gavin et al., 2003	Gavin et al., 2003	49.3911	-125.748781	PNW	Tree stump
Glassow et al., 2012	Glassow et al., 2012	33.960648	-119.817915	SW	Archeological record
Hallett and Anderson 2010	Hallett and Anderson 2010	37.90857222	-119.2864	SW	Lake sediment
	Hallett and Anderson 2010	37.59570278	-119.0067	SW	Lake sediment
Hallett et al., 2003	Hallett et al., 2003	49.36	-121.4666667	PNW	Lake sediment
	Hallett et al., 2003	49.266667	-121.516667	PNW	Lake sediment
Hermann et al 2018	Hermann et al 2018	review paper			
Heusser 1978	Heusser 1978	34.266667	-120.066667	SW	Marine sediment
Heusser 1983	Heusser 1983	48.59065	-123.503333	PNW	Marine sediment
Heusser 1998	Heusser 1998	review paper			Marine sediment
Hiner et al 2016	Hiner et al 2016	36.231354	-121.482348	SW	Lake sediment
Ingram 1998	Ingram 1998	37.576171	-122.261235	SW	Archaeological record
Jones and Kennett 1999	Jones and Kennett 1999	36.288439	-121.853672	SW	Archaeological record
	Jones and Kennett 1999	35.642784	-121.177744	SW	Archaeological record
	Jones and Kennett 1999	36.045231	-121.584481	SW	Archaeological record
Jones et al., 2008	Jones et al., 2008	35.668278	-121.284271	SW	Archaeological record
	Jones et al., 2008	36.070611	-121.582634	SW	Archaeological record
Kaufman et al., 2020	Kaufman et al., 2020	global synthesis			
	Kennett and Ingram 1995	34.2875	-120.036667	SW	Marine sediment
Kennett and Kennett 2000	Kennett and Kennett 2000	34.2875	-120.036667	SW	Marine sediment
Kennett et al., 2007	Kennett et al., 2007	34.2875	-120.036667	SW	Marine sediment
Kim et al 2004	Kim et al., 2004	48.912	-126.89	PNW	Marine sediment
	Kim et al., 2004	22.99	-109.47	SW	Marine sediment
	Kim et al., 2004	34.535	-121.107	SW	Marine sediment
	Kim et al., 2004	41.682	-124.93	PNW	Marine sediment
Kirby et al 2007	Kirby et al 2007	33.37	-117.22	SW	Lake sediment
Kirby et al 2010	Kirby et al 2010	33.37	-117.22	SW	Lake sediment
Kirby et al 2012	Kirby et al 2012	34.253472	-116.920249	SW	Lake sediment
Kirby et al 2014	Kirby et al 2014	34.77	-120.1162	SW	Lake sediment
Kirby et al 2015	Kirby et al 2015	33.37	-117.22	SW	Lake sediment
Kirby et al 2019	Kirby et al 2019	33.6733	-117.3542	SW	Lake sediment
	Kirby et al 2019	33.6734	-117.3641	SW	Lake sediment
Konrad and Clarke, 1998	Konrad and Clarke 1998	37.970176	-119.318354	SW	Lake sediment
	Konrad and Clarke 1998	37.140252	-118.629612	SW	Lake sediment

Lightfoot and Cuthrell 2015	Lightfoot and Cuthrell 2015	37.16305	-122.338183	SW	Archaeological record
Lindstrom, 1990	Lindstrom 1990	38.942579	-120.053067	SW	Tree stump
Long and Whitlock 1998	Long and Whitlock 1998	44.167778	-123.582222	PNW	Lake sediment
Lyle et al., 2012	Lyle et al., 2012	review paper			
Macdonald and Case 2005	Macdonald and Case 2005	34.066667	-116.483333	SW	Tree ring
MacDonald et al., 2016	MacDonald et al 2016	38.3395	-119.4984	SW	Lake sediment
Malamud-Roam et al 2006	Malamud-Roam et al 2006	37.997233	-122.453821	SW	Marine sediment
Marchitto et al 2010	Marchitto et al., 2010	25.2	-112.7	SW	Marine sediment
Marcott et al., 2013	Marcott et al., 2013	review paper			
Marlon et al., 2006	Marlon et al. 2006	48.168	-114.368	PNW	Lake sediment
	Marlon et al. 2006	44.288	-110.178	PNW	Lake sediment
	Marlon et al. 2006	44.928	-110.358	PNW	Lake sediment
	Marlon et al. 2006	44.668	-110.628	PNW	Lake sediment
	Marlon et al. 2006	45.848	-113.448	PNW	Lake sediment
	Marlon et al. 2006	45.898	-114.268	PNW	Lake sediment
	Marlon et al. 2006	46.328	-114.658	PNW	Lake sediment
	Marlon et al. 2006	45.708	-114.998	PNW	Lake sediment
	Marlon et al. 2006	46.088	-123.908	PNW	Lake sediment
Mayewski et al., 2004	Mayewski et al., 2004	review paper			
McGann 2008	McGann 2008	37.6305	-122.3665	SW	Marine sediment
McGann 2011	McGann 2011	37.223333	-123.243333	SW	Marine sediment
McGann 2015	McGann 2015	36.392167	-123.342	SW	Marine sediment
McQuiod and Hobson 2001	McQuiod and Hobson 2001	48.633333	-123.5	PNW	Marine sediment
Mix et al., 1999	Mix et al 1999	42.117	-125.75	PNW	Marine sediment
	Mix et al 1999	41.682	-124.93	PNW	Marine sediment
Moffitt et al., 2014	Moffitt et al., 2014	34.37	-121.13	SW	Marine sediment
Moffitt et al., 2015	Moffitt et al., 2015	34.37	-121.13	SW	Marine sediment
Mohr et al., 2000	Mohr et al., 2000	41.4	-122.583	PNW	Lake sediment
	Mohr et al., 2000	41.333	-122.55	PNW	Lake sediment
Nederbragt and Thurow 2001	Nederbragt and Thurow 2001	48.59065	-123.503333	PNW	Marine sediment
	Nederbragt and Thurow 2001	48.590617	-123.503417	PNW	Marine sediment
Negrini et al., 2006	Negrini et al., 2006	36.004447	-119.785517	SW	Lake sediment
Oster et al., 2017	Oster et al., 2017	37	-122.1833333	SW	Speleothem
Pellatt et al., 2001	Pellatt et al., 2001	48.59065	-123.503333	PNW	Marine sediment
Platzman and Lund 2019	Platzman and Lund 2019	35.3	-120.05	SW	Lake sediment
Rasmussen et al 2006	Rasmussen et al 2006	32.159	-104.523	SW	Speleothem
Reyes and Clague, 2004	Reyes and Clague 2004	50.75	-123.766667	PNW	Moraine
Rick, 2011	Rick 2011	34.003841	-120.176931	SW	Archeological record
Roark et al 2003	Roark et al 2003	34.2875	-120.036667	SW	Marine sediment
Schimmelmann et al., 2013	Schimmelmann et al., 2013	34.2875	-120.036667	SW	Marine sediment
Shuman et al 2018	Shuman et al 2018	review paper			
Spaulding et al 1991	Spaulding 1990	35.45	-115.1	SW	Terrestrial midden
Steinman et al., 2019	Steinman et al 2019	48.5417	-119.5818	PNW	Lake sediment
	Steinman et al 2019	48.5394	-119.5615	PNW	Lake sediment
Steinman et al., 2016	Steinman et al., 2016	50.82	-116.39	PNW	Lake sediment
Stine 1990	Stine 1990	38.008101	-119.016233	SW	Lake shore
Stine 1994	Stine 1994	37.950538	-119.01395	SW	Tree stump
Taylor et al. 2016	Taylor et al. 2016	40.7	-121.59	PNW	Fire scar

Tomasovych and Kidwell 2017	Tomosovych and Kidwell 2018	33.48	-118.59	SW	Marine sediment
	Tomosovych and Kidwell 2018	32.7555	-117.3617	SW	Marine sediment
Tunnicliffe et al 2001	Tunnicliffe et al 2001	48.59065	-123.503333	PNW	Marine sediment
	Tunnicliffe et al 2001	48.590617	-123.503417	PNW	Marine sediment
van Geen et al 2003	van Geen et al 2003	34.2875	-120.036667	SW	Marine sediment
Viau et al., 2006	Viau et al., 2006	review/modeling paper			
Walsh et al. 2017	Walsh et al. 2017	46.9231	-121.5836	PNW	Lake sediment
	Walsh et al. 2017	46.9198	-121.5886	PNW	Lake sediment
	Walsh et al. 2017	46.9114	-121.6571	PNW	Lake sediment
Whitlock et al 2008	Whitlock et al 2008	41.21	-122.5	PNW	Lake sediment
	Whitlock et al 2008	41.35	-122.56	PNW	Lake sediment
	Whitlock et al 2008	41.4	-122.58	PNW	Lake sediment
	Whitlock et al 2008	42.02	-123.46	PNW	Lake sediment
	Whitlock et al 2008	45.81	-123.57	PNW	Lake sediment
	Whitlock et al 2008	44.16	-123.58	PNW	Lake sediment
	Whitlock et al 2008	46.08	-123.9	PNW	Lake sediment

Appendix 5: Appendix to Chapter 3. Results of coded analysis of previously published records.

Paper	Region	Early Fire	Early Temp	Early Hydro	Mid Fire	Mid Temp	Mid Hydro	Late Fire	Late Temp	Late Hydro
Addisson et al 2017	PNW			dry						
Anderson and Byrd 1998	SW			dry			wet			
Asmerom et al 2013	SW			dry						
Bacon et al 2018	SW			dry						
Bacon et al., 2006	SW			dry						
Barron and Bukry, 2007	PNW		warm	dry		cold				
Barron et al., 2017	PNW			dry		cold			warm	wet
Barron et al., 2003	PNW		warm	dry		cold			warm	wet
Barron et al., 2010	SW			dry						
Barron et al., 2019	SW		warm	dry		cold			warm	wet
Beatty and Taylor 2009	SW	low			high			low	cold	dry
Beck et al 2018	PNW			wet						
Benson et al 2002	PNW			wet		warm	dry			wet
Bird & Kirby 2006	SW			wet						
Bird et al., 2010	SW			wet						
Braje et al 2012	SW			wet						
Briles et al., 2005	PNW		warm	wet				high	cold	dry
Brown and Hebda 2002	PNW		high	wet	low			low/high	cold	dry

Paper	Region	Early Fire	Early Temp	Early Hydro	Mid Fire	Mid Temp	Mid Hydro	Late Fire	Late Temp	Late Hydro
Byrne et al., 2001	SW			wet						
Cannariato and Kennett 1999	SW			wet						
Cole and Liu 1994	SW			wet			dry			wet
Cole and Wahl 2000	SW			wet						
Du et al., 2018	SW						wet			
Fisler and Hendy 2008	SW		cold			warm				wet
Friddell et al 2003	SW		cold			warm				wet
Hallett and Anderson 2010	SW	low			high	warm	dry	high	cold	dry
Hallett et al., 2003	PNW	high	warm				wet		cold	dry
Kennett et al., 2007	SW					warm	dry			wet
Kirby et al 2007	SW						dry			wet
Kirby et al 2010	SW						dry			wet
Kirby et al 2014	SW						dry			wet
Kirby et al 2015	SW						dry			
Kirby et al 2019	SW						wet			
Konrad and Clarke 1998	SW						wet			
Lindstrom 1990	SW						dry			

Paper	Region	Early Fire	Early Temp	Early Hydro	Mid Fire	Mid Temp	Mid Hydro	Late Fire	Late Temp	Late Hydro
Long and Whitlock 1998	PNW	high	warm		low	cold	wet	low	cold	dry
MacDonald et al 2016	SW					warm	dry			wet
Malamud-Roam et al 2006	SW					cold	wet		cold	
Marchitto et al., 2010	SW		cold			cold				
Marlon et al. 2006	PNW	low	warm		high	cold	wet	high	cold	dry
McGann 2011	SW		warm			warm	dry		warm	wet
McGann 2015	SW		warm				dry			wet
Mix et al 1999	PNW		warm			cold			warm	wet
Mohr et al., 2000	PNW	low	warm		high	cold	wet	high	cold	dry
Nederbragt and Thurow 2001	PNW						wet			
Pellatt et al., 2001	PNW		warm							
Spaulding 1990	SW						dry			
Steinman et al 2019	PNW						wet	high	cold	dry
Whitlock et al 2008	PNW	low				cold	wet	high	cold	dry

Appendix 6: Appendix to Chapter 3. Table of data accessed for time series plots (Figure 4 and 5).

Paper	Latitude	Longitude	Region	Archive	Figure Number	Accessed From	Link
Addisson et al 2017	40.8656	-124.573	PNW	Marine sediment	4	NOAA Paleoclimate Database	https://www.ncdc.noaa.gov/paleo-search/study/21650
Barron et al 2003	42.682	-124.93	PNW	Marine sediment	4	NOAA Paleoclimate Database	https://www.ncdc.noaa.gov/paleo-search/study/5867
Braje et al 2012	34.038578	-120.37907	SW	Archaeological Record	5	In original paper: Table 1	https://www.sciencedirect.com/science/article/abs/pii/S1040618211005301
Kennett et al., 2007	34.2875	-120.036667	SW	Marine sediment	5	Author webpage	http://php.scripts.psu.edu/dept/liberalarts/sites/kennett/data.php
Kirby et al 2015	33.37	-117.22	SW	Lake sediment	5	NOAA Paleoclimate Database	https://www.ncdc.noaa.gov/paleo-search/study/20106
Long and Whitlock 1998	44.167778	-123.582222	PNW	Lake sediment	4	NOAA Paleoclimate Database	https://www.ncdc.noaa.gov/paleo-search/study/2252
MacDonald et al 2016	38.3395	-119.4984	SW	Lake sediment	5	Harvard Dataverse	https://dataverse.harvard.edu/dataset.xhtml?persistentId=doi:10.7910/DVN/P3MCFX
McGann 2015	36.392167	-123.342	SW	Marine sediment	5	In original paper: Table 2	https://www.sciencedirect.com/science/article/pii/S1040618215000610?casa_token=PAo4SBfUSPMAAAAA:g2YzlQACCS_MKrtKGcIN8PbTF0vc44mFxqyNfO_1ojeGltRavFpodrSo1aT7mUaM_KuPUM3aupM
Steinman et al 2016	50.82	-116.39	PNW	Lake sediment	4	NOAA Paleoclimate Database	https://www.ncdc.noaa.gov/paleo-search/study/21250